



Prospects of Measuring
 $qq \rightarrow qqH$ and $gg \rightarrow H$ Cross Sections
at the LHC with CMS

or

the *Higgs files*

Diploma thesis

Anne-Sylvie Nicollerat

performed at CERN
under supervision of

Dr. Michael Dittmar, ETHZ
Prof. Felicitas Pauss, ETHZ
Prof. Tatsuya Nakada, Université de Lausanne

October 2000 to March 2001

Abstract

The possibility to observe a Higgs boson having a mass between 300 and 600 GeV and to measure its couplings to vector bosons and top quark with CMS at the LHC is studied. The different signatures:

$$H \rightarrow ZZ \rightarrow \ell^+ \ell^- \ell^+ \ell^-$$

$$H \rightarrow ZZ \rightarrow \ell^+ \ell^- \nu \bar{\nu}$$

$$H \rightarrow ZZ \rightarrow \ell^+ \ell^- q \bar{q}$$

$$H \rightarrow ZZ \rightarrow \nu \bar{\nu} q \bar{q}$$

$$H \rightarrow WW \rightarrow \ell \nu \ell \nu$$

$$H \rightarrow WW \rightarrow \ell \nu q \bar{q}$$

are analyzed. The possibility to separate the Higgs events produced through weak boson fusion ($qq \rightarrow qqH$) from the Higgs produced through gluon fusion ($gg \rightarrow H$) using the forward going jets emitted in the weak boson fusion process is discussed for each of these different channels. The results are then used to determine the possible statistical errors on the ratio between the two Higgs decay branching fractions $H \rightarrow ZZ$ and $H \rightarrow WW$ and on the weak boson fusion and gluon fusion cross sections after one year of LHC running.

Contents

Introduction	5
1 The Large Hadron Collider	9
2 Basic Higgs properties	13
3 General ideas to get a signal	19
4 Analysis	31
5 Discussion	73
Summary	89
Bibliography	91
Acknowledgments	95

Introduction

or how to explain to my friends what I did during four months...

During the late sixties, Salam, Glashow and Weinberg proposed a Model, the *Standard Model of electroweak interactions*¹, which was giving a new description of the interactions between the basic components of matter. Based on the same principles (the gauge symmetries), a Model which describes interactions of quarks and gluons was developed later, the so-called Quantum Chromodynamic (QCD)². These models are now gathered under the name of *Standard Model of Particle Physics* and provide a description of the basic components of matter and its interactions. Since that time, the Standard Model gave predictions which were well confirmed by observations. Within that Model and given the experimental results, all the known matter can be described with 12 fundamental entities, named fermions (spin 1/2 particles), together with some interaction carriers, named vector bosons (spin 1 particles).

These particles can interact via three types of forces³, see Table 1: The electromagnetic interaction, the strong interaction (which binds the quarks together, e.g. in the protons) and the weak interaction (used for the description of radioactivity, β decay).

Interaction	Vector boson	Mass (GeV)	Fermions involved
Strong	8 gluons	0	quarks
Electromagnetic	γ	0	all charged particles
Weak	W^\pm, Z^0	80, 91	all left-handed particles

Table 1: Interactions of the Standard Model.

The interactions are carried by particles named vector bosons. To understand the idea of an interaction carried by a particle, let's take the image of two children playing with a ball. As they are throwing the ball, they cannot move too far away

¹ The idea of Salam, Glashow and Weinberg [1] was to propose a gauge theory which unify weak and electromagnetic interactions using the symmetry groups $SU(2)$ of 'weak isospin' and $U(1)$ of 'weak hypercharge'.

² In that theory a new symmetry group was added, describing the strong interactions, $SU(3)$, completing the Standard Model gauge group: $SU(3)_c \times SU(2)_I \times U(1)_Y$.

³We exclude here the gravity, which is not described in that model.

from each other, as the ball will not reach a too long distance because of its weight. They are somehow bound to each other, by the presence of the ball. In today used representation of interactions, the particles can be considered like the children and vector bosons like the ball.

The twelve fundamental fermions can be sorted out using their different behavior under the interactions. For example, quarks are defined as particles which feel the strong interaction and leptons as particles which does not. These twelve particles can also be sorted out in three doubleted families, each family having the same general behavior under the weak interaction. These families are shown in Table 2. One achievement of the late CERN accelerator, LEP, was to show that there is no fourth family.

Everyday matter is made out of the components from the first family (*electrons* and *electron neutrino*, *up* and *down* quarks). For example, a proton is made out of one *d* and two *u* quarks. The two other generations (*muon* and *muon neutrino*, *c* and *s* quarks, *tau* and *tau neutrino*, *t* and *b* quarks) are used to describe high energy states like the ones which were present at the beginning of the Universe and can now be created in the particle accelerators.

1st family		2nd family		3rd family	
Leptons					
	Mass		Mass		Mass
$\begin{pmatrix} \nu_e \\ e \end{pmatrix}$	$<0.003 \text{ MeV}$ 0.511 MeV	$\begin{pmatrix} \nu_\mu \\ \mu \end{pmatrix}$	$<0.17 \text{ MeV}$ 106 MeV	$\begin{pmatrix} \nu_\tau \\ \tau \end{pmatrix}$	$<18.2 \text{ MeV}$ 1777 MeV
Quarks					
	Mass		Mass		Mass
$\begin{pmatrix} u \\ d \end{pmatrix}$	$\sim 6 \text{ MeV}$ $\sim 3 \text{ MeV}$	$\begin{pmatrix} c \\ s \end{pmatrix}$	$\sim 1'250 \text{ MeV}$ $\sim 115 \text{ MeV}$	$\begin{pmatrix} t \\ b \end{pmatrix}$	$175'000 \text{ MeV}$ $\sim 4'250 \text{ MeV}$

Table 2: The building blocks of matter given by the Standard Model.

All these elementary particles have very different masses: For instance the top quark is almost about one million times heavier than the electron. The Standard Model as it was initially developed cannot explain such a variety in the masses of the particles. Even worse, it predicted all particles to be massless ... To solve that problem, a British physicist, Peter Higgs, introduced a new field in the Standard Model, named the Higgs field, which through the mechanism of *spontaneous symmetry breaking*, would give their mass to the particles [2]. To understand better how this works, let's quote David Miller from the Department of Physics and As-

tronomy of the University College of London:

Imagine a cocktail party of political party workers who are uniformly distributed across the floor, all talking to their nearest neighbors. The ex-Prime Minister enters and crosses the room. All of the workers in her neighborhood are strongly attracted to her and cluster round her. As she moves she attracts the people she comes close to, while the ones she has left return to their even spacing. Because of the knot of people always clustered around her she acquires a greater mass than normal, that is she has more momentum for the same speed of movement across the room. Once moving she is hard to stop, and once stopped she is harder to get moving again because the clustering process has to be restarted.

In this story, the Higgs field would be represented by the people taking part to the party and the particles would be the ex-Prime Minister. But now, how can we see that such a field exists? In Quantum Mechanics, fields can be seen as particles and vice versa. The idea will be to detect the particle associated to that field, namely the *Higgs boson* (a spin 0 particle). To illustrate this, let's go on with the story:

(...) Now consider a rumor passing through our room full of uniformly spread political workers. Those near the door hear of it first and cluster together to get the details, then they turn and move closer to their next neighbors who want to know about it too. A wave of clustering passes through the room. It may spread to all the corners or it may form a compact bunch which carries the news along a line of workers from the door to some dignitary at the other side of the room. Since the information is carried by clusters of people, and since it was the clustering that gave extra mass to the ex-Prime Minister, then the rumor-carrying clusters also have mass.

The Higgs boson is indeed predicted to be just such a clustering in the Higgs field. We will find it much easier to believe that this field describes a physical reality, and that the mechanism for giving other particles masses is true, if we actually see the Higgs particle itself.

This particle is the only predicted particle of the Standard Model which still remains to be found. The theory does not make prediction for the mass of that new particle. Lower and upper limits to its mass can nevertheless be set [3]: The Standard Model is assumed to give predictions only up to an energy Λ . Above that limit, the method used to make calculations cannot be applied any more. The mass of the Higgs and Λ are not independent and a light Higgs allows Λ to be higher. If Λ is large, calculations with the Standard Model will be possible up to higher energies and more energetic states of the Universe will be described by that Model. However arguments on the vacuum stability suggest a lower Higgs mass limit. Figure 1 shows how the Higgs mass can be constrained in respect to the parameter Λ . For the Standard Model to be valid up to energies as high as possible, the Higgs mass should lie between 140 and 180 GeV. A higher or a lower Higgs mass restricts the region in which the Standard Model could describe Nature. Today, physics is tested only up to a mass scale of about 100 to 200 GeV (notice that the plot begins at energies of 1000 GeV !) and almost all the measurements agree with the Standard Model. The observation of a Higgs boson is a crucial test

of the Standard Model and at the same time the value of its mass will determine up to which energy the Standard Model could make predictions.

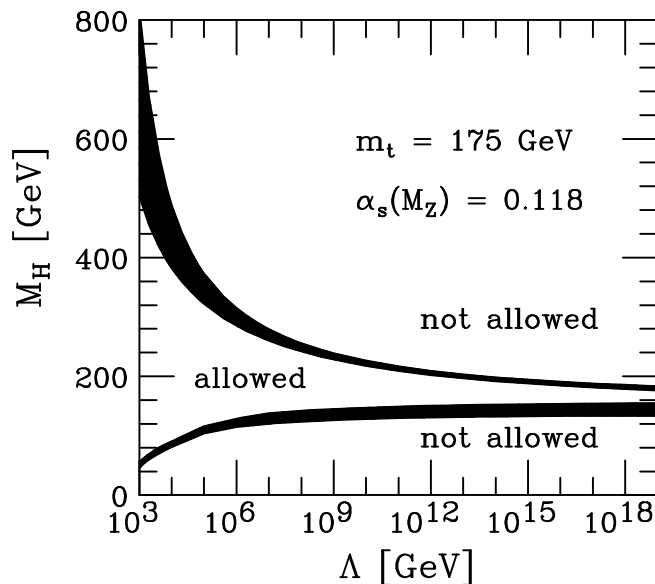


Figure 1: The area between black curves shows the allowed Higgs mass range assuming the validity of the Standard Model up to an energy scale of Λ , [3].

Thus today the Higgs boson can be considered like the Holy Grail of Particle Physics and if it is eventually found, it will be by far the most expensive particle of the Universe, given all the efforts that are and will be done to find it. The final answer to the question of its existence will probably be given in about five years either at the Fermilab accelerator Tevatron or at the CERN's new Collider, LHC. Story to be continued ...

The work I did started from the hypothesis that the Higgs boson has a mass between 300 and 600 GeV. It was interesting to study this mass region as it was not deeply analyzed yet in opposition to the lighter Higgs mass sector. I studied how a heavy Higgs might be discovered and what one might learn about its properties.

The first chapter gives a short description of the Large hadron Collider (LHC), the CERN's new accelerator and of one of its detectors (CMS), with which we hope to find the Higgs. It also describes the simulation used.

The second chapter reviews the important physical characteristics of the Higgs, like its production and decays modes. The next chapter gives the general ideas used in that study to find the selection cuts. The fourth chapter goes through the different Higgs search channels studied and presents the results obtained. Finally a discussion is made, analyzing the different properties of the Higgs which could be measured with the previously obtained results.

Chapter 1

The Large Hadron Collider

CERN started to build a new accelerator, the Large Hadron Collider (LHC), whose main task will be to find the Higgs boson. Situated in the 27-kilometer of the now former LEP tunnel, it will bring protons into head-on collisions at expected center of mass energies of 14 TeV and should be ready to run in Spring 2006.

1.1 LHC characteristics

An important parameter, used to characterize an accelerator needs to be defined first, namely, the luminosity, \mathcal{L} . It determines, together with the cross section, σ , the event rate produced in a given process:

$$N_{evts} = \sigma \mathcal{L}$$

While the cross section depends on the physical characteristics of the process, the luminosity depends on the characteristics of the accelerator. For a circular accelerator, it is given by:

$$\mathcal{L} = \frac{N^2 k f \gamma}{4\pi \epsilon_n \beta^*}$$

where N is the number of particles in each of the k circulating bunches, f the revolution frequency, β^* the value of the betatron function at the crossing point and ϵ_n the emittance corresponding to the one σ contour of the beam, normalized by multiplying by the Lorentz factor $\gamma = (E/m_0 c^2)$.

In the first years, LHC should reach a luminosity of $10^{33} \text{ cm}^{-2} \text{ s}^{-1}$ which represents an integrated luminosity of 10 fb^{-1} per year. Then it will be raised till a maximum of 100 fb^{-1} per year. The designed frequency is about 40 MHz, which is equivalent to a bunch crossing approximatively every 25 nanosecond. Each crossing contains about 20 events, as the total cross-section at hadron colliders is very large, about 100 mb for the LHC.

The detection of processes with a signal to total cross section ratio of about 10^{-12} ,

like for a 120 GeV Higgs decaying into two photons, will be a difficult experimental challenge. Note that the interesting signatures for detecting the Higgs particle are often characterized by charged leptons or photons, since its hadronic decays is overwhelmed by a huge QCD background. Purely leptonic modes lead to very small branching fractions. In order to observe such signals, a machine with a high constituents center-of-mass energy and a high luminosity is required.

Four detectors will be built around the LHC : ATLAS (A Toroidal LHC Apparatus), CMS (Compact Muons Solenoid), ALICE (A Large Ion Collider Experiment) and LHCb. The first two are dedicated to Higgs searches and to the exploration of possible new physics beyond the Standard Model at high masses, whereas ALICE will analyze the collisions of heavy ions. LHCb will study CP violation and other rare phenomena in the decay of beauty particles.

1.2 The Compact Muon Solenoid (CMS) detector

Before describing the detector, it is important to say some words about the rapidity. The rapidity, y , of a particle is defined like:

$$y = \frac{1}{2} \ln \left(\frac{E + p_z}{E - p_z} \right)$$

The rapidity is defined compared with a direction, z , usually given by the beam axis. If $p \gg m$, the rapidity can be approximated in the following way and we get the *pseudorapidity*, η :

$$\eta = -\ln(\tan(\theta/2))$$

We see that the pseudorapidity is directly linked with the angle between the particle momentum and the beam pipe, θ . A pseudorapidity of 1, represents an angle of 40 degrees, a pseudorapidity of 2.5, an angle of 9 degree and a pseudorapidity of 4.5 an angle of 1 degree. What is interesting with the rapidity, is that in opposition to θ , it is only shifted by a constant under Lorentz transformations, leading to flat distributions. The density of rapidity is then independent of the chosen referential. Rapidity is thus preferably used to describe the event geometry than θ . Figure 1.1 give a comparison between the η and θ distribution obtained in the reaction $qq \rightarrow qq$ for the pions present in event.

The rapidity range in which the particles can be detected is an important characteristic of a detector.

CMS (see Ref. [4]) is a detector optimized for the search of the Standard Model Higgs over a mass range from 100 GeV to 1 TeV. The detector has a length of 21.6 m, a diameter of 14.6 m and a total weight of 14500 tons. It will be able to identify and measure isolated muons, photons and electrons with high precision. The expected energy resolution for the above particles will be less than 1% at 100 GeV. The proposed CMS detector has a large superconductive solenoid with a radius of about 2.9 m, generating an uniform magnetic field of 4 T. The choice of a

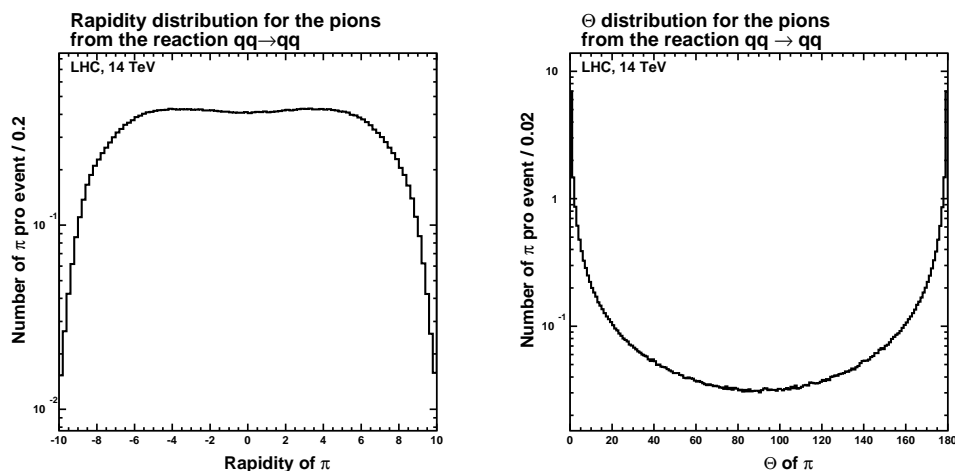


Figure 1.1: (Left) Rapidity distribution of the pions pro event of the QCD process $qq \rightarrow qq$ (all p_t and all rapidities allowed) (Right) Θ distribution of the pions for the same process.

strong magnetic field leads to a compact design for the muon spectrometer without compromising the momentum resolution up to pseudorapidities of 2.5.

Right around the beam pipe a tracking system will allow the detection of charged particles. Then comes the electronic calorimeter (ECAL) which will detect photons and electrons. Around it, lies the hadronic calorimeter (HCAL) which measures the energy of hadronically interacting particles (π^\pm , K^\pm , K_L^0 , p , \bar{p} , n , \bar{n}). Finally the detector is surrounded by muons chambers which will detect the muons. The expected transversal impulse resolution is given, for high p_t particles by $\Delta p/p \approx 0.1 p_t$ (p_t in TeV) in the range $|\eta| < 2.5$. As the electromagnetic calorimeter is essentially designed to detect the Higgs in the two photons channel, it has a small expected energy resolution ($\Delta E/E \approx 2\%/\sqrt{E}$). For the hadronic calorimeter, a resolution of $\Delta E/E \approx 65\%/\sqrt{E}$ is expected. Muons should be detected up to $|\eta| = 2.4$ and for $p_t > 4$ GeV. Forward calorimeter will measure the energy of hadrons up to a rapidity of $|\eta| \approx 5$.

1.3 The PYTHIA event generator

PYTHIA is the standard event generator used by the LHC collaborations to study the physics performance of their detectors. Like the ancient Greeks who used to consult the Pythia to know their destiny, modern physicists use PYTHIA to get a feeling for the kind of events one may expect/hope to find, and at which rates. An event generator simulates data, with more or less the same average behavior and fluctuations as the real data. In PYTHIA, data are simulated through Monte Carlo

techniques.

PYTHIA gives the list of all particles together with their physical and kinematical properties involved in a given process. The detector responses are still needed. For the study described in the following, a 'fast detector simulation' of CMS was made, where different requirements were asked for a particle to be detected:

- Only stable particles can be detected, i.e. π^\pm , K^\pm , K_L^0 , p , \bar{p} , n , \bar{n} for the hadrons, e^\pm , μ^\pm for the leptons and photons.
- The detected particles have to have $p_t > 0.5 \text{ GeV}$ and $|\eta| < 4.5$.
- Isolated electrons, photons and muons can be detected up to rapidity of $|\eta| < 2.5$.
- Jets can be detected up to a rapidity of $|\eta| < 4.5$.

Other important detector characteristics like the energy and momentum resolutions were not simulated. However for electrons, photons and muons the resolution effects are small for the region of interest (about 1%) and should not have a large effect on the obtained results.

Jet mass reconstruction is more difficult, as it involves the combination of several detector elements over large rapidity ranges for many particles. To take this effect into account, larger selected W and Z mass ranges ($\pm 20 \text{ GeV}$) were taken than the simulated ones ($\pm 10 \text{ GeV}$).

This fast simulation of the CMS detector should be sufficient to get a first idea of the detector capacity and to estimate the possible experimental accuracy that can be reached at CMS.

Chapter 2

Basic Higgs properties

Twelve years of direct Higgs searches at LEP show that the Higgs mass should be higher than 113 GeV¹. Many detailed Higgs studies for the LHC (for example [5] and [6]) give confidence that the Higgs boson with Standard Model - like couplings can be discovered at the LHC.

The experimental observation of one or several Higgs bosons will be fundamental for a better understanding of the mechanism of electroweak symmetry breaking. In the Standard Model, one doublet of scalar fields is assumed, leading to the existence of one neutral scalar particle, the Higgs, with an essentially unconstrained mass. An upper limit of about 1 TeV can be derived from unitarity arguments. Assuming the Standard Model to be valid up to an energy scale Λ , the allowed Higgs range can be calculated. For Λ set at Planck scale, the Higgs should have a mass lying between 140 and 180 GeV. However these bounds become weaker if new physics appears at lower mass scale. If Λ is chosen to be 1 TeV, the Higgs boson mass is constrained to be in the range $50 \text{ GeV} < m_H < 800 \text{ GeV}$.

Assuming the overall validity of the Standard Model, a global fit to all electroweak data leads to $m_H = 76_{-47}^{+85} \text{ GeV}$ and its mass is less than 210 GeV with 95% confidence level. However, in a recent paper [7], Peskin and Wells study a variety of new physics models which might have a heavy Higgs and simultaneously some other new physics. They review how these Models could allow a heavy Higgs boson being consistent with the precision electroweak constraints and come to the conclusion that the electroweak fit constraint the Higgs to small masses, only if no other new physics enters in.

2.1 Higgs production mechanisms

We will review here the different production mechanisms of the Higgs boson within the Standard Model framework.

¹Last year, LEP II reached that limit and observed signs for a Higgs boson of 115 GeV with a 2.9 σ deviation, see [10].

The total production cross section for the Standard Model Higgs at the LHC is dominated by the *gluon fusion process* (see Figures 2.1 and 2.2), which largely proceeds via a top quark loop, directly sensitive to the $t\bar{t}H$ coupling.

The second interesting production process for the heavy Higgs boson is the *weak boson fusion*, where two quarks emit vector bosons which interact to create a Higgs (see Figure 2.1). Its cross section is about 5 to 10 times smaller than the gluon fusion cross section. This process is then sensitive to the Higgs coupling to the weak vector bosons. The ratio of the two cross sections provides the information how the Higgs couples to fermions and bosons. This is then a crucial test whether the heavy Higgs is within the Standard Model or beyond. The possibility to make such a measurement at the LHC will be one of the main purposes of this study.

Another possible Higgs production mechanisms is the *associated Higgs production*: $q_i\bar{q}_j \rightarrow WH$ or $q_i\bar{q}_j \rightarrow ZH$, where an off-shell vector boson is produced and radiates a Higgs. This process has a sizable cross section for a Higgs with low masses (see Figure 2.2). Like for the weak boson fusion process, its cross section depends on the Higgs coupling to vector bosons.

The last production mechanism is the *Higgs Bremsstrahlung*: $gg, q_i\bar{q}_j \rightarrow t\bar{t}H$ where top quarks are produced and radiate a Higgs. Notice that in this case, the cross section depends on the Higgs coupling at fermions, like for the gluon fusion case.

Unfortunately, in the mass region considered for this study, these two last production mechanisms have a cross section about 100 times smaller than the gluon fusion process, leading to essentially undetectable signals.

2.2 Higgs decays

The strategy to find the Higgs changes depending on its mass. Figure 2.3 give the necessary luminosity for a five standard deviations², for different Higgs masses and channels.

For Higgs masses between 110 GeV and 130 GeV, the most significant channel is the decay $H \rightarrow \gamma\gamma$.

If the Higgs mass is lying between 130 GeV and 180 GeV, the expected discovery channel is then the $H \rightarrow WW^{(*)} \rightarrow \ell^+\nu\ell^-\bar{\nu}$ decay as the $H \rightarrow ZZ^* \rightarrow 4\ell^\pm$ has there a very low branching ratio, due to the production of two on-shell W 's.

For $2 \times m_Z \leq m_H \leq 400$ GeV, the decay $H \rightarrow ZZ \rightarrow 4\ell^\pm$ provides the easiest discovery signature as the events should contain four isolated leptons with high transversal momentum, p_t .

For higher Higgs masses, additional signatures involving hadronic W and Z decays as well as invisible Z decays like $H \rightarrow ZZ \rightarrow \ell^+\ell^-\nu\bar{\nu}$ have been investigated and promising signals have been obtained. These channels will also be studied in detail in that report.

²Five standard deviations from the expected background, which corresponds to a probability of $5.9 \cdot 10^{-7}$, is the usual requirement to claim for a discovery.

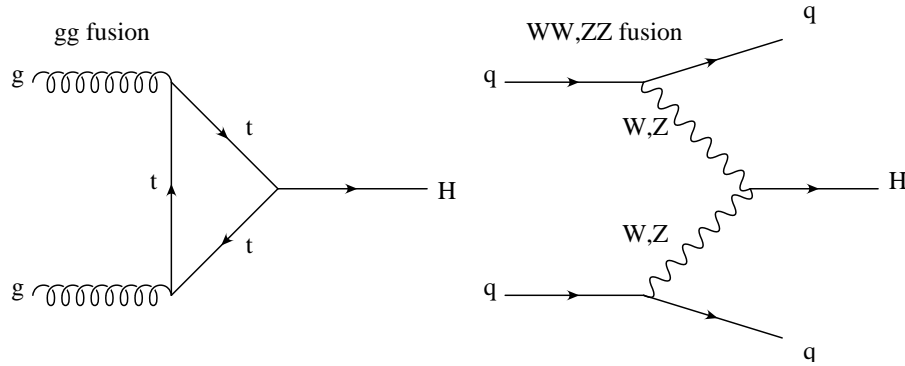


Figure 2.1: Feynman diagrams for two production mechanisms of Higgs. (Left) gluon fusion (Right) weak boson fusion.

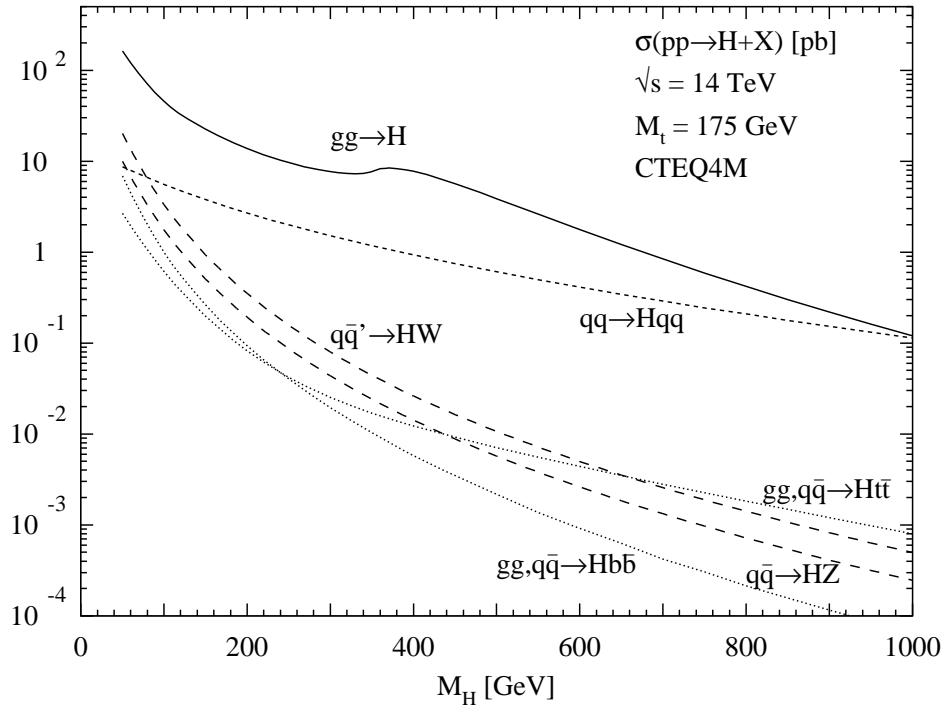


Figure 2.2: Cross sections of different production mechanisms of Higgs as a function of the Higgs mass, given at the next to leading order, Ref. [8].

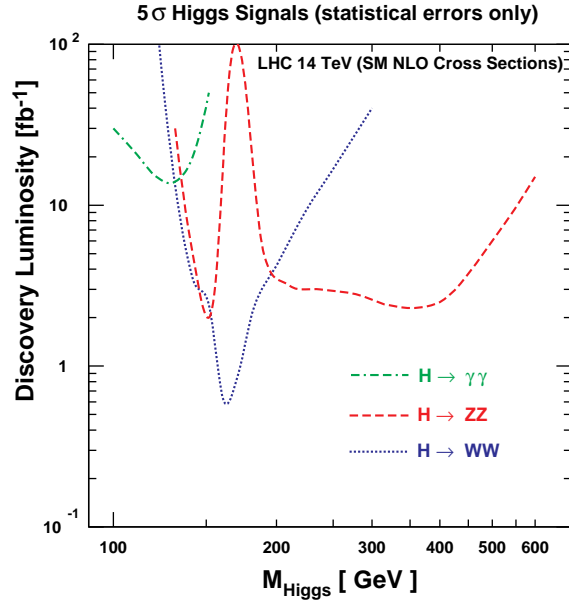


Figure 2.3: Discovery luminosity as a function of the Higgs mass as given in Ref. [9].

For a deeper study of the Higgs discovery channels see [6] and [12].

The obvious next question, if we assume that the Higgs has been found, is then how well the Higgs sector can be tested at the LHC. As it was already said before, the purpose of this work is to treat that question for the case of a heavy Higgs. As we worked with Higgs masses between 300 and 600 GeV, we can see on Figure 2.4 that the $H \rightarrow WW$ and $H \rightarrow ZZ$ decay are, within the Standard Model, by far the dominant branching ratios.

For high Higgs masses, we see on Figure 2.4 that the Higgs can also decay in top quarks, with a branching ratio of about 10 to 20%. However this channel is currently believed to be unmeasurable at the LHC, given the presence of a too important background.

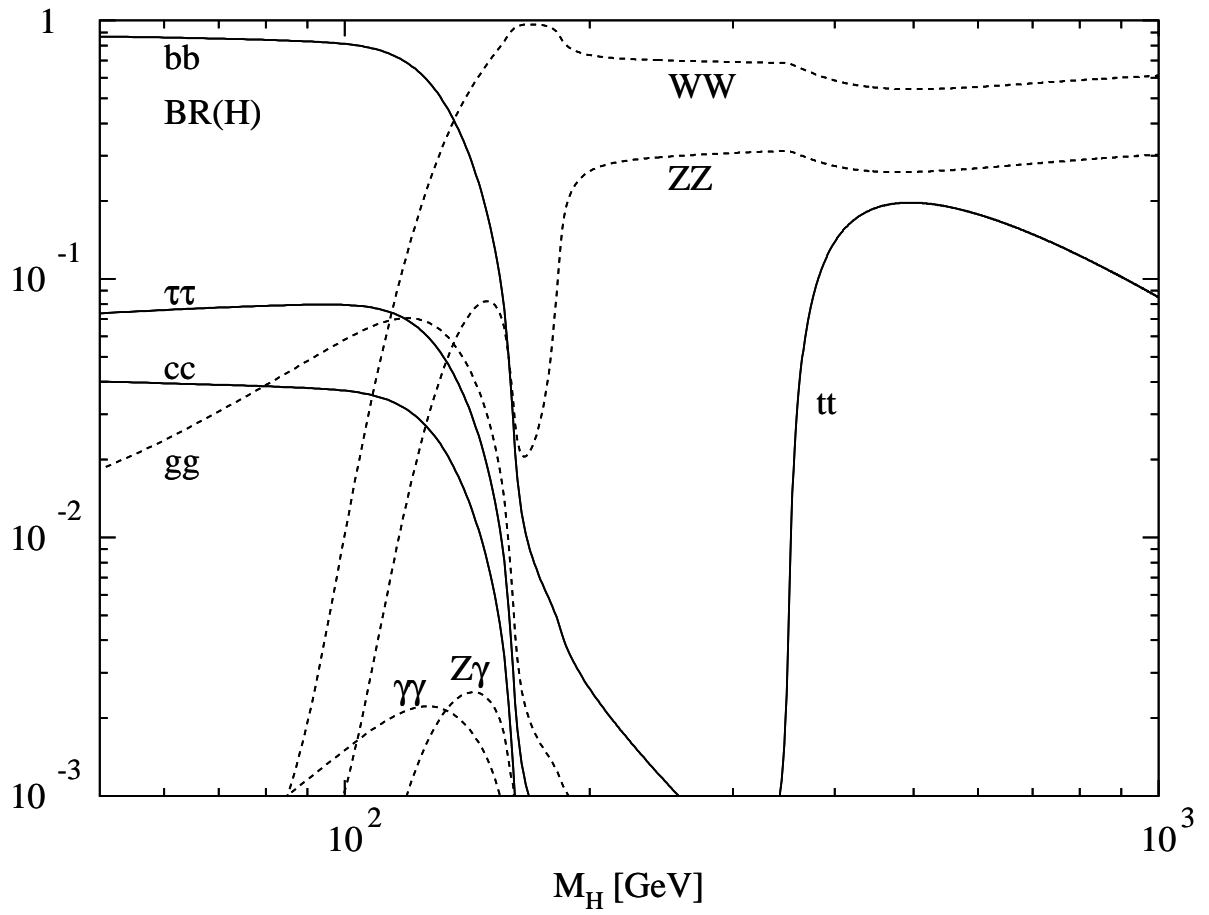


Figure 2.4: Decay branching ratios of the Higgs as a function of its mass, Ref. [11].

Chapter 3

General ideas to get a signal

As discussed in the previous chapter, a SM Higgs with a mass between 300 and 600 GeV is produced mainly through weak boson fusion ($q_i q_j \rightarrow q_i q_j H$) and gluon fusion ($gg \rightarrow H$) and cross sections for other processes are 100 to 1000 times smaller. A heavy Higgs will then mainly decay in vector bosons through the processes $H \rightarrow WW$ and $H \rightarrow ZZ$. The branching ratio for the first decay mode is about two times higher than that for $H \rightarrow ZZ$.

The branching fractions for the decays of the W and Z vector bosons are well known from LEP and agree with the Standard Model expectations. These vector bosons can decay either hadronically ($W \rightarrow q_i q_j$ or $Z \rightarrow q_i \bar{q}_i$, with a branching ratio of about 70%) or leptonically ($W \rightarrow \ell \nu$, $Z \rightarrow \ell^+ \ell^-$ or $Z \rightarrow \nu \nu$ with branching ratios of respectively 30%, 10% and 20%, if the taus are included in the leptons). Hadronic decays have a higher branching ratio but are harder to detect than leptonic decays, characterized by high p_t leptons and/or missing energy coming from neutrinos.

The decay of a heavy Higgs boson can thus lead to very different signatures: only leptons, leptons together with neutrinos and only neutrinos, for the fully leptonic signatures and leptons together with jets, neutrinos together with jets and only jets for the hadronic signatures. These signatures will have to be studied separately.

In the first part of this chapter, the different Higgs signatures are described. This is followed by some words about how vector bosons can be detected and combined to reconstruct the Higgs. Then, independently of the channel, we will analyze how one can use the kinematical properties of an Higgs event to improve the efficiency of the selection cuts. Finally, we will explain the method used to distinguish the Higgs production process through weak boson fusion.

3.1 Signatures of a heavy Higgs

Starting from the assumption that the Higgs decays into either two W or two Z bosons, the different Higgs signatures are all the combinations of the possible W and Z decay modes. However, some channels can be immediately discarded as

they do not give measurable signatures, like for instance $H \rightarrow ZZ \rightarrow \nu_i \bar{\nu}_i \nu_j \bar{\nu}_j$ were nothing about the Higgs can be reconstructed or $H \rightarrow WW, ZZ \rightarrow q_i q_j q_k q_l$ which is overwhelmed by backgrounds. The signatures which can possibly be seen in the CMS detector are summed up in Table 3.1. Note that in this Table, ℓ refers to electrons and muons, as the taus events are always removed by the selection cuts¹.

Note that the channel $H \rightarrow ZZ \rightarrow \nu_i \bar{\nu}_i q_i \bar{q}_i$ stays at the border of the observable channels.

Channel	$\sigma \times BR$ (normalized)	Main backgrounds studied for this channel
$H \rightarrow ZZ \rightarrow \ell^+ \ell^- \ell^+ \ell^-$	1	$q_i \bar{q}_i \rightarrow ZZ$
$H \rightarrow ZZ \rightarrow \ell^+ \ell^- \nu_i \bar{\nu}_i$	6	$q_i \bar{q}_i \rightarrow ZZ, q_i \bar{q}_j \rightarrow WZ$ $q_i \bar{q}_i \rightarrow gZ, q_i g \rightarrow q_i Z$ $q_i \bar{q}_i \rightarrow t\bar{t} \rightarrow WbWb$
$H \rightarrow WW \rightarrow \ell \nu \ell \nu$	27	$q_i \bar{q}_i \rightarrow WW$ $q_i \bar{q}_i \rightarrow gZ, q_i g \rightarrow q_i Z$ $q_i \bar{q}_i \rightarrow Z$ $q_i \bar{q}_i \rightarrow t\bar{t} \rightarrow WbWb$
$H \rightarrow WW \rightarrow \ell \nu q_i q_j$	135	$q_i \bar{q}_i \rightarrow WW$ $q_i \bar{q}_j \rightarrow gW^+, q_i g \rightarrow q_k W^+$ $q_i \bar{q}_i \rightarrow t\bar{t} \rightarrow WbWb$
$H \rightarrow ZZ \rightarrow \ell^+ \ell^- q_i \bar{q}_i$	21	$q_i \bar{q}_i \rightarrow ZZ$ $q_i \bar{q}_i \rightarrow gZ, q_i g \rightarrow q_i Z$ $q_i \bar{q}_i \rightarrow t\bar{t} \rightarrow WbWb$
$H \rightarrow ZZ \rightarrow \nu_i \bar{\nu}_i q_j \bar{q}_j$	64	$q_i \bar{q}_i \rightarrow ZZ$ $q_i \bar{q}_i \rightarrow gZ, q_i g \rightarrow q_i Z$ $q_i \bar{q}_i \rightarrow t\bar{t} \rightarrow WbWb$ QCD events

Table 3.1: Heavy Higgs decay channels together with their potential sources of background. Only the channels which could give a detectable signature are given here. ℓ refers to electrons and muons.

The following criteria have to be considered in order to judge the feasibility of detecting a Higgs signal for a given decay channel:

- In which way is it possible to reconstruct the Higgs mass peak and what is the obtained mass resolution? This is especially important for a discovery where the exact Higgs mass is not known.
- Is the cross section of the channel big enough to get a signal?

¹ Studies like [13] were done about the possibility to include taus in the leptonic signatures and showed that the significance could be raised. However, such treatment will not be considered in this study.

- Has the channel a lot of backgrounds, is it easy to get rid of them ?

Given these criteria, we can compare the different channels. For instance, the four leptons channel has an advantage as the Higgs mass peak can be nicely reconstructed, but its branching fractions are small. On the contrary, all channels involving hadronic decays have higher branching fractions, but also have backgrounds with huge cross sections that have to be suppressed with tighter cuts. For instance, in the $H \rightarrow ZZ \rightarrow \ell^+ \ell^- q_i \bar{q}_i$ channel, the Higgs mass peak can be reconstructed and its branching fraction is twenty times higher than the one for four leptons channel, but too many sources of background prevent it to be a really significant Higgs discovery channel.

Background is clearly a crucial issue in this study. Table 3.1 gives of list of these different backgrounds for the channels we studied.

The sources of background can be divided in three categories with different physical properties:

- The *continuum backgrounds*: $q_i \bar{q}_i \rightarrow ZZ$, $q_i \bar{q}_i \rightarrow WW$ and $q_i \bar{q}_j \rightarrow WZ$.
- The *single boson production with multi jets*: $q_i \bar{q}_j \rightarrow gW^+$, $q_i g \rightarrow q_k W^+$, $q_i \bar{q}_i \rightarrow gZ$ and $q_i g \rightarrow q_i Z$.
- The *Top-antitop production*: $q_i \bar{q}_i \rightarrow t\bar{t} \rightarrow WbWb$.

Different cuts will have to be found to reduce these three types of backgrounds.

3.2 Reconstruction of the event

The signal is reconstructed in two steps:

First we try to find the two Z 's or the two W 's present in the event. This first step would be for example useful against *Single boson production backgrounds* but not against *Continuum backgrounds* in which anyway two vector bosons are produced. The Higgs is then reconstructed in combining the two W 's or the two Z 's. If possible, a cut on the mass of the reconstructed Higgs was done.

Subsequently the kinematics of the Higgs event is exploited and cuts on the p_t 's of the reconstructed vector bosons and/or the Higgs are added.

Detecting the Z 's in the event

The Z has the following decay modes (note that in the following, ℓ stands for electrons, muons and taus):

- $Z \rightarrow \ell^+ \ell^-$ with a branching ration of 3×0.033
- $Z \rightarrow jet\ jet$ with a branching ration of 0.70
- $Z \rightarrow \nu \bar{\nu}$ with a branching ration of 0.20

When it decays into leptons, the Z can simply be identified by asking two isolated leptons² in event which form an invariant mass within an interval of 10 or 20 GeV (depending on the resolution we had in the simulation, see for instance Figure 3.1, left) centered in the Z mass (91 GeV).

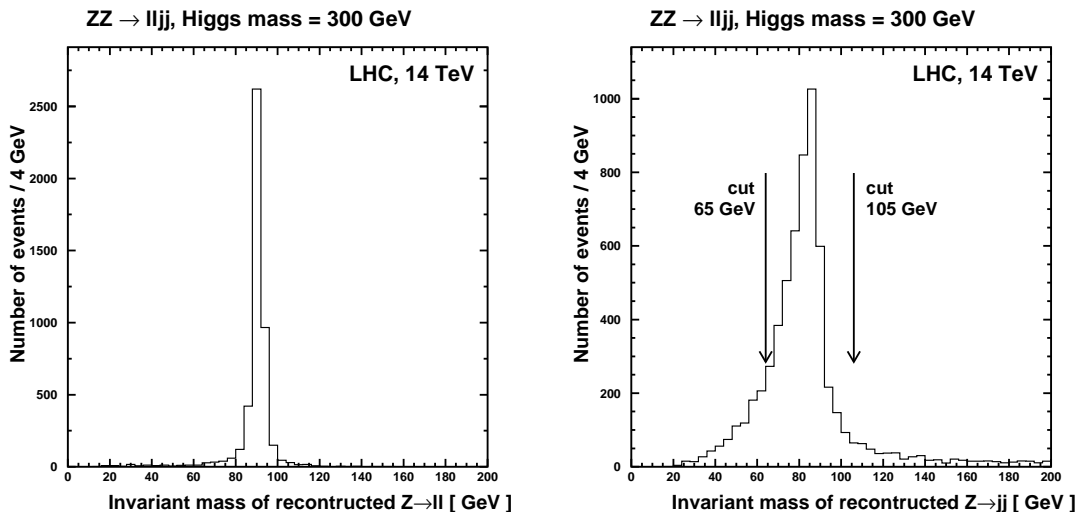


Figure 3.1: Reconstructed Z 's in the channel $gg \rightarrow H \rightarrow ZZ \rightarrow \ell\ell jj$ for a 300 GeV Higgs after minimal cuts (e.g. asking two isolated leptons and more than two jets). (Left) $Z \rightarrow \ell\ell$ (Right) $Z \rightarrow jj$.

When the Z decays in hadrons generating jets³, we have basically two problems: The invariant mass resolution is not as good as for leptons, as it can be seen on Figure 3.1 and the Z mass peak is shifted from 91 GeV to 85 GeV. As we cannot detect particles with an energy smaller than 500 MeV, this means that there will be missing particles in the jet and this latter will have a smaller reconstructed invariant mass. The jet jet invariant mass is asked to be within an interval of 40 GeV centered in 85 GeV. As it can be seen on Figure 3.1, this mass window could be chosen to be smaller. However the measured jet resolution is expected to be lower than the one given by the Monte Carlo. In order to be closer to the real experiment, a wider

² For this study an *isolated lepton* or more generally an *isolated particle* is a particle with a rapidity smaller than 2.5, a transverse momentum higher than 10 GeV and whose energy represents 90% of the energy within a cone of $\Delta R = \sqrt{\Delta\eta^2 + \Delta\phi^2} = 0.5$ around it. Even more, the total mass of all particles present in this cone, should be smaller than 2 GeV and only one other particle with a p_t higher than 0.1 GeV can be next to the 'isolated' particle.

³The jets are reconstructed in the following way: We take a stable particle with a transversal momentum larger than 5 GeV. Then we take all stable particles with a transversal momentum higher than 500 MeV (this is the smallest energy we assume to detect) in a cone of $\Delta R = 0.5$ around the first particle, and add up all these particles. This gives us the jet. Moreover the jet has to have a transversal momentum higher than 20 GeV and a rapidity smaller than 4.5.

mass range was chosen here.

When more than two jets are reconstructed in one event, all the possible jet mass combinations were done and only the ones whose mass was in an interval of 40 GeV centered in the shifted Z mass, 85 GeV, were kept. From the remaining combinations, the hypothetical Z with the highest p_t was selected as the 'true' Z , as this particle is supposed to have a large p_t .

The reconstruction of Z decaying into neutrinos is more problematic as its decay products cannot be detected. An event with large missing transverse momentum is then required (the value we chose for it depended on the channel studied, as well as on the Higgs mass generated). The $Z \rightarrow \nu\bar{\nu}$ four vector is reconstructed in the following way:

$$(p_x^{Z\nu\nu} ; p_y^{Z\nu\nu} ; p_z^{Z\nu\nu} ; E^{Z\nu\nu}) = \left(- \sum_{lep,jets} p_x^i ; - \sum_{lep,jets} p_y^i ; 0. ; \sqrt{(p_t^{Z\nu\nu})^2 + m_Z^2} \right)$$

The p_x and p_y coordinates of the Z are the opposed ones of the vector obtained by adding up the four vectors of all the jets and leptons present in the event. The p_z is set to zero and the energy is calculated by assuming a Z mass of 91 GeV.

Sources of background come as well from events which contain neutrino, as from events where the jets or the leptons were not accurately measured, leading to an artificial missing energy in the detector.

Detecting the W 's in the event

The W has the following decay modes :

- $W \rightarrow jet\ jet$ with a branching ration of 0.69
- $W \rightarrow l\nu$ with a branching ration of 3×0.11

When the W decays in jets, the same criteria were used to reconstruct it than the ones for the Z with the invariant mass of the jets to be within an interval of 40 GeV centered in 73 GeV, which is where the shifted W mass peak is sitting.

In the channel $WW \rightarrow l\nu jj$, when one W decays to a lepton and a neutrino, the neutrino four vector is reconstructed exactly in the same way than for the $Z \rightarrow \nu\bar{\nu}$. But in that case, we can besides try to determine its p_z component: Assuming that the reconstructed W 's mass is 83 GeV and that the neutrino mass is zero and after some algebra, we have two solutions for the neutrino's p_z :

$$\alpha \stackrel{\text{def}}{=} \frac{m_W^2}{2} + p_x^{lept} p_x^\nu + p_y^{lept} p_y^\nu$$

$$p_z^\nu = \frac{\alpha \cdot p_z^{lept} \pm \sqrt{\alpha^2 (p_z^{lept})^2 - [(E^{lept})^2 - (p_z^{lept})^2][(E^{lept})^2 (p_t^\nu)^2 - \alpha^2]}}{(E^{lept})^2 - (p_z^{lept})^2}$$

The question is now, which p_z to chose. As we expect the event to be central, the smallest absolute value for the p_z^{neut} was chosen. But this criterion is not very good

since we only get the right solution in 50% of the cases ! Unfortunately no smarter criterion was found. However we showed that this did not really affect the final mass peak.

When the Higgs decays in leptons and neutrinos only, as in the channel $WW \rightarrow \ell\nu\ell\nu$, we cannot reconstruct a W mass peak. We then had to find special kinematic properties of that channel to get a signal.

Knowing that the vector bosons come from the Higgs

Now that we 'know' that there are two vector bosons in the event, we can reconstruct the Higgs out of them and try to use the expected physical properties of a Higgs event to enhance a signal.

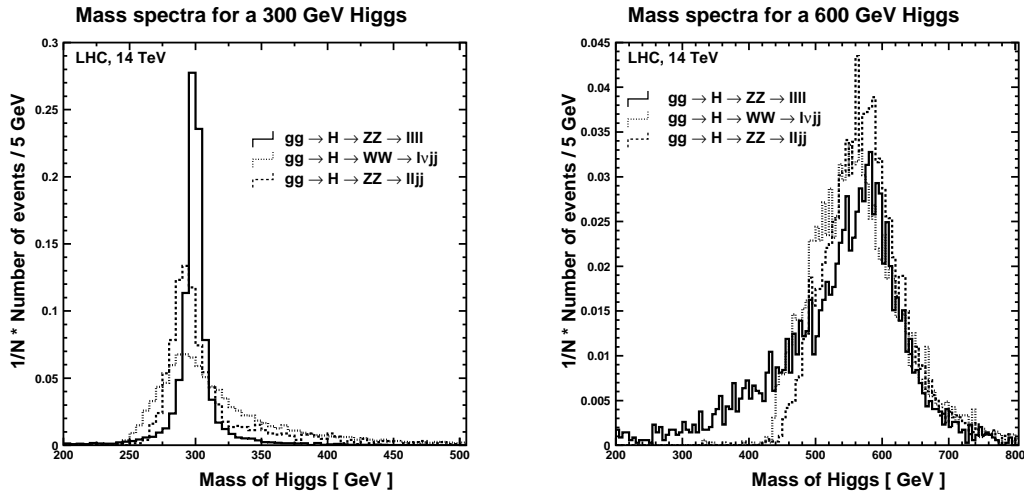


Figure 3.2: Comparison between the mass resolution the reconstructed Higgs mass spectrum for different signatures. The plots are made after the reconstruction cuts. The Higgs is produced through the gluon fusion. (Left) for a 300 GeV Higgs (Right) for a 600 GeV Higgs.

Figure 3.2 shows the invariant mass of the two vector bosons for the signal in different channels. All the plots were normalized so that the integral of the curves gives 1. As expected, the best mass resolution is obtained with the four leptons channels for a 300 GeV Higgs. Broader peaks are seen for the other channels. The $H \rightarrow WW \rightarrow \ell\nu jj$ channel gives a large tail for the higher mass region in the case of a 300 GeV Higgs, due to the presence of the neutrino which cannot be well reconstructed. As already pointed out, the jets are not as well reconstructed as in that simulation and the expected measured mass peak should be wider.

The natural width of the Higgs increases with its mass. Then, the different channels give more or less the same resolution. The natural width of the Higgs

here dominates the uncertainty in the reconstruction. For the high Higgs masses, the four leptons channel has a longer tail in the low mass region compared to the other channels. This is due to the large value of the p_t 's cuts applied in these other channels, whose effects are to cut the low mass region in the reconstructed Higgs mass spectrum.

The reconstruction of the Higgs mass peak is the best way to discover this particle. However, other criteria can improve the signal significance. Furthermore, when the backgrounds are too important, new cuts have to be found.

One possibility is to cut on the p_t of the vector bosons and/or of the Higgs. More specifically, in the weak boson fusion processes, the Higgs is always produced together with jets, which allows it to have a large p_t . As we can see on Figure 3.3, events produced through weak boson fusion have a higher mean transverse momentum than events produced through gluon fusion. As it usually does not contain jets, the ZZ continuum background leads to small mean values for the p_t of the generated ZZ system.

Notice that the mean p_t for that background is even smaller than the mean p_t for gluon fusion, as gluons can radiate jets with higher probability than quarks. A cut on the reconstructed Higgs p_t will be very efficient against the continuum backgrounds. For instance in the channel $ZZ \rightarrow \ell\ell\ell\ell$, where the only background is $qq \rightarrow ZZ$, a cut on the Higgs transverse momentum was found to improve the signal significance considerably.

However, we found more significant to cut on the p_t of the reconstructed W or Z , as soon as backgrounds like W , Z production and $t\bar{t}$ were important. Figure 3.4 shows the different p_t distributions for the signal and these backgrounds for a 600 GeV Higgs in the channel $H \rightarrow \ell\ell jj$.

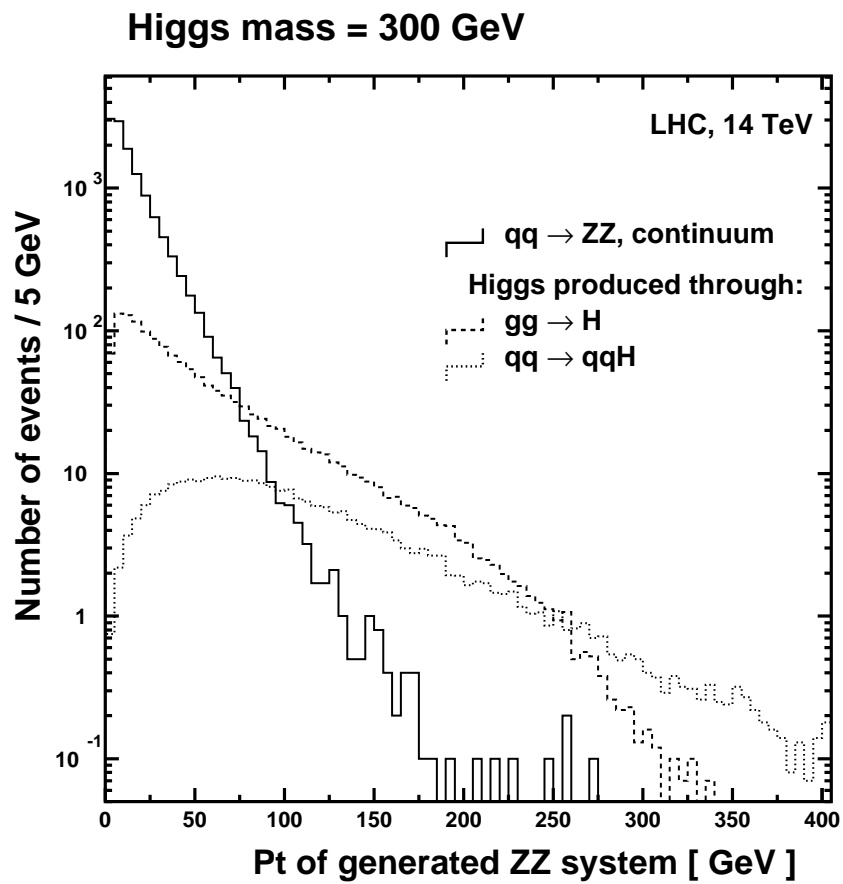


Figure 3.3: Generated transverse momentum for a 300 GeV Higgs for the two signal processes (with K-factors) and for the ZZ continuum.

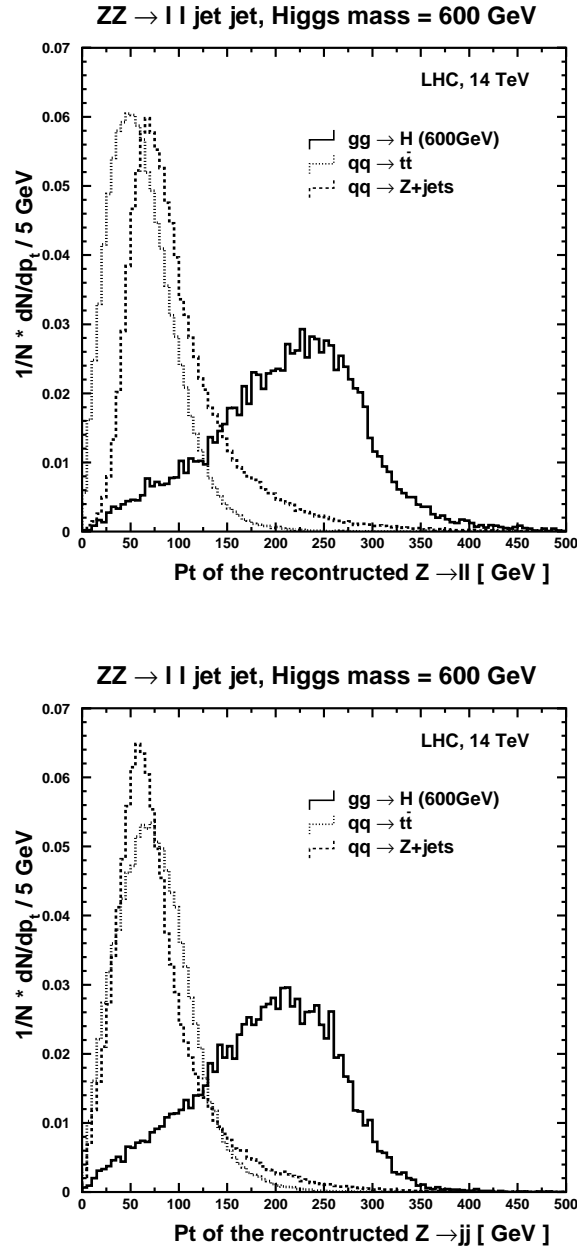


Figure 3.4: p_t spectra of the reconstructed Z for a 600 GeV Higgs and for different backgrounds in the $H \rightarrow ZZ \rightarrow \ell\ell jj$ channel, before the selection cuts and normalized to the total number of events. (Up) p_t spectrum for the reconstructed Z decaying leptonically (Down) p_t spectrum for the reconstructed Z decaying hadronically.

3.3 Reconstruction of the $qq \rightarrow qqH$ signal

Up to now, to isolate a signal, only the Higgs decay characteristics were used in the selection cuts. It is also interesting to consider the way the Higgs was produced, especially when it is produced through weak boson fusion. This production process leads to a very specific signature, which can be used to get a signal in some particular Higgs search channels, which contains jets and where the reconstruction of the event only through the Higgs decay products is not sufficient, and also to isolate that process from the other Higgs production processes (in our case, gluon fusion).

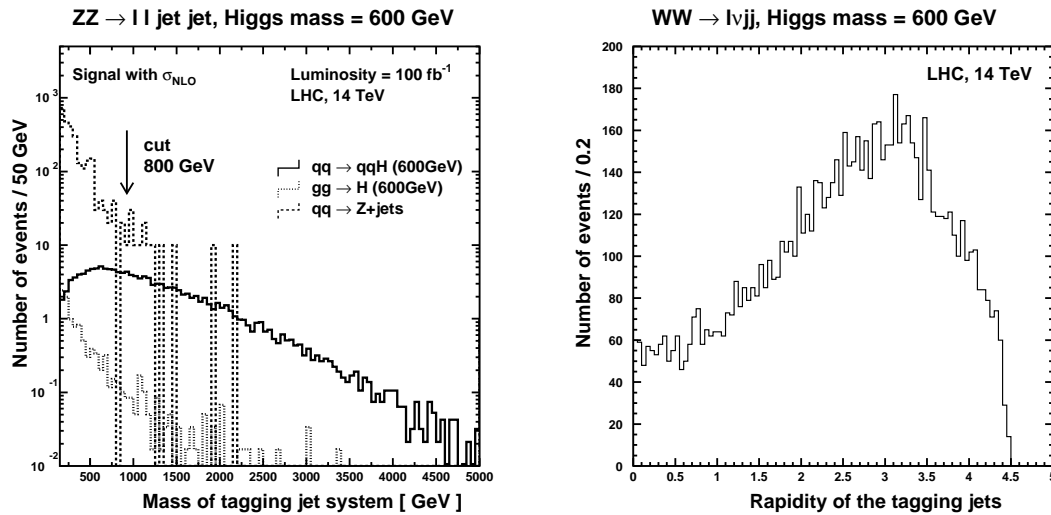


Figure 3.5: Characteristics of the tagging jets system: (Left) Mass of the tagging jet system for different processes in the channel $qq \rightarrow qqH \rightarrow ZZ \rightarrow \ell\ell jj$ (Right) Rapidity of the tagging jets for the channel $qq \rightarrow qqH \rightarrow WW \rightarrow \ell\nu jj$.

One of the characteristics of the $qq \rightarrow qqH$ signal is that the Higgs tends to be produced centrally and yields central decay products. In contrary, the two quarks which emitted the vector bosons enter the detector at large rapidities and have a transverse momentum in the 20 to 100 GeV range, thus leading to two observable forward tagging jets. To isolate such type of events, we can cut on the invariant mass of the two jets, asking it to be higher than 800 GeV. This cut will be called in the following, the *jet tagging technique*. It is very efficient since the distribution of the invariant mass of the two jets is drastically different for $qq \rightarrow qqH$ than for all the other backgrounds, as it is rare for the backgrounds to have two jets emitted with such a high mass. The tagging jets mass spectrum, as well as their p_t distribution is shown on Figure 3.5 for a 600 GeV Higgs.

Suppressing the top-antitop production background

As soon as we are dealing with jets and W 's, a main source of background comes from the top-antitop production : $qq \rightarrow t\bar{t} \rightarrow WbWb$. The top quark decays into a W and a b quark with a branching ratio of almost 100%. This background will thus be characterized by two W 's and two jets. It is an important background source for the channels $qq \rightarrow qqH \rightarrow WW$ and $WW \rightarrow \ell\nu\ell\nu$ or $WW \rightarrow \ell\nu jj$.

However, since the W and the jet are decay products of a top quark, their invariant mass has to give the top quark mass, that is 175 GeV. A good way to eliminate top-antitop production is to cut on the mass of top decay products, which are here a W and a jet. As we have two reconstructed W 's in event and two supplementary jets, we have several possibilities to reconstruct the top. Out of the masses we get from the different W -jet combinations, the mass closest to the top mass was chosen, which was called m_{Wjet} . In order to remove as much $t\bar{t}$ events as possible, we demand m_{Wjet} much more larger than the top mass. For the signal events, always high m_{Wjet} are found as the tagging jets are emitted with a high rapidity.

An example of the efficiency of this cut in the $H \rightarrow WW \rightarrow \ell\nu jj$ channel is given in Figure 3.6. Note that the curves were normalized to 1. On this Figure, notice also that the single W production background is reduced by a factor 3. Actually this last background was generated with a cut on the mass of the total system (as we will explain later), namely asking it to be higher than 300 GeV. This requirement cuts the low masses of the m_{Wjet} mass spectrum. The cut on m_{Wjet} is even more efficient against single W production if this background is simulated without kinematical cuts.

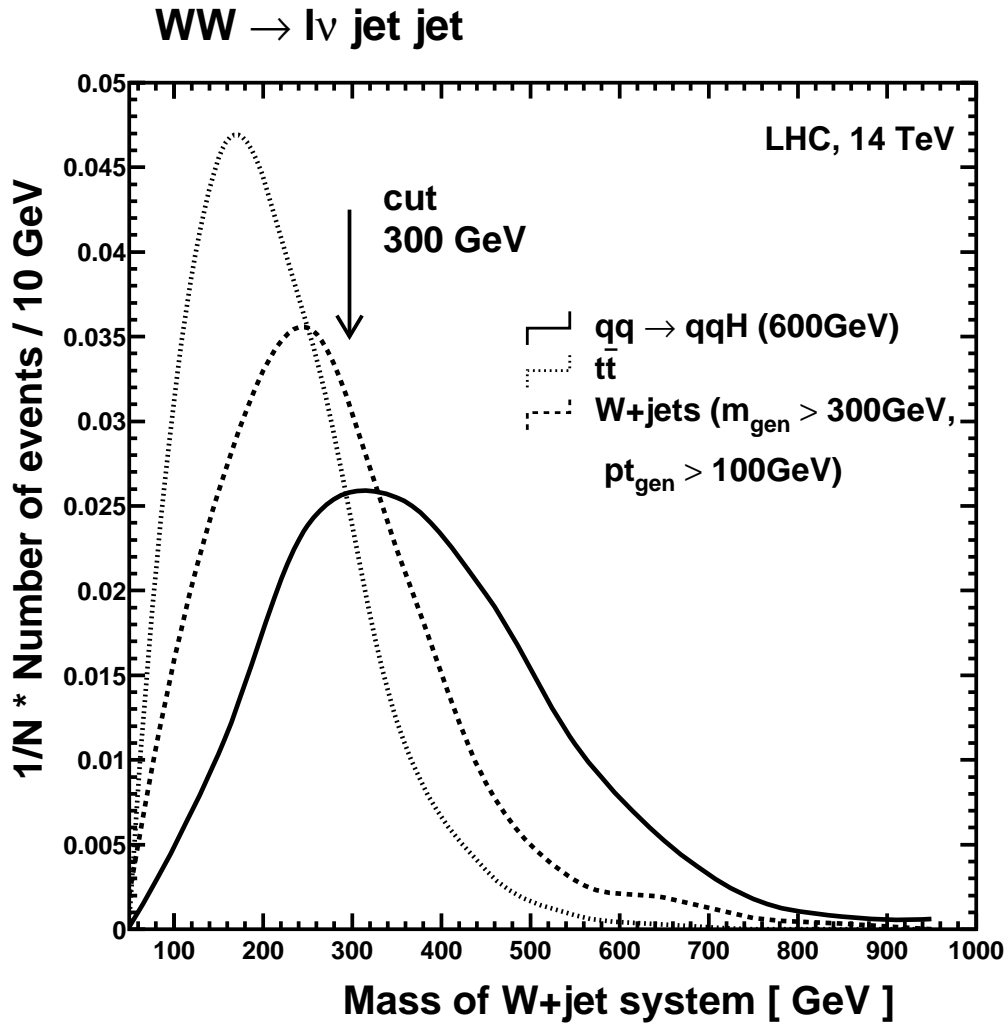


Figure 3.6: Distribution of the $m_{W\text{jet}}$ candidates for the signal, the top-antitop and W + jets backgrounds. The curves are normalized to 1.

Chapter 4

Analysis

The cuts used to isolate a given signature are always applied in two steps: First we try to get a signal without taking into account the way the Higgs was produced. Subsequently, we concentrate on signal events where the Higgs was produced through weak boson fusion and combine the usual selection cuts with a cut using the presence of the forward emitted jets in that process, like it was described on page 28.

In the text, these two ways of getting a Higgs signal are differentiated by saying 'with' and 'without tagging'.

This chapter begins with a few words about how the signal and the different backgrounds were simulated. In the next sections, the results for the different channels studied are presented separately.

4.1 Simulating the different processes

Running PYTHIA

Version 6.1 [15] of PYTHIA set at a center of mass energy of 14 TeV was used for this study.

GRV (LO) [16] was used for the proton structure function and the top quark mass was set to 175 GeV.

Before starting the event selection, we always ask no events with high p_t isolated photons or hadrons.

Determination of the cross sections of the processes

At the end of every simulation, PYTHIA gives an estimate of the cross section of the process which was simulated. However, all PYTHIA cross sections and branching ratio estimates are based on leading order (LO) calculations. Often these leading order cross sections differ significantly from the next to leading order (NLO) QCD calculations. The ratio of $\sigma(NLO)/\sigma(LO)$ defines the so-called K-factor.

For a Higgs produced in the gluon fusion process, it has been shown [17] that the next to leading order corrections consist mainly in soft gluon radiation. That means that the expected event kinematics with NLO estimates should not differ too much from LO distributions. A simple scaling with the K-factor should thus be a good approximation of the NLO corrections. Ref [18] gives the values for the K-factors for different production mechanisms and Higgs masses. We see that for gluon fusion processes, these K-factors are rather important (about 1.6) in contrast to weak boson fusion where K-factors of about one have been calculated. To simulate correctly the different signal processes, we took the cross section given by PYTHIA and multiplied it by the corresponding K-factor. Table 4.1 gives the K-factor for the two Higgs production processes and for different Higgs masses.

	weak boson fusion $qq \rightarrow qqH$	gluon fusion $gg \rightarrow H$
Mass of Higgs	K-factor	K-factor
300 GeV	0.88	1.48
450 GeV	0.94	1.66
600 GeV	1.06	1.69

Table 4.1: K-factors for the two Higgs production mechanisms and for different Higgs masses, as given in [18].

Not all backgrounds have been calculated in NLO, as some of the calculations are quite complex and until today, no consistent simulations for all backgrounds are available. This could lead to some analysis modifications in the future, as some kinematics of the background events could be changed if NLO corrections are added. For example, as we will show later, in the four leptons channel, a cut on the p_t of the reconstructed Higgs is proposed. Such a selection in a LO Monte Carlo has been found to improve the experimental sensitivity by a relatively large factor. However, as has been pointed out (Ref. [18] and [19]), the NLO backgrounds have higher statistic for the large p_t 's of the reconstructed ZZ system than the corresponding LO results. Thus, a hard cut on the p_t of the reconstructed ZZ system would not be as efficient as expected (if for example $p_t > 100$ GeV is asked). However, the efficiency of a soft p_t cut (for example $p_t > 30$ GeV), as we proposed in sections 4.2, 4.3 and 4.6, should not be too much influenced by the introduction of NLO corrections in the future (see Figure 4.1).

Note that as the signal significance is proportional to $1/\sqrt{B}$, the addition of a K-factor higher than one in the background will reduce the significance by a factor $\sqrt{K_B}$, whereas for the signal, the introduction of a K-factor higher than one increases the significance by a factor K_S .

For that study, no K-factors were taken for the backgrounds. However this is something which will need to be studied in more details in the following years.

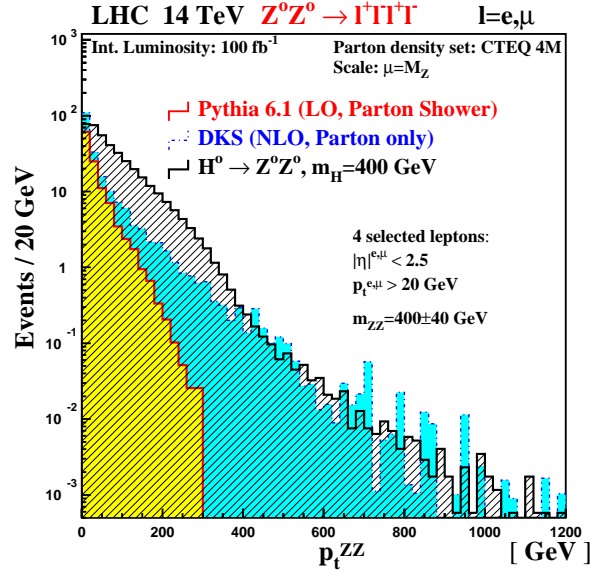


Figure 4.1: Transverse momentum of the ZZ system in the four leptons channel for signal and background (LO and NLO) [19].

Simulating the Higgs with PYTHIA

The Higgs signals were generated using the PYTHIA processes 123 and 124 for the weak boson fusion, $qq \rightarrow qqH$, and 102 for the gluon fusion, $gg \rightarrow H$.

In contrast to previous studies, like for instance [6], in all the simulations a new parameterization for the Higgs width (described in [20]) was used. Figure 4.2 gives a comparison of the Higgs mass spectra obtained with the old and the new parameterizations for different Higgs masses and the two Higgs production processes.

The use of the new parameterization increases up to 10% the signal cross section. The plots are thus made for a number of events corresponding to a luminosity of $100fb^{-1}$ and NLO cross sections. There is no real difference between the two parameterizations for a 300 GeV Higgs. A noticeable difference between the two parameterizations appears for a 600 GeV Higgs produced through gluon fusion. Actually this new parameterization tends to give larger tails to the Higgs lineshape. Moreover the simulated mass spectrum is the convolution between the parton distribution function and the natural Higgs width. As the gluons have a smaller mean momentum than the valence quarks, the tail in the Higgs mass distribution will be more significant for lower Higgs masses as soon as gluons are involved. The plot for a 600 GeV Higgs produced through gluon fusion clearly shows that: More events with a mass around 400 GeV are expected with the new parameterization compared to what older simulations give.

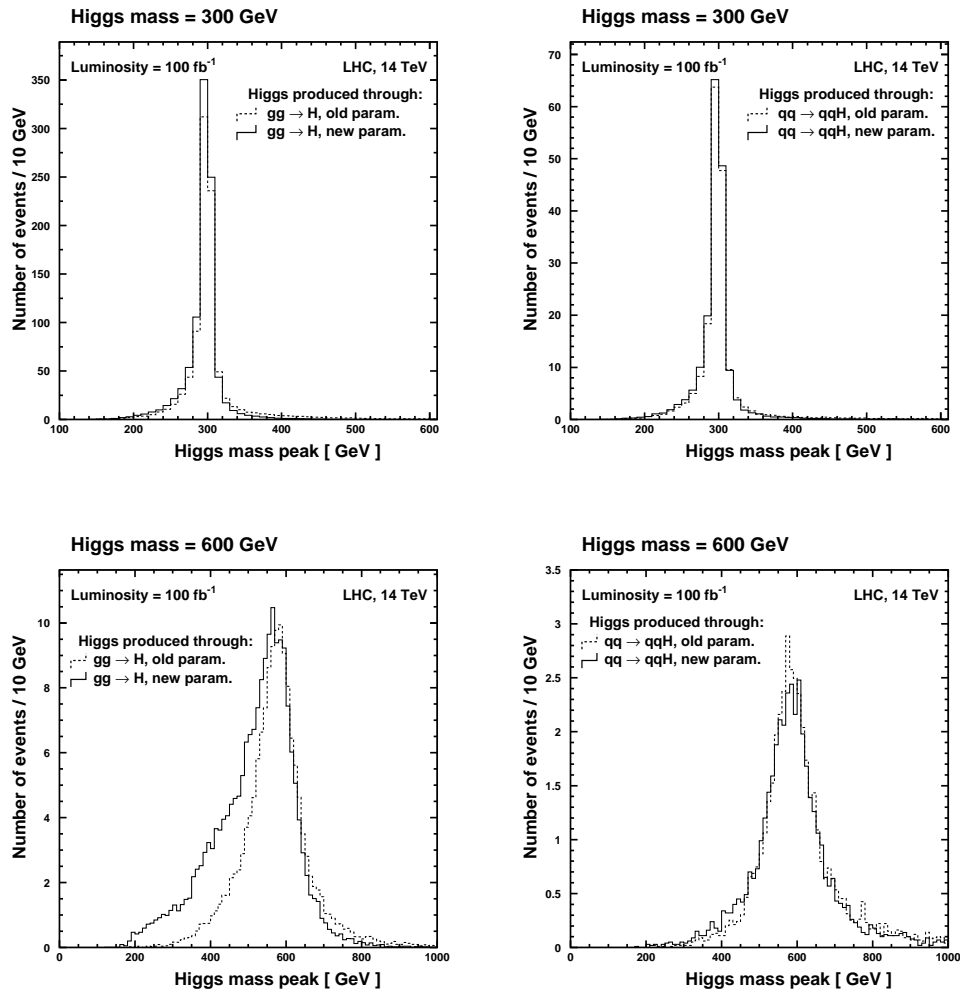


Figure 4.2: Difference between the generated Higgs mass peak obtained with the old and the new parameterization. Upper plots correspond to a 300 GeV Higgs and lower plots to a 600 GeV Higgs. The Higgs events on the left plots were produced through gluon fusion and on the right plots through weak boson fusion. The plots are made on the generator level, without any selection cuts and NLO cross sections are used.

What we conclude from this is that this effect should be taken into account for high Higgs masses and when gluons are involved in the production mechanism.

Simulating the continuum vector boson production with PYTHIA

The continuum boson production was generated using the PYTHIA processes 22 for $qq \rightarrow ZZ$, 23 for $qq \rightarrow WZ$ and 25 for $qq \rightarrow WW$.

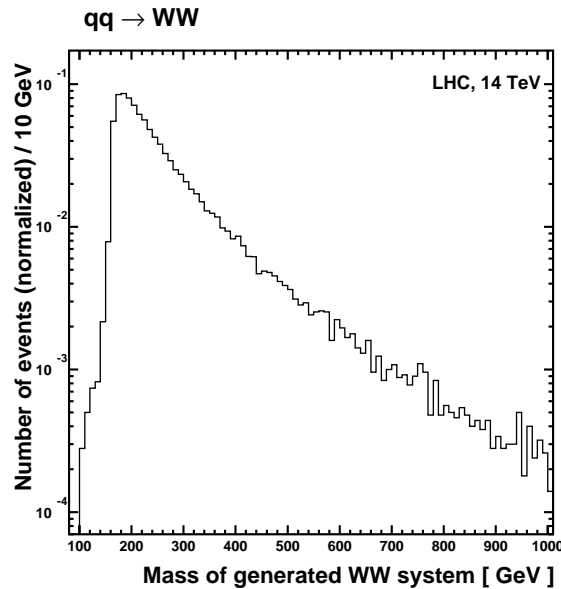


Figure 4.3: Mass spectrum of the generated WW system, produced through $qq \rightarrow WW$.

It is interesting to consider the shape of the generated ZZ , WW or WZ mass spectrum. Figure 4.3 shows the mass spectrum of the generated $qq \rightarrow WW$ process. The mass spectrum shows a maximum around $2m_W$ and tends then to decrease exponentially with the WW mass. Therefore there are much more events around 300 GeV than around 600 GeV. More background events of that kind will also be present around 300 GeV than around a 600 GeV. But as the Higgs width is smaller when its mass is 300 GeV than 600 GeV, we compensate this effect by taking narrower mass windows in the selection cuts.

Simulating the single boson production with PYTHIA

The single W, Z production with multi jets was generated using the PYTHIA processes 15 and 30 for $qq \rightarrow Z + jets$ and 16 and 31 for $qq \rightarrow W + jets$.

These processes have matrix elements which are divergent for $p_t \rightarrow 0$ and therefore should not be used down to the low- p_t region. We then generated them asking

the p_t 's of the initial system being larger than 50 GeV to avoid that type of problems.

As the cross section of those kind of processes are too large to allow a simulation of all events required, a way of generating less background events had to be found. A solution was to generate the single boson production with a cut on the total generated system mass, \hat{m} , and on the p_t of the total system, \hat{p}_t . It lowers the background cross section and allows less events to be generated for the same luminosity. By simulating smaller background samples, we verified that the events which were not generated in the analysis would not have survived the cuts anyway. For instance, in the channel $H \rightarrow WW \rightarrow l\nu jj$, the backgrounds $qq \rightarrow gW^+$ and $gg \rightarrow qW^+$ have to be generated. If it is done with $\hat{m} > 300$ GeV and $\hat{p}_t > 100$ GeV, their cross section falls from 3600 pb with $\hat{m} > 100$ GeV and $\hat{p}_t > 50$ GeV (the minimal requirements) to 360 pb. We need thus to generate ten times less events for the same final number of events !

Even with those generation cuts, these background cross sections are very high. Sometimes a number of events corresponding to a luminosity of only $10 fb^{-1}$ instead of $100 fb^{-1}$ could be generated. And even with this luminosity, the number of events to generate was about 10^7 !

Simulating the top antitop production with PYTHIA

The top antitop production, $qq \rightarrow t\bar{t} \rightarrow WbWb$, was generated using the processes 81 and 82 in PYTHIA.

The cross section for this process is also very high ($\approx 600 pb$) and the presence of many jets in the events slowed a lot the simulation. We could not generate the number of events requested for a luminosity of $100 fb^{-1}$ and therefore we have the same problem for this background than for the single W, Z production backgrounds.

To limit the number of background events to generate, we also forced the vector bosons to decay only in the dangerous channels for the signature studied. For example, in the channels where only leptonic decays were present, like in the $H \rightarrow WW \rightarrow l\nu l\nu$ one, we could reduce the number of $t\bar{t}$ events to generate by a factor 10 by forcing the W 's to decay into leptons. The assumption was made that the events where the W 's did not decay leptonically were excluded by the selection cuts, as the event had to contain isolated leptons.

4.2 $H \rightarrow ZZ \rightarrow \ell^+\ell^-\ell^+\ell^-$

The first signature studied is the so-called *gold plated channel*, namely the $H \rightarrow ZZ \rightarrow \ell^+\ell^-\ell^+\ell^-$ signature. It takes its name from the fact that a Higgs mass peak can be nicely reconstructed, as leptons can be detected with a very good resolution. Essentially only one source of background needs to be studied in detail, the ZZ continuum production. The different cross sections for the signal and the background are given in Table 4.2.

We give the cross sections times branching ratio directly at the next to leading order, as the corresponding K-factors are given on page 32. Note that here and also for the other channels, Z and W can decay into τ 's, even if almost all the signal events get lost with the selection cuts. However, for backgrounds, $Z \rightarrow \tau^+\tau^-$ and $W \rightarrow \tau\nu$ branching ratios can be a danger and need to be simulated. Therefore, if not explicitly specified, ℓ will refer to electrons, muons *and* taus.

<i>Signal</i>		
Channel:	$qq \rightarrow qqH \rightarrow ZZ \rightarrow \ell\ell\ell\ell$	$gg \rightarrow H \rightarrow ZZ \rightarrow \ell\ell\ell\ell$
Mass of Higgs (GeV)	$\sigma \times BR$, NLO (fb)	$\sigma \times BR$, NLO (fb)
300	4.3	22.1
450	1.7	15.3
600	1.0	4.5
<i>Background</i>		
Channel	$\sigma \times BR$ (fb)	
$qq \rightarrow ZZ \rightarrow \ell\ell\ell\ell$	163	

Table 4.2: Cross sections times branching ratio for the signal (NLO) and background in the channel $H \rightarrow ZZ \rightarrow \ell^+\ell^-\ell^+\ell^-$.

The following cuts were used to isolate the Higgs signal when no jet tagging was made:

- There must be four isolated leptons in the event (e or μ with $p_t > 10$ GeV and $|\eta| < 2.5$).
- The two Z are reconstructed by pairing the leptons so that the chosen combination out of the possible ones give masses lying as close as possible to the real Z mass (91 GeV). The mass of the dilepton, which is closest to the Z one, has to be in an interval of 10 GeV centered in 91 GeV. The other reconstructed Z mass has to be in an interval of 20 GeV centered in 91 GeV.
- Only events where the mass of the reconstructed ZZ system is within an interval of 16, 60 and 200 GeV centered in respectively 300, 450 and 600 GeV were kept. Note that the half of the size of the interval chosen, 8, 30 and

100 GeV, correspond to one sigma of variation around the Higgs reconstructed mass peak.

- As the only background is the continuum ZZ production, we will make a soft cut on the reconstructed Higgs p_t , rather than on the p_t 's of the Z 's alone. (see page 25), $p_t(ZZ) > 30$ GeV was chosen.

The cuts used to isolate the Higgs produced through weak boson fusion, with the jet tagging technique are the following:

- The events must survive the same cuts as explained before, except for the p_t cut on the reconstructed Higgs, since almost all the continuum background events are removed with the jet tagging requirements.
- Exactly 2 jets must be in the event, with $p_t > 20$ GeV and $|\eta| < 4.5$. Their invariant mass has to be higher than 800 GeV.

The expected results for $\mathcal{L} = 100 fb^{-1}$ are given in Table 4.3. We give first the number of events left after the minimal reconstruction cuts, ie. when no cuts on the Higgs p_t is done. Then the number of events left after all cuts without and with the jet tagging is given. We see that very good signal to background ratios can be obtained. As pointed out before, the cut on the reconstructed Higgs p_t removes 90% of the background in the considered Higgs mass window, while only 50% of the signal events are removed, improving considerably the signal to background ratio.

The jet tagging removes almost all the background events, while the weak boson fusion signal events are remaining, but the statistics is small (between 5 and 15 events for a luminosity of $100 fb^{-1}$).

We can now calculate the necessary luminosity to get a 5 standard deviation. We find, for example, for a 600 GeV Higgs, a luminosity of approximately $30 fb^{-1}$ without jet tagging. The number of expected events in the signal for this luminosity is 12 and in the background 3. The probability to observe 15 events when the expected number of events is 3 is about 10^{-6} , assuming that the number of events follows a Poisson distribution. This probability corresponds approximately to the probability of a 5σ deviation in a Gaussian distribution and this is the usual requirement for a discovery.

These discovery luminosities are given in Table 4.4.

We find 4, 8 and $10 fb^{-1}$ for a 300, 450 and 600 GeV Higgs respectively. These numbers are in agreement with the previous studies (see for instance Ref [6]). Finally one should keep in mind that the detector inefficiencies are not taken into account. For isolated leptons, they are expected to be high and therefore these luminosities might be increased. For example, if we assume that the isolated leptons are detected with an efficiency of 90%, then the number of measured signal events will be $N_s^{measured} = 0.65 \cdot N_s^{expected}$, which leads to a loss of 19% in the significance of the signal $\frac{N_s^{measured}}{\sqrt{B}} = \frac{0.65 \cdot N_s^{expected}}{\sqrt{0.65 \cdot B}}$.

In Figure 4.4, we can see how a mass peak for a 300 GeV Higgs would look like in that channel and for a number of events corresponding to the discovery luminosity.

$H \rightarrow ZZ \rightarrow \ell^+\ell^-\ell^+\ell^-$				
Channel	Number of events			
	Generated	Min. rec. cuts	p_t cut	Jet tag.
$m_{Higgs} = 300$ GeV				
$qq \rightarrow qqH \rightarrow llll$	430	50	50	15
$gg \rightarrow H \rightarrow llll$	2'210	180	90	2
$qq \rightarrow ZZ \rightarrow llll$	16'300	50	4	0
$m_{Higgs} = 450$ GeV				
$qq \rightarrow qqH \rightarrow llll$	170	20	20	6
$gg \rightarrow H \rightarrow llll$	1'530	120	70	1
$qq \rightarrow ZZ \rightarrow llll$	16'300	30	6	0
$m_{Higgs} = 600$ GeV				
$qq \rightarrow qqH \rightarrow llll$	100	15	15	5
$gg \rightarrow H \rightarrow llll$	450	40	25	0
$qq \rightarrow ZZ \rightarrow llll$	16'300	30	10	0

Table 4.3: Expected results for $\mathcal{L} = 100 fb^{-1}$ and for different Higgs masses in the $H \rightarrow ZZ \rightarrow \ell^+\ell^-\ell^+\ell^-$ channel, NLO cross sections. After the number of generated events, the third column shows the number of events left after all cuts except the one on the reconstructed Higgs p_t (Min. rec. cuts). The two last columns give the number of events left after all cuts with and without the use of the jet tagging technique.

However, we would like to draw attention to the y-axis, which represents a small and non-integer number of events. Actually, in order to get rid of the statistical fluctuations, the signal was simulated for a number of events corresponding to a luminosity $10'000 fb^{-1}$ and the background for a number of events corresponding to a luminosity of $1'000 fb^{-1}$. However, in a real experiment, we would rather get something like in Figure 4.5, where only the number of events corresponding to the discovery luminosity were generated. For a 300 GeV Higgs, as the discovery luminosity is $4fb^{-1}$, it represented 106 signal events and 652 background events. We get 5 signal events in the good mass region against 2 background event. The expected values are of 5.6 signal events and 0.16 background events. We see than that we were not really lucky with our 'experiment', as the background is a bit high ! The plots on the left and on the right on Figure 4.5 represent exactly the same events, but with a binning of 5 GeV and 10 GeV. While a signal has to be guessed on the plot on the left, a Higgs peak becomes visible on the plot on the right.

Finally Figure 4.6 shows the mass peak we can get with a luminosity of $100 fb^{-1}$ without jet tagging for a 300 and a 600 GeV Higgs.

When the jet tagging technique is used, all the background events are removed, as continuum ZZ production contains few jets. However, not enough events are

$H \rightarrow ZZ \rightarrow \ell^+ \ell^- \ell^+ \ell^-$				
Higgs mass (GeV)	Signal	Background	S/B	$\mathcal{L}_{disc} (fb^{-1})$
300	140	4	35	4
450	90	6	15	8
600	40	10	4	30

Table 4.4: Expected discovery luminosities for the channel $H \rightarrow ZZ \rightarrow \ell^+ \ell^- \ell^+ \ell^-$, without systematic errors taken into account. The number of events for signal and background corresponds to a luminosity of $100 fb^{-1}$.

left to draw any significant conclusion: 17, 7 and 5 events are left for a 300, 450 and 600 GeV Higgs respectively.

For this channel, the Higgs search without tagging is giving excellent results, with a good signal to background ratio. The four leptons channel is thus a good candidate for a discovery channel. On the other hand, the jet tagging technique do not give here significant results, due to a too small statistic.

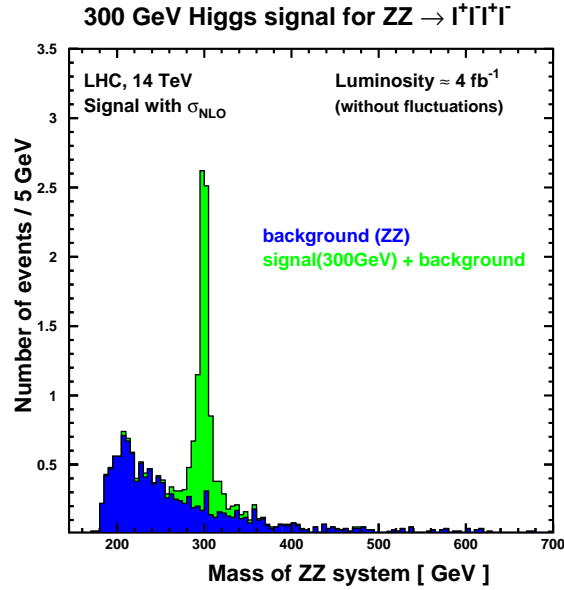


Figure 4.4: Higgs mass peak for a Higgs mass of 300 GeV, when no jet tagging is done. The signal and background were generated in a way to reduce as much as possible the statistical fluctuations.

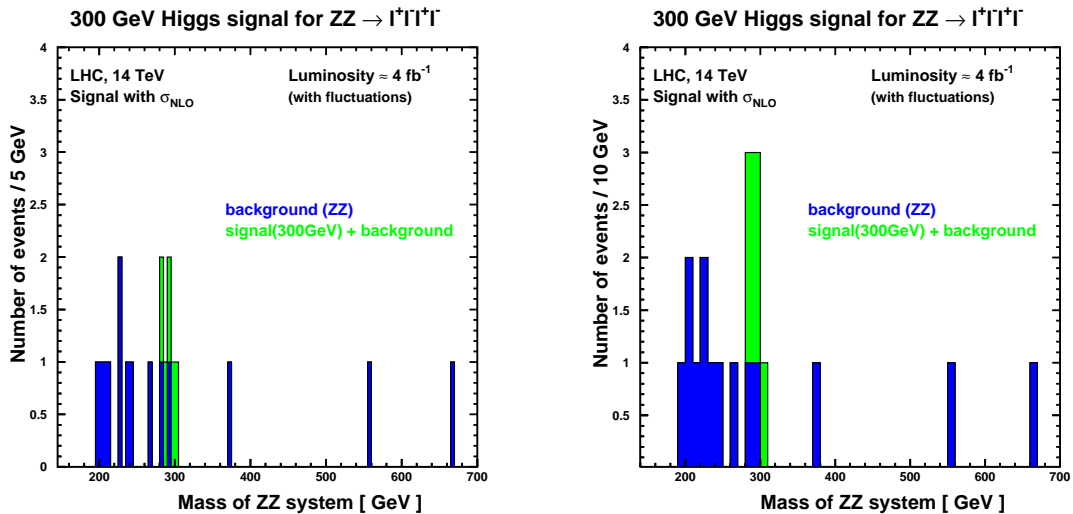


Figure 4.5: Higgs mass peak for a Higgs mass of 300 GeV, for a 'real' experiment and two different binnings, the 5 GeV bins are optimized according to our high luminosity plot while the 10 GeV bins are more for the small statistic samples.

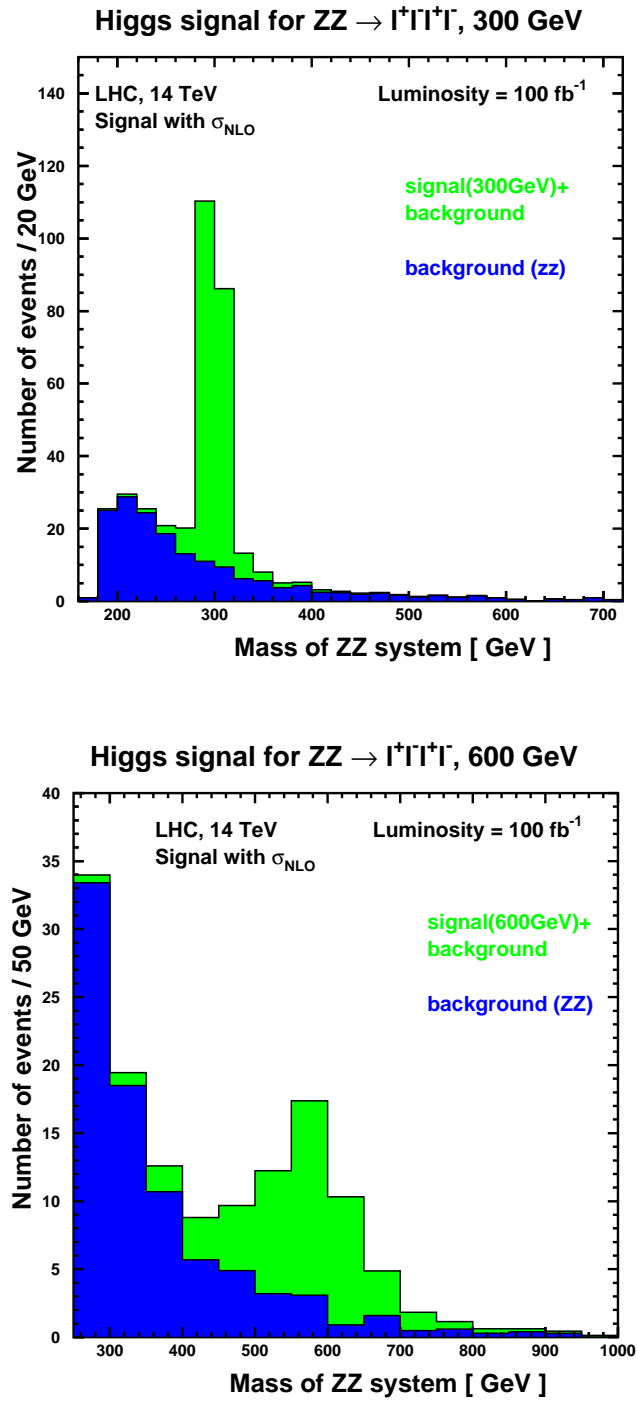


Figure 4.6: Mass spectrum for a 300 (Up) and 600 (Down) GeV Higgs for a luminosity of 100 fb^{-1} , without jet tagging.

4.3 $H \rightarrow ZZ \rightarrow \ell^+ \ell^- \nu \bar{\nu}$

This signature was already studied in detail (for instance see Ref. [14]) and it is known to give good signals for Higgs masses between 500 and 800 GeV. For such high masses, it seems to be superior to the four leptons channel. Notice that the branching fraction for this channel is six times larger than the one for the four leptons channel. Even if the Higgs mass peak cannot be totally reconstructed, the presence of the two leptons and a large missing energy gives this signature enough specifications to be isolated for large Higgs masses.

The signal cross sections times branching ratio for this signature are given in Table 4.5 for the two most significant production mechanisms of the Higgs.

<i>Signal</i>		
Channel:	$qq \rightarrow qqH \rightarrow ZZ \rightarrow \ell \ell \nu \nu$	$gg \rightarrow H \rightarrow ZZ \rightarrow \ell \ell \nu \nu$
Mass of Higgs (GeV)	$\sigma \times BR$, NLO (fb)	$\sigma \times BR$, NLO (fb)
300	16	90
450	7	60
600	4	23

Table 4.5: Cross sections times branching ratio for the signal in the channel $H \rightarrow ZZ \rightarrow \ell^+ \ell^- \nu \bar{\nu}$, given at the NLO.

The main feature of this signature is thus two isolated leptons, coming from a Z decay and a large missing p_t . The potential backgrounds are then all the processes which can produce two isolated leptons and missing p_t as given in Table 4.6.

<i>Backgrounds</i>	
Channel	$\sigma \times BR$ (fb)
$qq \rightarrow ZZ \rightarrow \ell \ell \nu \nu$	502
$qq \rightarrow WW \rightarrow \ell \nu \ell \nu$	8'050
$qq \rightarrow WZ \rightarrow \ell \nu \ell \ell$	950
$qq \rightarrow Z + jets$ ($Z \rightarrow \ell \ell$)	486'000 ($\hat{p}_t > 50$ GeV)
$qq \rightarrow t\bar{t} \rightarrow WbWb \rightarrow \ell \nu b \ell \nu b$	65'400

Table 4.6: Cross sections times branching ratio for the potential backgrounds in the channel $H \rightarrow ZZ \rightarrow \ell^+ \ell^- \nu \bar{\nu}$.

When there are jets in the event, to get rid of the ZZ continuum production, a cut on the p_t of the reconstructed ZZ system was made, which reduces this background by a factor 3 while the signal is only reduced by a factor 1.5 (if there are no jets in the event, the reconstructed Higgs has obviously $p_t = 0$).

The $Z + jets$ background can be reduced strongly with cuts on the reconstructed Z p_t 's.

The $t\bar{t}$ background is not really a problem here, as the isolated leptons do not give the Z mass.

The Higgs signal events are isolated with the following cuts:

- We ask for two isolated leptons from the same flavor in event (e, μ with $p_t > 10$ GeV and $|\eta| < 2.5$), whose invariant mass has to be within an interval of 10 GeV centered in 91 GeV.
- Then we ask, as a pre-cut, the missing p_t in the event to be higher than 75 GeV. The p_t of the reconstructed Z decaying into leptons has to be higher than 75 GeV.
- As explained before, when there are jets in the event, the p_t of the reconstructed Higgs has to be larger than 50 GeV.
- A harder cut on the missing p_t is finally done: $p_t^{miss} > 150(175, 225)$ GeV, for a 300(450, 600) GeV Higgs.

A background which remains problematic when the jet tagging is done, is the single Z production with jets. It definitely looks like a signal event if the Z decays into leptons and the jets emitted together with the Z play the role of the tagging jets. The missing p_t comes from badly reconstructed jets. However the jets identified as the tagging jets are more centrally emitted than the ones coming from the signal events and the cut on their invariant mass reduces this background by a factor of 40 against a factor of 2 for the signal. Furthermore, the missing p_t spectrum for the main background is falling much more steeply than the one for the signal, as there are no neutrinos in the event. A final cut on the missing p_t will then be lethal for that background. Cuts on the p_t 's of the reconstructed ZZ system and the reconstructed Z 's allows finally to get a better efficiency. The cuts used to isolate weak boson fusion are the following:

- The events must survive the above cuts, except for the final p_t cuts.
- Exactly 2 jets must be in the event with $p_t > 20$ GeV and $|\eta| < 4.5$. Their invariant mass has to be higher than 800 GeV.
- A last cut on the missing p_t is done: $p_t^{miss} > 100(125, 150)$ GeV, for a 300(450, 600) GeV Higgs.

The expected results for $\mathcal{L} = 100 fb^{-1}$ and for different Higgs masses are given in Table 4.7. We see that the main background is $qq \rightarrow Z + jets$. The cut which will be efficient against it will be the final cut on the missing p_t which reduces this background from a factor 25.

Is this possible to discover the Higgs in that channel? It is interesting to calculate the necessary luminosity for a 5 standard deviation with and without the use of the jet tagging technique. For the search without tagging, as we have

$H \rightarrow ZZ \rightarrow \ell^+ \ell^- \nu \bar{\nu}$				
Channel	Number of events			
	Generated	Min. rec. cuts	p_t cuts	Jet tag.
$m_{Higgs} = 300 \text{ GeV}$				
$qq \rightarrow qqH \rightarrow ZZ \rightarrow \ell\nu\nu$	1'600	260	55	55
$gg \rightarrow H \rightarrow ZZ \rightarrow \ell\nu\nu$	9'000	1'500	90	7
Sum of all backgrounds	56'090'200	37'960	2'115	66
Detailed backgrounds				
$qq \rightarrow ZZ \rightarrow \ell\nu\nu$	50'200	2'600	500	0
$qq \rightarrow WW \rightarrow \ell\nu\nu$	805'000	300	10	0
$qq \rightarrow WZ \rightarrow \ell\nu\ell\ell$	95'000	1'000	155	0
$qq, gg \rightarrow Z + jets \quad (Z \rightarrow \ell\ell)$	48'600'000	30'000	1'100	60
$qq \rightarrow t\bar{t} \rightarrow WbWb \rightarrow \ell\nu b \ell\nu b$	6'540'000	4'060	350	6
$m_{Higgs} = 450 \text{ GeV}$				
$qq \rightarrow qqH \rightarrow ZZ \rightarrow \ell\nu\nu$	700	190	110	55
$gg \rightarrow H \rightarrow ZZ \rightarrow \ell\nu\nu$	6'000	1'300	700	10
Sum of all backgrounds	56'090'200	37'960	1'313	33
Detailed backgrounds				
$qq \rightarrow ZZ \rightarrow \ell\nu\nu$	50'200	2'600	350	0
$qq \rightarrow WW \rightarrow \ell\nu\nu$	805'000	300	3	0
$qq \rightarrow WZ \rightarrow \ell\nu\ell\ell$	95'000	1'000	110	0
$qq, gg \rightarrow Z + jets \quad (Z \rightarrow \ell\ell)$	48'600'000	30'000	670	30
$qq \rightarrow t\bar{t} \rightarrow WbWb \rightarrow \ell\nu b \ell\nu b$	6'540'000	4'060	180	3
$m_{Higgs} = 600 \text{ GeV}$				
$qq \rightarrow qqH \rightarrow ZZ \rightarrow \ell\nu\nu$	400	120	80	40
$gg \rightarrow H \rightarrow ZZ \rightarrow \ell\nu\nu$	2'300	710	330	7
Sum of all backgrounds	56'090'200	37'960	401	12
Detailed backgrounds				
$qq \rightarrow ZZ \rightarrow \ell\nu\nu$	50'200	2'600	150	0
$qq \rightarrow WW \rightarrow \ell\nu\nu$	805'000	300	1	0
$qq \rightarrow WZ \rightarrow \ell\nu\ell\ell$	95'000	1'000	40	0
$qq, gg \rightarrow Z + jets \quad (Z \rightarrow \ell\ell)$	48'600'000	30'000	170	10
$qq \rightarrow t\bar{t} \rightarrow WbWb \rightarrow \ell\nu b \ell\nu b$	6'540'000	4'150	40	2

Table 4.7: Expected results for $\mathcal{L} = 100 \text{ fb}^{-1}$ and for different Higgs masses in the $H \rightarrow ZZ \rightarrow \ell^+ \ell^- \nu \bar{\nu}$, channel, NLO cross sections. After the total number of events generated for each process, we give the number of events left after the minimal reconstruction cuts, which means all cuts before the cut on the missing p_t and the number of events left without and with the jet tagging technique. Notice than looser p_t cuts are done if the jet tagging technique is used.

here more statistic, we can approximate the Poisson distribution with a Gaussian distribution and the formula for the discovery luminosity simplifies to:

$$\mathcal{L}_{disc} = 2'500 \frac{B}{S^2}$$

where B and S are the number of background and signal events corresponding to a luminosity of 100 fb^{-1} . For the results obtained with the jet tagging technique, the Poisson distribution has to be used. These results are given in Table 4.8. For Higgs masses higher than 450 GeV, interesting signals with good signal to background ratios are obtained.

$H \rightarrow ZZ \rightarrow \ell^+ \ell^- \nu \bar{\nu}$				
	Signal	Background	S/B	$\mathcal{L}_{disc} (\text{fb}^{-1})$
$m_{Higgs} = 300 \text{ GeV}$				
no tagging	145	2115	0.07	251
tagging	62	66	0.94	43
$m_{Higgs} = 450 \text{ GeV}$				
no tagging	810	1'313	0.62	5
tagging	65	33	1.97	27
$m_{Higgs} = 600 \text{ GeV}$				
no tagging	410	400	1.03	6
tagging	47	12	3.92	30

Table 4.8: Expected discovery luminosities for the channel $H \rightarrow ZZ \rightarrow \ell^+ \ell^- \nu \bar{\nu}$, without systematic errors taken into account. The number of events for signal and background corresponds to a luminosity of 100 fb^{-1} .

We conclude from this that it would be interesting to combine this channel with the four leptons channel in the search of the Higgs.

In Figures 4.8, 4.9 and 4.10 we can see the missing transverse momentum in the event for a 300, 450 and respectively 600 GeV Higgs signal, plotted above the different backgrounds. The plot on the left is made before jet tagging and the plot on the right after the use of the jet tagging technique.

Notice that without tagging, no excess can be seen for a 300 GeV Higgs. The problem is that for low Higgs masses, the peak in the missing transverse energy is just sitting where the background is huge. That means that it will be very difficult to measure an excess in that region. For higher Higgs masses the peak gets shifted and coincide with a region where the background is not that important any more and an excess can be seen. To get an idea of where the peak in the signal is sitting, see Figure 4.7, which shows the p_t spectrum of the signal. Actually the missing energy is correlated to the mass of the system. This can be explained in the following way: In the center of mass referential, the two vector bosons are emitted back to back.

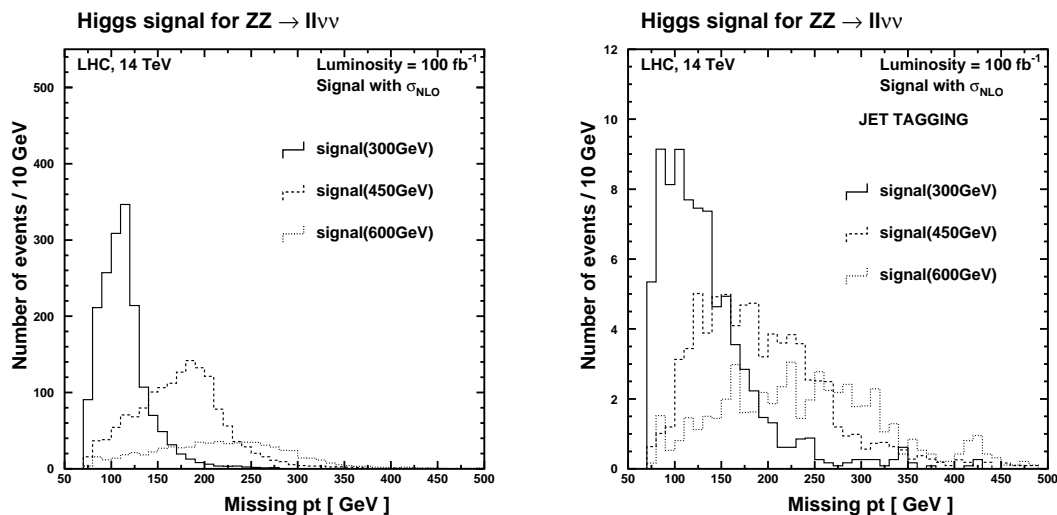


Figure 4.7: Missing p_t spectrum for a 300, 450 and 600 GeV Higgs without the backgrounds. (Left) without tagging (Right) with tagging. We can clearly see in all cases a peak in the distribution.

Then the W 's get a boost along the z -axis and their p_t remain unchanged. Thus the higher their transverse momentum is, the larger the mass of the system will be. Making a cut on the missing transverse momentum will then automatically make a cut on the mass of the system.

Notice also (on Figures 4.8, 4.9 and 4.9) that the low missing p_t region could be used to normalize the background. It is good to keep that region in order to check if the background is indeed well described by the simulation. This was the reason to use first some softer cuts on the p_t 's, in our case asking them to be higher than 75 GeV, and subsequently make harder cuts to get a good efficiency.

This channel is thus giving interesting results for Higgs masses higher than 300 GeV. The jet tagging technique allows to get better signal to background ratios and for a 300 GeV Higgs, we have a smaller discovery luminosities when the jet tagging is used.

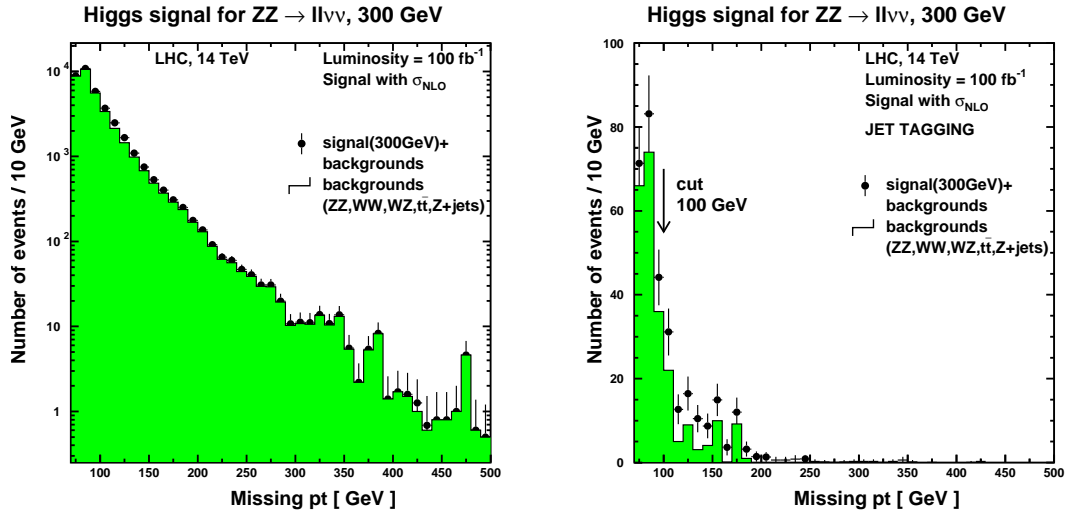


Figure 4.8: Missing p_t spectrum for a 300 GeV Higgs signal with the backgrounds. (Left) without tagging (Right) with tagging.

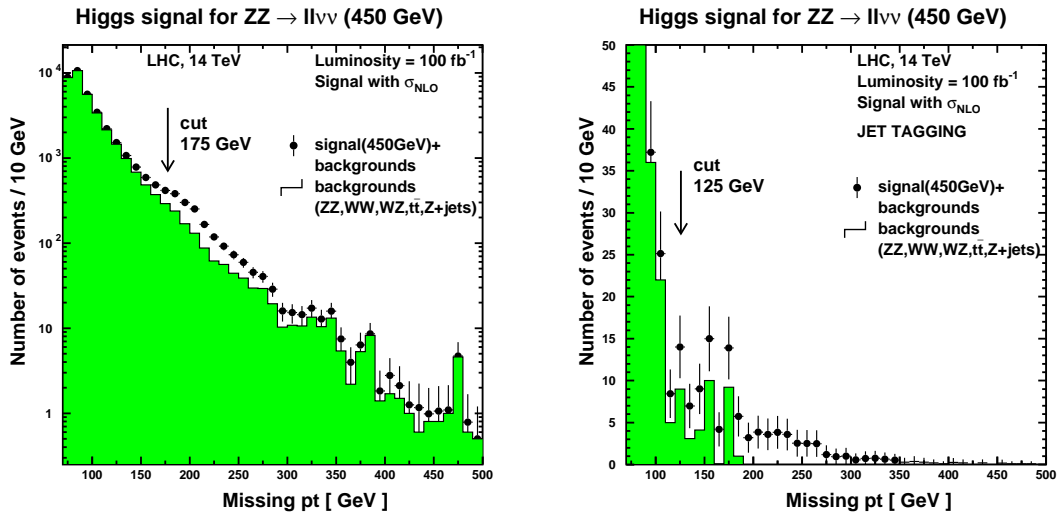


Figure 4.9: Missing p_t spectrum for a 450 GeV Higgs signal with the backgrounds. (Left) without tagging (Right) with tagging.

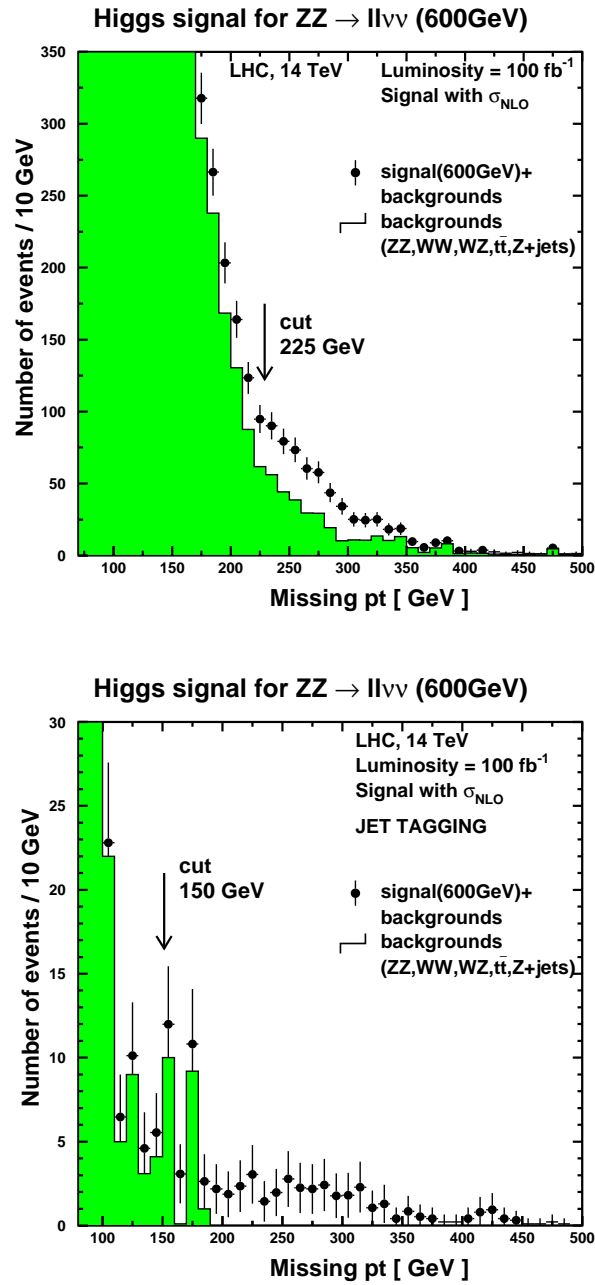


Figure 4.10: Missing p_t spectrum for a 600 GeV Higgs signal with the backgrounds. (Up) without tagging (Down) with tagging.

4.4 $H \rightarrow WW \rightarrow \ell\nu\ell\nu$

This channel is a bit different from the channels studied so far, since with that signature, it is impossible to reconstruct the Higgs mass and the cuts to isolate the signal have to rely only on the kinematic properties of the signal. Note that in spite of this, it was shown [21] that it gives a very good signal for Higgs masses between 150 and 200 GeV. To get a signal in that mass region, the spin correlations properties of the W 's coming from the Higgs were used as well as the differences in the p_t spectrum of the leptons coming from the decays of the W 's. However if we go to higher Higgs masses, the strong angular correlations that the W 's had for masses around 160 GeV are not present any more, due to the large boost that the W are receiving. New kinematical cuts have then to be found.

The cross section times branching ratio for the two most significant production mechanisms of the Higgs for this channel are given in Table 4.9.

<i>Signal</i>		
Channel:	$qq \rightarrow qqH \rightarrow WW \rightarrow \ell\nu\ell\nu$	$gg \rightarrow H \rightarrow WW \rightarrow \ell\nu\ell\nu$
Mass of Higgs (GeV)	$\sigma \times BR$, NLO (fb)	$\sigma \times BR$, NLO (fb)
300	88	533
450	40	332
600	22	130

Table 4.9: Cross sections times branching ratio for the signal in the channel $H \rightarrow WW \rightarrow \ell\nu\ell\nu$, given at the NLO.

The potential backgrounds for this signatures are all the processes which can produce two isolated leptons and possibly missing p_t . They are given in Table 4.10. We demand, for the signature when no jet tagging is applied, no jets in event to reduce the top-antitop background.

To get rid of most of the single Z production, the invariant mass of the leptons is asked not to be the Z mass.

Finally note that, as a jet veto in the selection cuts without jet tagging is made, two different processes for the single vector boson production have to be generated: Either $qq, gg \rightarrow Z$ or $qq, gg \rightarrow Z + jets$, corresponding to two different PYTHIA processes and depending on the signature we want to study (with or without tagging). The $qq, gg \rightarrow Z + jets$ background was generated with generation cuts as explained on page 36.

The Higgs events are isolated with the following cuts:

- We ask for two isolated leptons in event (e, μ with $p_t > 10$ GeV and $|\eta| < 2.5$), whose invariant mass should not to be within an interval of 20 GeV centered in 91 GeV, in order to reduce the single Z production background.

<i>Backgrounds</i>	
Channel	$\sigma \times BR$ (fb)
$qq \rightarrow WW \rightarrow \ell\nu\ell\nu$	8'050
$qq, gg \rightarrow Z \rightarrow \ell\ell$	230'000
$qq, gg \rightarrow Z + jets \rightarrow \ell\ell + jets$	52'000 ($\hat{p}_t > 100$ GeV, $\hat{m} > 300$ GeV)
$qq \rightarrow t\bar{t} \rightarrow WbWb \rightarrow \ell\nu b \ell\nu b$	65'400

Table 4.10: Cross sections times branching ratio for the potential backgrounds in the channel $H \rightarrow WW \rightarrow \ell\nu\ell\nu$.

- This channel is also characterized by a missing p_t , that is asked to be higher than 50 GeV.
- A cut on the p_t of the lepton which has the highest p_t from the two is also done, asking $p_t^\ell(max) > 100(150)$ GeV for Higgs masses of 300 and 600 GeV respectively.
- We finally cut on the angle that make the leptons in the transversal plane, $\varphi_{\ell\ell}$, asking them not being emitted back to back: $\varphi_{\ell\ell} < 140^\circ(175^\circ)$, for Higgs masses of 300 and 600 GeV respectively.

The cuts used for a 450 GeV Higgs mass are the same than the ones used for a 600 GeV mass. Figure 4.11 shows the p_t spectrum of the lepton which has the highest p_t from the two for a 600 GeV Higgs produced through weak boson fusion and for the backgrounds just before the cut on that p_t is applied.

The cuts with the jet tagging are a bit different. This comes from the fact that the main signal process will be then weak boson fusion which have other kinematic properties than the main signal process when no tagging is done, the gluon fusion. When the jet tagging is done, we do not use the cut on $\varphi_{\ell\ell}$ but rather make a cut on the angle between the two leptons, $\theta_{\ell\ell}$.

A cut against the top-antitop background is also made, as explained on page 29. In that case, we combine one jet with one lepton and keep the combination, whose mass, $m_{\ell jet}$, is closest to the mass of the top to make the cut.

The cuts used for the $H \rightarrow WW \rightarrow \ell\nu\ell\nu$ channel when the jet tagging is done are the following:

- Exactly 2 jets must be in the event with $p_t > 20$ GeV and $|\eta| < 4.5$. Their invariant mass has to be higher than 800 GeV.
- As explained above, we ask $m_{\ell jet}$ to be higher than 200 GeV, to reduce the $t\bar{t}$ background.
- The missing p_t in event should be higher than 50 GeV.

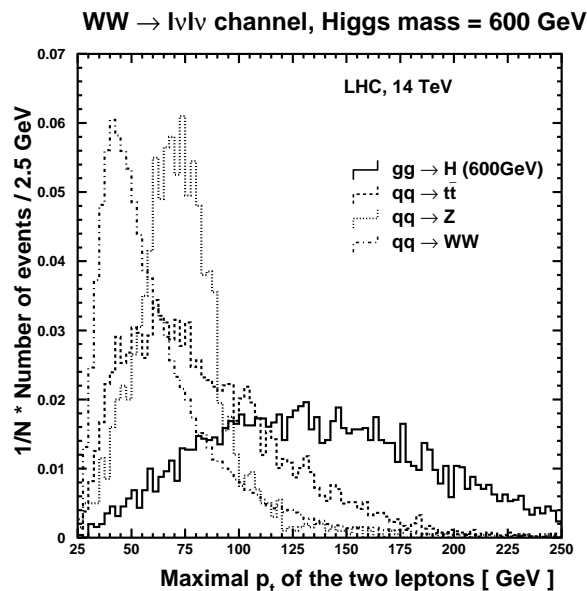


Figure 4.11: p_t spectrum of the lepton which has the highest p_t from the two, for a 600 GeV Higgs produced through weak boson fusion and for the backgrounds just before the cut on that p_t is applied in the $WW \rightarrow \ell\nu\ell\nu$ channel. The curves are normalized to 1.

- The p_t of the lepton with the highest p_t from the two must be higher than 50 GeV.
- We make a cut on the angle between the two leptons asking its cosine to be negative, ie. that the leptons are flying more back to back: $\cos\theta_{\ell\ell} < 0$.

Some other cuts were tried, like a cut on the rapidity difference between the leptons or on the invariant mass of the two leptons. But with these other cuts, we did not manage to improve the significance of the signal in any significant way.

The expected results for $\mathcal{L} = 100 \text{ fb}^{-1}$ and for different Higgs masses are given in Table 4.11. We see that the jet tagging technique works very well here and manage to rise the signal to background ratio from about 0.1 up to a factor 1.

Now let's calculate the luminosity for a 5 standard deviation with and without the jet tagging. The results are given in Table 4.12.

Once again, we see that it would be interesting to combine the results obtained with the jet tagging with the results of the other channels for the Higgs search. However, notice that it is hard to find the Higgs with this channel as no mass peak can be reconstructed. In order to determine the Higgs mass, we could fit for instance the transversal mass¹ distribution. This lead to a supplementary uncertainty on

¹The transversal mass of a particle is the mass it would have if its p_z is set to zero.

$H \rightarrow WW \rightarrow \ell\nu\ell\nu$				
Channel	Number of events			
	Generated	Min. rec. cuts	Full cuts (No tag.)	Jet tag.
$m_{Higgs} = 300 \text{ GeV}$				
$qq \rightarrow qqH \rightarrow \ell\nu\ell\nu$	8'800	25	7	80
$gg \rightarrow H \rightarrow \ell\nu\ell\nu$	53'300	980	460	10
Sum of all backgrounds	35'545'000	9'860	2'800	90
Detailed backgrounds				
$qq \rightarrow WW \rightarrow \ell\nu\ell\nu$	805'000	5'120	1'400	0
$qq, gg \rightarrow Z \rightarrow \ell\ell$	23'000'000	1'400	100	-
$qq, gg \rightarrow Z + jets \rightarrow \ell\ell + jets$	5'200'000	-	-	10
$qq \rightarrow t\bar{t} \rightarrow WbWb \rightarrow \ell\nu b \ell\nu b$	6'540'000	3'340	1300	80
$m_{Higgs} = 450 \text{ GeV}$				
$qq \rightarrow qqH \rightarrow \ell\nu\ell\nu$	4'000	30	5	140
$gg \rightarrow H \rightarrow \ell\nu\ell\nu$	33'200	1'570	530	10
Sum of all backgrounds	35'545'000	9'860	2'550	90
Detailed backgrounds				
$qq \rightarrow WW \rightarrow \ell\nu\ell\nu$	805'000	5'120	1500	0
$qq, gg \rightarrow Z \rightarrow \ell\ell$	23'000'000	1'400	300	-
$qq, gg \rightarrow Z + jets \rightarrow \ell\ell + jets$	5'200'000	-	-	10
$qq \rightarrow t\bar{t} \rightarrow WbWb \rightarrow \ell\nu b \ell\nu b$	6'540'000	3'340	750	80
$m_{Higgs} = 600 \text{ GeV}$				
$qq \rightarrow qqH \rightarrow \ell\nu\ell\nu$	2'200	20	10	110
$gg \rightarrow H \rightarrow \ell\nu\ell\nu$	13'000	550	310	20
Sum of all backgrounds	35'545'000	9'860	2'550	90
Detailed backgrounds				
$qq \rightarrow WW \rightarrow \ell\nu\ell\nu$	805'000	5'120	1500	0
$qq, gg \rightarrow Z \rightarrow \ell\ell$	23'000'000	1'400	300	-
$qq, gg \rightarrow Z + jets \rightarrow \ell\ell + jets$	5'200'000	-	-	10
$qq \rightarrow t\bar{t} \rightarrow WbWb \rightarrow \ell\nu b \ell\nu b$	6'540'000	3'340	750	80

Table 4.11: Expected results for $\mathcal{L} = 100 \text{ fb}^{-1}$ and for different Higgs masses in the $H \rightarrow WW \rightarrow \ell\nu\ell\nu$ channel, NLO cross sections. After the total number of events generated for each process, we give the number of events left after the minimal reconstruction cuts, which means $p_t^{miss} > 50 \text{ GeV}$, $p_t^\ell(max) > 100 \text{ GeV}$ and $\varphi_{\ell\ell} < 175^\circ$. The number of events left without and with the jet tagging are given in the two last columns.

$H \rightarrow WW \rightarrow \ell\nu\ell\nu$				
	Signal	Background	S/B	$\mathcal{L}_{disc} (fb^{-1})$
$m_{Higgs} = 300 \text{ GeV}$				
no tagging	467	2'800	0.19	32
tagging	90	90	1	28
$m_{Higgs} = 450 \text{ GeV}$				
no tagging	535	2'550	0.22	20
tagging	150	90	1.67	12
$m_{Higgs} = 600 \text{ GeV}$				
no tagging	320	2'550	0.13	62
tagging	130	90	1.44	13

Table 4.12: Expected discovery luminosities for the channel $H \rightarrow WW \rightarrow \ell\nu\ell\nu$, without systematic errors taken into account. The number of events for signal and background corresponds to a luminosity of $100 fb^{-1}$.

the simulation used to make the fit.

Figures 4.12 and 4.13 show how the transversal mass of the 'leptons plus missing energy' system for a 300 and a 600 GeV Higgs would look like, after the cuts, with and without forward jet tagging. A signal can clearly be seen when the tagging is made. The observation of a signal when no tagging is done implies a good knowledge of the background, as the signal peak stands right where the background has a maximum.

In the $H \rightarrow WW \rightarrow \ell\nu\ell\nu$ channel, when the jet tagging is added in the selection cuts, the signal is reduced by a factor 3 and the background by a factor 30, thus allowing a Higgs signal to be seen. The jet tagging improves the signal to background ratio of this signature from about a factor 10. As we will see later, this assumption will be true also for other channels studied.

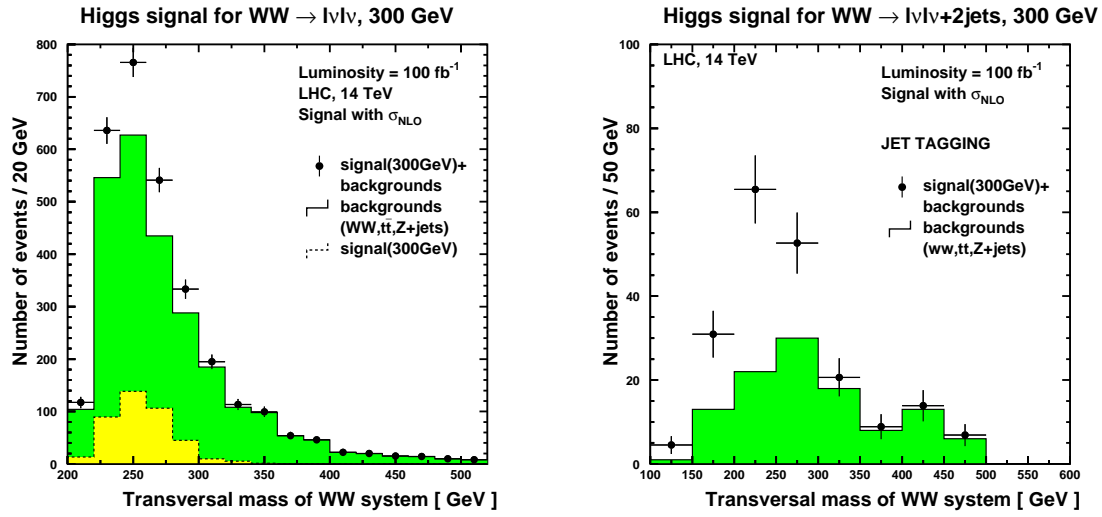


Figure 4.12: Transverse mass of the WW system for a 300 GeV Higgs, before tagging (Left) and after tagging (Right).

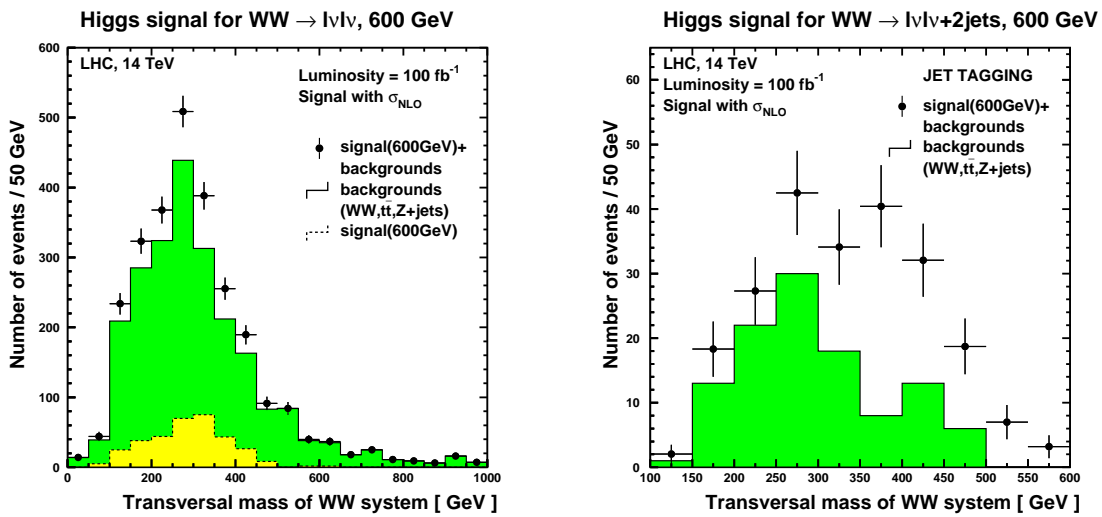


Figure 4.13: Transverse mass of the WW system for a 600 GeV Higgs. (Left) before tagging (Right) after tagging.

4.5 $H \rightarrow WW \rightarrow \ell\nu jj$

This channel is characterized by a large branching fraction (135 times larger than for $H \rightarrow ZZ \rightarrow 4\ell^\pm$). It is unfortunately also characterized by sources of backgrounds with huge cross sections due to the presence of jets in the signature. However thanks to the large number of signal events, harder cuts to isolate the signal can be made.

The cross sections times branching ratio for this channel are given in the Table 4.13.

<i>Signal</i>		
Channel:	$qq \rightarrow qqH \rightarrow WW \rightarrow \ell\nu jj$	$gg \rightarrow H \rightarrow WW \rightarrow \ell\nu jj$
Mass of Higgs (GeV)	$\sigma \times BR$, NLO (fb)	$\sigma \times BR$, NLO (fb)
300	370	2126
450	158	1350
600	90	518

Table 4.13: Cross sections times branching ratio for the signal in the channel $H \rightarrow WW \rightarrow \ell\nu jj$, given at the NLO.

This signature is characterized by one isolated lepton and at least two jets. The potential backgrounds are then all the processes which can produce one isolated lepton, jets and missing p_t . They are listed in Table 4.14. The $qq, gg \rightarrow W + jets \rightarrow \ell\nu + jets$ background can be generated with generation cuts, like explained on page 36. This is a main difference between the study we did and the study previously made by the Atlas group [6].

<i>Backgrounds</i>	
Channel	$\sigma \times BR$ (fb)
$qq \rightarrow WW \rightarrow \ell\nu jj$	32'340
$qq, gg \rightarrow W + jets \rightarrow \ell\nu + jets$	358'000 ($\hat{p}_t > 100$ GeV, $\hat{m} > 300$ GeV)
$qq \rightarrow t\bar{t} \rightarrow WbWb \rightarrow \ell\nu b \ell\nu b$	623'000

Table 4.14: Cross sections times branching ratio for the potential backgrounds in the channel $H \rightarrow WW \rightarrow \ell\nu jj$.

Here is a summary of the cuts to get a signal without jet tagging:

- We ask for one isolated lepton (e or μ with $p_t > 10$ GeV and $|\eta| < 2.5$) and at least two jets (with $p_t > 20$ GeV and $|\eta| < 4.5$).
- We reconstruct the first W by asking the two jets to have a mass within a interval of 40 GeV centered in the shifted W mass (here 73 GeV).

- Cuts are done on the p_t of the lepton and on the missing p_t : $p_t(\ell) > 25$ GeV and $p_t^{miss} > 25$ GeV. The W decaying into a lepton and a neutrino is reconstructed as explained on page 23. We make a loose cut on the W 's transversal mass, asking it to be between 20 and 100 GeV.
- Only events where the invariant mass of the WW system is within an interval of 70 (100, 200) GeV centered in 300 (450, 600) GeV were kept.
- Finally, cuts on the p_t 's of the reconstructed W 's are done:
 $p_t(W_{jj}, W_{\ell\nu}) > 100$ (150, 200) GeV, for a 300 (450, 600) GeV Higgs.

The cuts applied to isolate weak boson fusion, ie. when the jet tagging technique is used, are the following:

- The events must survive the same cuts as before.
- Exactly four jets with $p_t > 20$ GeV and $|\eta| < 4.5$ are asked in event (two jets to reconstruct the Z and two jets to be the tagging jets). The invariant mass of the tagging jets has to be higher than 800 GeV.
- As explained on page 29, a cut against the $t\bar{t}$ background is added, namely the mass of the W plus jet system, m_{Wjet} , has to be higher than 300 GeV.

The expected results for $\mathcal{L} = 100 fb^{-1}$ and for different Higgs masses are given in Table 4.15. We do not get very interesting results when no jet tagging technique is used. This is mainly caused by the presence of the huge $t\bar{t}$ background.

Like in the $H \rightarrow WW \rightarrow \ell\nu\ell\nu$ channel, we see that the jet tagging technique improves a lot the signal to background ratio, making it rise from 1/20 to about 1. One main source of background, the top antitop production, is strongly reduced with the cut on the m_{Wjet} . We find that when it is applied just after asking the cut on the invariant mass of the two tagging jets and before the cuts on the p_t 's, it makes us loose a factor 1.5 (for 600 GeV) and 2 (for 300 GeV) in the signal and 5 in the top-antitop background. To visualize the effect of that cut, see Figure 3.6 on page 30.

The other important background is the single W production, which is also strongly reduced thanks to the cuts on the m_{Wjet} and on the mass of the tagging jets requirement. The reason is that the jets for this background are emitted rather centrally and cannot lead to so high masses like the forward going jets coming from the weak boson fusion process.

As usual, let's calculate necessary luminosity for a 5 standard deviation, with and without the jet tagging technique. These results are given in Table 4.16.

It is interesting to discuss the results obtained without jet tagging. That this channel seems to lead to small discovery luminosities, at least as good as the ones obtained in the four leptons channels. Actually one thing need to be pointed out here. Even if the signal significance without tagging is very good, due to the large amount of events, the signal to background ratio is really low. That means that

$H \rightarrow WW \rightarrow \ell\nu jj$				
Channel	Number of events			
	Generated	Min. rec. cuts	p_t cuts	Jet tag.
$m_{Higgs} = 300 \text{ GeV}$				
$qq \rightarrow qqH \rightarrow \ell\nu jj$	37'000	5'000	1'900	290
$gg \rightarrow H \rightarrow \ell\nu jj$	212'600	28'000	14'700	40
Sum of all backgrounds	65'234'000	1'750'000	530'000	280
Detailed backgrounds				
$qq \rightarrow WW \rightarrow \ell\nu jj$	3'234'000	60'000	10'000	0
$qq, gg \rightarrow W + jets \rightarrow \ell\nu + jets$	35'800'000	290'000	160'000	130
$qq \rightarrow t\bar{t} \rightarrow WbWb \rightarrow \ell\nu b \ell\nu b$	26'200'000	1'400'000	360'000	150
$m_{Higgs} = 450 \text{ GeV}$				
$qq \rightarrow qqH \rightarrow \ell\nu jj$	15'800	2'400	1'650	330
$gg \rightarrow H \rightarrow \ell\nu jj$	135'000	19'000	14'000	90
Sum of all backgrounds	65'234'000	760'000	304'000	200
Detailed backgrounds				
$qq \rightarrow WW \rightarrow \ell\nu jj$	3'234'000	20'000	4'000	0
$qq, gg \rightarrow W + jets \rightarrow \ell\nu + jets$	35'800'000	270'000	150'000	120
$qq \rightarrow t\bar{t} \rightarrow WbWb \rightarrow \ell\nu b \ell\nu b$	26'200'000	470'000	150'000	80
$m_{Higgs} = 600 \text{ GeV}$				
$qq \rightarrow qqH \rightarrow \ell\nu jj$	9'000	1'500	900	220
$gg \rightarrow H \rightarrow \ell\nu jj$	51'800	6'400	4'700	40
Sum of all backgrounds	65'234'000	462'000	153'000	150
Detailed backgrounds				
$qq \rightarrow WW \rightarrow \ell\nu jj$	3'234'000	12'000	3'000	0
$qq, gg \rightarrow W + jets \rightarrow \ell\nu + jets$	35'800'000	190'000	85'000	100
$qq \rightarrow t\bar{t} \rightarrow WbWb \rightarrow \ell\nu b \ell\nu b$	26'200'000	260'000	65'000	50

Table 4.15: Expected results for $\mathcal{L} = 100 \text{ fb}^{-1}$ and for different Higgs masses in the $H \rightarrow WW \rightarrow \ell\nu jj$ channel, NLO cross sections. After the total number of events generated for each process, we give the number of events left after the minimal reconstruction cuts, which means all cuts except the ones on the p_t 's of the reconstructed W 's. In the two last columns, the expected number of events left without and with the jet tagging technique is given.

$H \rightarrow WW \rightarrow \ell\nu jj$				
	Signal	Background	S/B	$\mathcal{L}_{disc} (fb^{-1})$
$m_{Higgs} = 300 \text{ GeV}$				
no tagging	16'600	530'000	0.03	5
tagging	330	280	1.18	6
$m_{Higgs} = 450 \text{ GeV}$				
no tagging	15'650	304'000	0.05	3
tagging	420	200	2.10	3
$m_{Higgs} = 600 \text{ GeV}$				
no tagging	5'600	153'000	0.04	12
tagging	260	150	1.73	6

Table 4.16: Expected discovery luminosities for the channel $H \rightarrow WW \rightarrow \ell\nu jj$, without systematic errors taken into account. The results without tagging give too small signal to background ratios and cannot be taken into account. The number of events for signal and background corresponds to a luminosity of $100 fb^{-1}$.

if the background is not known with a precision of 3%, the error on the number of events in the background will be bigger than the expected signal itself ! Since the signal to background ratio is small, systematic errors have to be taken into account to get relevant results. Moreover if we look at the mass plots for a 300 and a 600 GeV Higgs without tagging (see Figure 4.14), no big excess is observable, which confirms this last remark !

One thing which is interesting to notice on the mass plots is that the background is not peaking around 200 GeV any more. It is a shifted. Actually, as soon as the high p_t cuts are made for the selection, the low mass region is much more strongly reduced than the high mass region. Figure 4.15 shows that the low-mass region in the WW mass spectrum for the backgrounds is much more reduced than the high mass region as soon as the cuts on the p_t s are applied. For a 300 GeV Higgs, the background maximum is then shifted to ≈ 350 GeV. However this is not the case for the signal, which still peaks around 300 GeV. The signal will then not stand where the background has a maximum (see Figure 4.14). Unfortunately, this is not the case any more for a 600 GeV Higgs.

As soon as the jet tagging technique is applied, the number of events is reduced, but a signal to background ratio larger than one is obtained with still a sizable number of events left. Figure 4.16 shows the reconstructed Higgs mass spectrum after the jet tagging. That means that even if the background is not well known, it should be possible to observe a signal. In that case, fluctuations in the background of for instance 10% allows nevertheless a signal to be observed. Moreover the mass plots show clearly a signal (see Figure 4.16). This channel might thus be very interesting if the tagging technique is used in the selection cuts.

It is finally interesting to point out that the number of jets in event influences

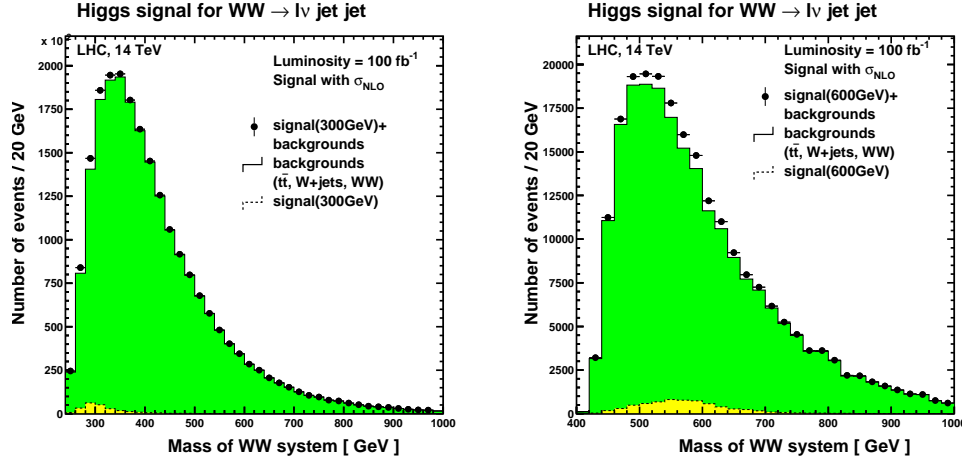


Figure 4.14: Mass spectrum of a 300 (Left) and a 600 GeV Higgs (Right) in the $H \rightarrow WW \rightarrow \ell\nu q\bar{q}$ channel, when no jet tagging is applied.

the signal to background ratio, especially when no jet tagging is done. A signal to background ratio of about 0.1 is obtained when there are two jets in event, while it falls to about 0.01 when more jets are present. Actually, as soon as there are more than two jets in the event, the $t\bar{t}$ background begins to be very important. This can be seen on the plots of the Figure 4.17, which shows the invariant mass distribution of the reconstructed WW system for a 300 GeV Higgs and the corresponding backgrounds, plotted for different numbers of jets in the event.

In the $H \rightarrow WW \rightarrow \ell\nu jj$ channel, very good results were obtained thanks to the jet tagging technique. We manage to get a signal to background ratio of about 2 together with a good statistic (about 300 events left for a luminosity of 100fb^{-1}). Moreover, somewhat better results were obtained than the ones obtained previously (for instance [6]). The reason appears to be the introduction of the cut on $m_{W_{jet}}$.

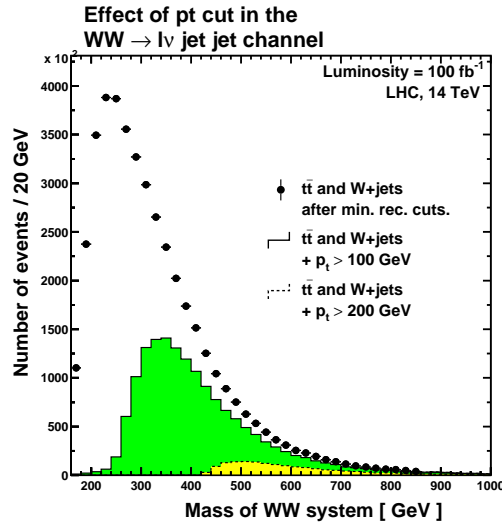


Figure 4.15: Effect of the cuts on the reconstructed WW mass spectrum. It is shown for $W + jets$ and $t\bar{t}$ backgrounds, with a number of events corresponding to a luminosity of $100fb^{-1}$. A first plot is done with the events that survived the minimal reconstruction cuts. As p_t cuts of 100 and 200 GeV were done to isolate a 300 and 600 GeV Higgs respectively, we show how the WW mass spectrum for background looks like after these two cuts.

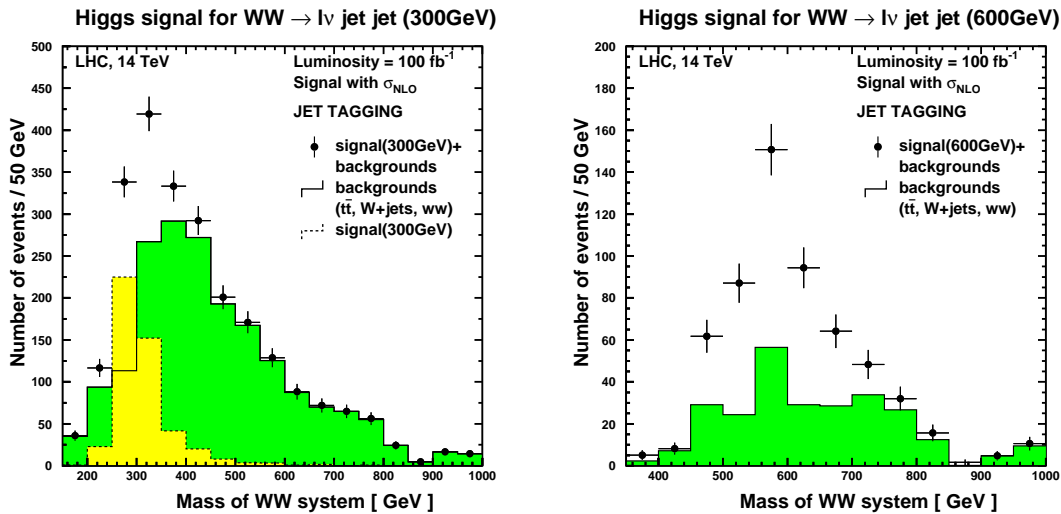


Figure 4.16: Mass spectrum of a 300 (Left) and a 600 GeV Higgs (Right) in the $H \rightarrow WW \rightarrow \ell\nu jj$ channel, with forward jet tagging.

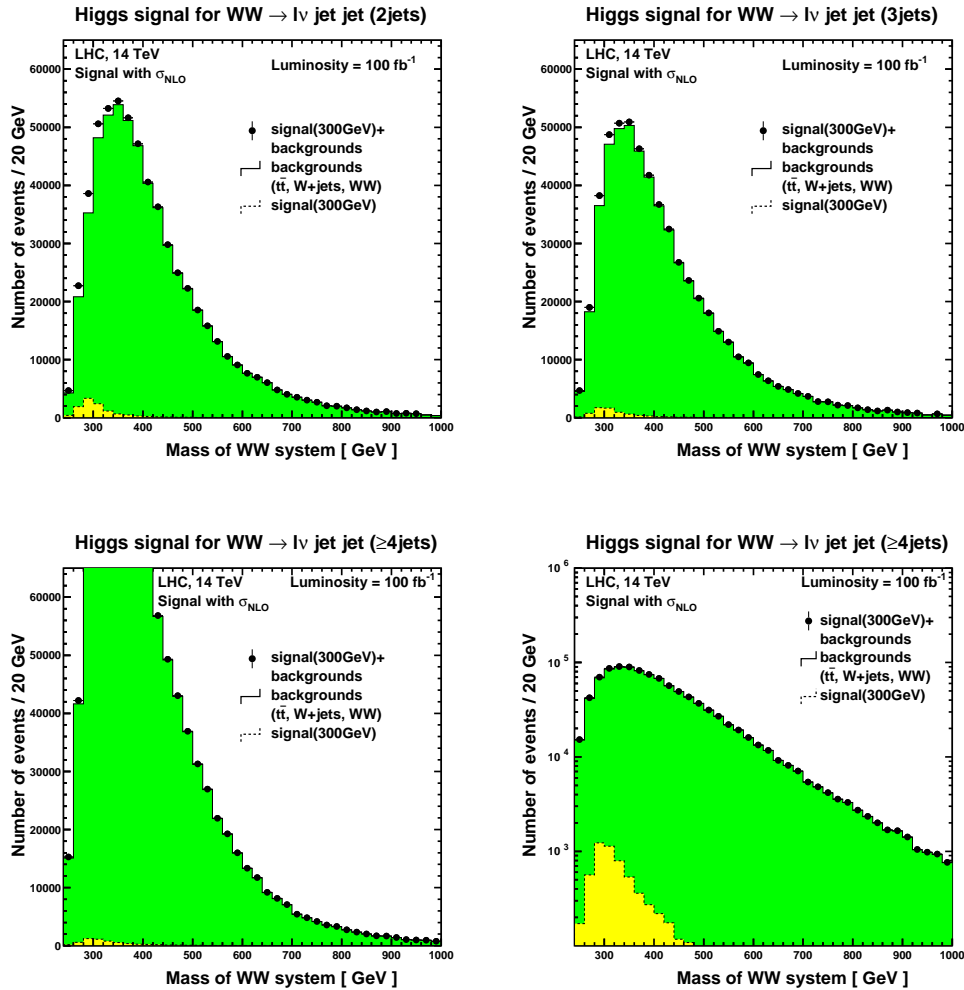


Figure 4.17: Mass spectrum of a 300 GeV Higgs in the $H \rightarrow WW \rightarrow \ell\nu jj$ channel, for different number of jets in event. (Up left) exactly 2 jets (Up right) exactly 3 jets (Down) more than 3 jets. (Left) with the same scale used than for the other plots (Right) with a logarithmic scale. As soon as there are more than 3 jets in events, the $t\bar{t}$ background begins to be important and overwhelm a possible signal. Furthermore the number of signal events produced through gluon fusion is strongly reduced as soon as the number of required jets is higher than 2.

4.6 $H \rightarrow ZZ \rightarrow \ell^+\ell^-jj$

This signature is not really different from the four leptons one, except for one Z which will decay in jets instead of leptons. The cuts to isolate this signal are then similar to the ones defined for the four leptons signature. However, problems arise from the fact that it is difficult to reconstruct the Z decaying into two jets (see page 22) and that new backgrounds with huge cross sections become dangerous due to the jets in the signature. Even if the branching fraction for this channel is 21 times bigger than the one of the four leptons channel, it is then hard to get a signal.

For this channel, the signal cross sections times branching ratio are given in the Table 4.17.

<i>Signal</i>		
Channel:	$qq \rightarrow qqH \rightarrow ZZ \rightarrow \ell\ell jj$	$gg \rightarrow H \rightarrow ZZ \rightarrow \ell\ell jj$
Mass of Higgs (GeV)	$\sigma \times BR$, NLO (fb)	$\sigma \times BR$, NLO (fb)
300	54	310
450	25	203
600	15	81

Table 4.17: Cross sections times branching ratio for the signal in the channel $H \rightarrow ZZ \rightarrow \ell^+\ell^-jj$, given at the NLO.

The signature is here two isolated leptons of the same flavor and at least two jets for the signature without jet tagging. The potential backgrounds are then all the processes which can produce two isolated leptons together with jets and are given in Table 4.18. Notice that for the $qq \rightarrow Z + jets$ background we did not let the Z decay into τ 's, because we checked that these events did not survive the selection cuts. This reduces the cross section for this background by a factor 2/3, allowing less events to be generated.

<i>Backgrounds</i>	
Channel	$\sigma \times BR$ (fb)
$qq \rightarrow ZZ \rightarrow \ell\ell jj$	1'700
$qq \rightarrow Z + jets$, ($Z \rightarrow e^\pm, \mu^\pm$)	320'000 ($\hat{p}_t > 50$ GeV)
$qq \rightarrow tt \rightarrow WbW\bar{b} \rightarrow \ell\nu b \ell\nu b$	65'400

Table 4.18: Cross sections times branching ratio for the potential backgrounds in the channel $H \rightarrow ZZ \rightarrow \ell^+\ell^-jj$.

The cuts used for the Higgs search without jet tagging in that channel are then the followings:

- We ask for two isolated leptons from the same flavor in the event (e, μ with

$p_t > 10 \text{ GeV}$ and $|\eta| < 2.5$), whose invariant mass has to be within 5 GeV around 91 GeV and at least 2 jets with ($p_t > 20 \text{ GeV}$ and $|\eta| < 4.5$).

- We then take all jets combinations which gave a mass within an interval of 40 GeV centered in the shifted Z mass (85 GeV) and from these good combinations, the one with the highest p_t was chosen.
- As the mass of the Z decaying into jets is shifted, the reconstructed ZZ system mass is also slightly shifted and the Higgs peak is around 285 GeV for a 300 GeV Higgs (for a 600 and a 450 GeV Higgs, as the peak is wider, the effect does not need to be taken into account). Only events where the invariant mass of the ZZ system is within an interval of 70 (100, 200) GeV centered in 285 (450, 600) GeV are kept.
- A cut on the p_t 's of the reconstructed vector bosons and of the reconstructed Higgs is finally done: $p_t(ZZ) > 50 \text{ GeV}$, $p_t(Z\ell\ell \text{ or } Zjj) > 100 (150, 200) \text{ GeV}$ for a 300 (450, 600) GeV Higgs

If the jet tagging is added, the following selection cuts are applied:

- The events must survive the above cuts.
- Exactly four jets are asked in event (two jets to reconstruct the Z and two jets to be the tagging jets). The invariant mass of the tagging jets has to be higher than 800 GeV.

The expected results for $\mathcal{L} = 100 \text{ fb}^{-1}$ and for different Higgs masses are given in Table 4.19. We give the expected number of events without the jet tagging technique before and after the application of the different cuts on the p_t 's. We see that the main background in that case is the single Z production. Because of that, it will be hard to see a signal if no jet tagging is made. We see that the cuts on the different p_t 's allows us to double the signal to background ratio. Since the jet tagging is done, we get a good signal to background ratio (more than 1) and a clear excess over the background is seen.

The luminosities required for a five standard deviation in that channel are given in Table 4.20.

Like for the $H \rightarrow WW \rightarrow \ell\nu jj$ channel, the results without jet tagging have to be taken with care, as the signal to background ratio is a bit too small to give relevant results when one does not take into account the systematic errors.

Figures 4.18, 4.19 and 4.20, show the mass of the ZZ system. When no tagging is done, for a 300 and a 600 GeV Higgs, it is clear that only a signal might be seen if the background is very well known. Nevertheless, a good peak can be obtained if the signal alone is considered. For a 450 GeV Higgs, a bigger excess can be seen. It confirms the good discovery luminosity we find there: 9 fb^{-1} . However the signal to background ratio is a bit low, 0.12.

As soon as the tagging is done, clear excesses become visible for every masses, as shown on Figures 4.18, 4.19 and 4.20.

$H \rightarrow ZZ \rightarrow \ell^+ \ell^- jj$				
Channel	Number of events			
	Generated	Min. rec. cuts	p_t cuts	Jet tag.
$m_{Higgs} = 300 \text{ GeV}$				
$qq \rightarrow qqH \rightarrow \ell\ell jj$	5'400	980	220	50
$gg \rightarrow H \rightarrow \ell\ell jj$	31'000	4'490	1'350	3
Sum of all backgrounds	38'710'000	193'280	27'750	46
Detailed backgrounds				
$qq \rightarrow ZZ \rightarrow \ell\ell jj$	170'000	3'400	400	0
$qq, gg \rightarrow Z + jets \rightarrow \ell\ell + jets$	32'000'000	186'000	27'000	40
$qq \rightarrow t\bar{t} \rightarrow WbWb \rightarrow \ell\nu b \ell\nu b$	6'540'000	3'880	350	6
$m_{Higgs} = 450 \text{ GeV}$				
$qq \rightarrow qqH \rightarrow \ell\ell jj$	2'500	460	260	60
$gg \rightarrow H \rightarrow \ell\ell jj$	20'300	3'070	2'030	15
Sum of all backgrounds	38'710'000	60'320	18'760	50
Detailed backgrounds				
$qq \rightarrow ZZ \rightarrow \ell\ell jj$	170'000	420	320	0
$qq, gg \rightarrow Z + jets \rightarrow \ell\ell + jets$	32'000'000	59'500	18'300	50
$qq \rightarrow t\bar{t} \rightarrow WbWb \rightarrow \ell\nu b \ell\nu b$	6'540'000	400	140	0
$m_{Higgs} = 600 \text{ GeV}$				
$qq \rightarrow qqH \rightarrow \ell\ell jj$	1'500	320	210	70
$gg \rightarrow H \rightarrow \ell\ell jj$	8'100	1'090	680	5
Sum of all backgrounds	38'710'000	43'970	11'211	25
Detailed backgrounds				
$qq \rightarrow ZZ \rightarrow \ell\ell jj$	170'000	760	210	0
$qq, gg \rightarrow Z + jets \rightarrow \ell\ell + jets$	32'000'000	43'000	11'000	25
$qq \rightarrow t\bar{t} \rightarrow WbWb \rightarrow \ell\nu b \ell\nu b$	6'540'000	210	1	0

Table 4.19: Expected results for $\mathcal{L} = 100 \text{ fb}^{-1}$ and for different Higgs masses in the $H \rightarrow ZZ \rightarrow \ell^+ \ell^- jj$ channel, NLO cross sections. After the total number of events generated for each process, we give the number of events left after the minimal reconstruction cuts, which means all cuts before the cut on the different p_t 's. The two last columns show the expected number of events left after all cuts without and with the jet tagging technique.

$H \rightarrow ZZ \rightarrow \ell^+ \ell^- jj$				
	Signal	Background	S/B	$\mathcal{L}_{disc} (fb^{-1})$
$m_{Higgs} = 300 \text{ GeV}$				
no tagging	1'570	27'750	0.06	28
tagging	53	46	1.15	41
$m_{Higgs} = 450 \text{ GeV}$				
no tagging	2'290	18'760	0.12	9
tagging	75	50	1.50	22
$m_{Higgs} = 600 \text{ GeV}$				
no tagging	890	11'211	0.08	35
tagging	75	25	3.00	20

Table 4.20: Expected discovery luminosities for the channel $H \rightarrow ZZ \rightarrow \ell^+ \ell^- jj$, without systematic errors taken into account. The number of events for signal and background corresponds to a luminosity of $100 fb^{-1}$.

Once more, only the number of events corresponding to a lower luminosity were generated for the background, which explains the big fluctuations on the plots in the distributions of the background.

This channel can lead an interesting contribution if it is combined to the results of the other channels. Due to the presence of high backgrounds, it does not lead alone to very useful results.

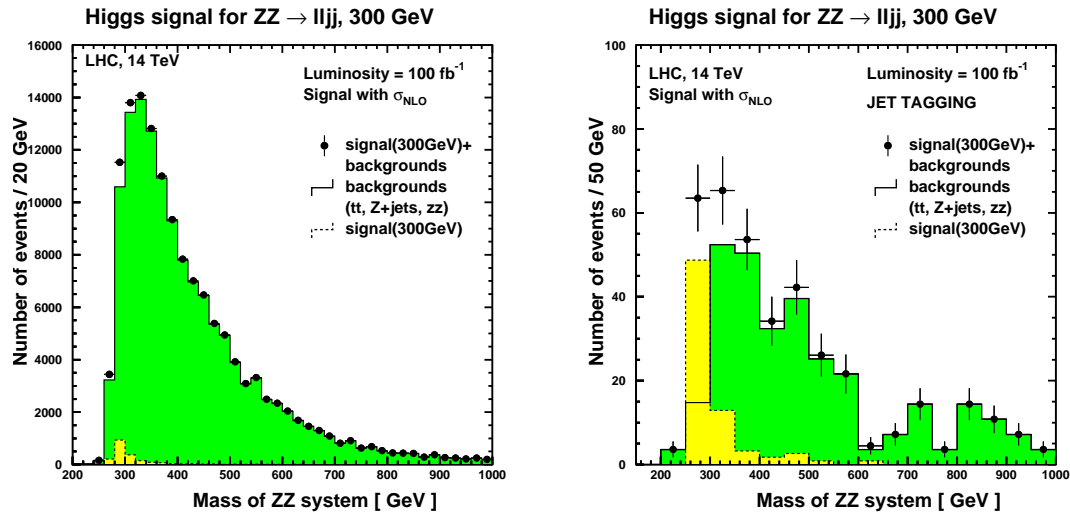


Figure 4.18: Mass spectrum of the reconstructed ZZ system for a 300 GeV Higgs. (Left) without jet tagging (Right) with jet tagging.

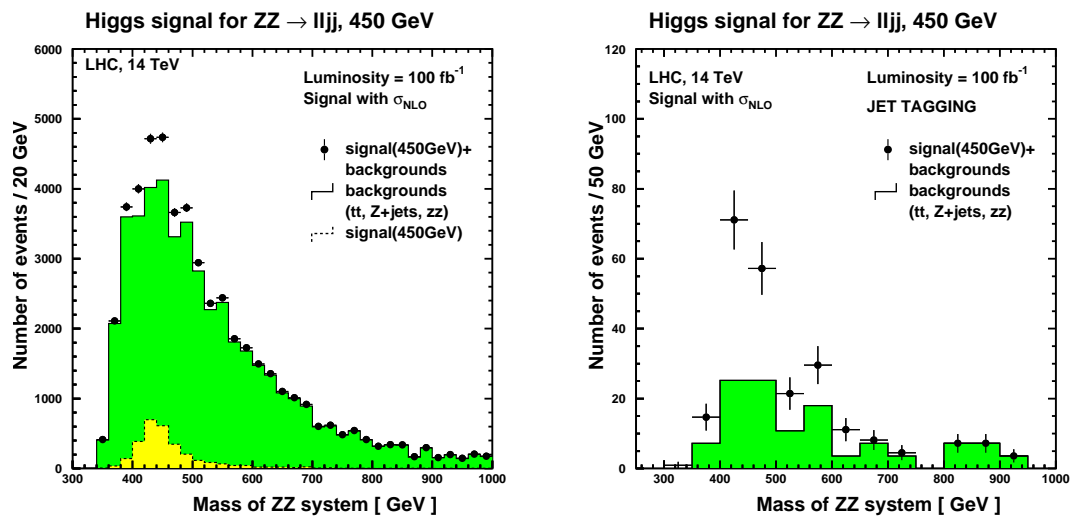


Figure 4.19: Mass spectrum of the reconstructed ZZ system for a 450 GeV Higgs. (Left) without jet tagging (Right) with jet tagging.

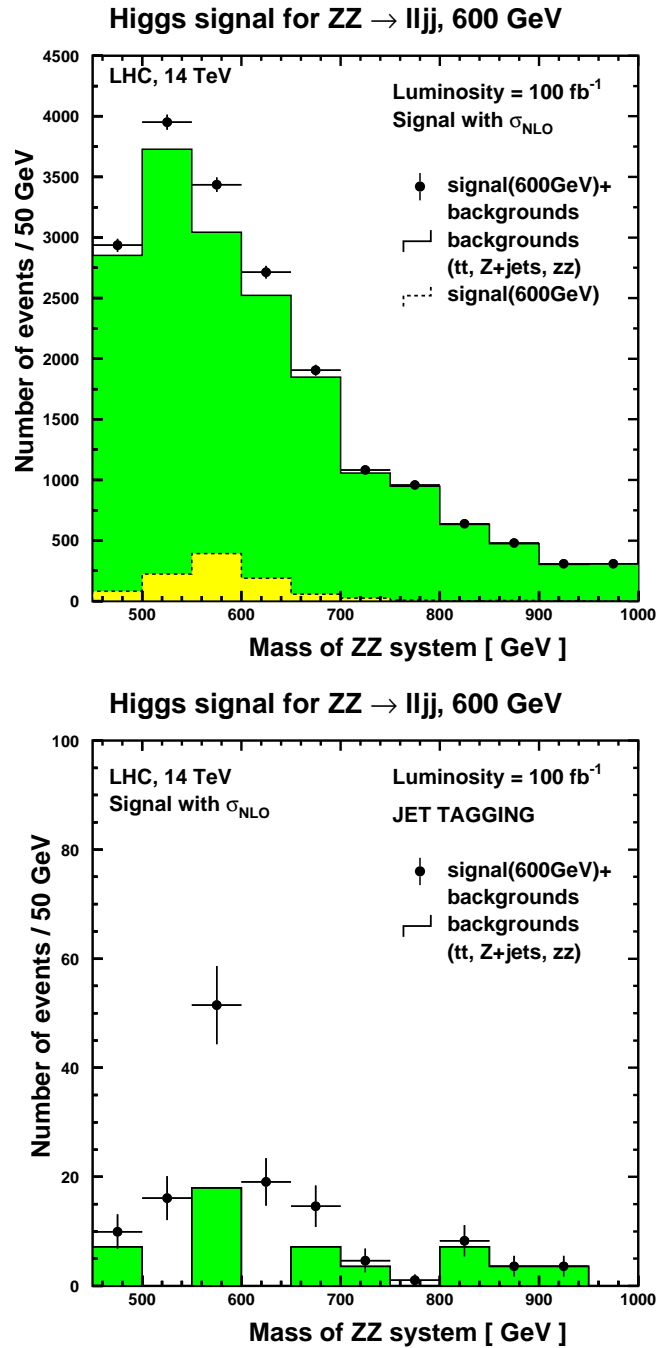


Figure 4.20: Mass spectrum of the reconstructed ZZ system for a 600 GeV Higgs. (Up) without jet tagging (Down) with jet tagging.

4.7 $H \rightarrow ZZ \rightarrow \nu\bar{\nu}jj$

This signature has not been really studied yet. Among the channels which contain Higgs decays into Z , it has the larger branching fraction: 64 times higher than the four leptons channels one and 10 times higher than the $H \rightarrow ZZ \rightarrow \ell\ell\nu\nu$ one. However, this signature is really hard to isolate due to the presence of the large QCD background. As no isolated leptons are present here, all the processes like $q_i q_j \rightarrow q_i q_j$ might be important background sources. However, as we find with the previous signatures that the jet tagging technique managed to rise considerably the signal to background ratios, it is interesting to study if, with the help of the jet tagging cut, one could nevertheless have a signal with that signature. We chose to consider only a 600 GeV Higgs, as harder cuts can be done than with a 300 GeV Higgs.

The cross sections times branching ratio at the next to leading order are given in the Table 4.21.

<i>Signal</i>		
Channel:	$qq \rightarrow qqH \rightarrow ZZ \rightarrow \nu\bar{\nu}jj$	$gg \rightarrow H \rightarrow ZZ \rightarrow \nu\bar{\nu}jj$
Mass of Higgs (GeV)	$\sigma \times BR$, NLO (fb)	$\sigma \times BR$, NLO (fb)
600	30	164

Table 4.21: Cross sections times branching ratio for the signal in the channel $H \rightarrow ZZ \rightarrow \nu\bar{\nu}jj$, given at the NLO.

<i>Backgrounds</i>	
Channel	$\sigma \times BR$ (fb)
$qq \rightarrow ZZ \rightarrow \nu\bar{\nu}jj$	3'200
$qq \rightarrow Z + jets$, ($Z \rightarrow \nu\bar{\nu}$)	811'000 ($\widehat{p}_t > 50 GeV$)
$qq \rightarrow t\bar{t} \rightarrow WbWb \rightarrow anything$	622'000
QCD backgrounds	$7 \cdot 10^7$ ($\widehat{m} > 1000 GeV$, $\widehat{p}_t > 100 GeV$)

Table 4.22: Cross sections times branching ratio for the potential backgrounds in the channel $H \rightarrow ZZ \rightarrow \nu\bar{\nu}jj$.

The backgrounds for this signature, which is characterized by two jets, which have to give the Z mass, a large missing p_t and no isolated leptons, are given in Table 4.22. What should be understood under *QCD backgrounds* are the following processes:

- $q_i q_j \rightarrow q_i q_j$
- $q_i \bar{q}_i \rightarrow q_k \bar{q}_k$

- $q_i \bar{q}_i \rightarrow gg$
- $q_i g \rightarrow q_i g$
- $gg \rightarrow q_i \bar{q}_i$
- $gg \rightarrow gg$

Actually these processes can be generated asking the mass of the total system, \hat{m} , being higher than 1000 GeV. This can be done, as a high \hat{m} is anyway asked by the selection cuts: The tagging jet system to have a mass higher than 800 GeV and the two other jets a mass close to 90 GeV.

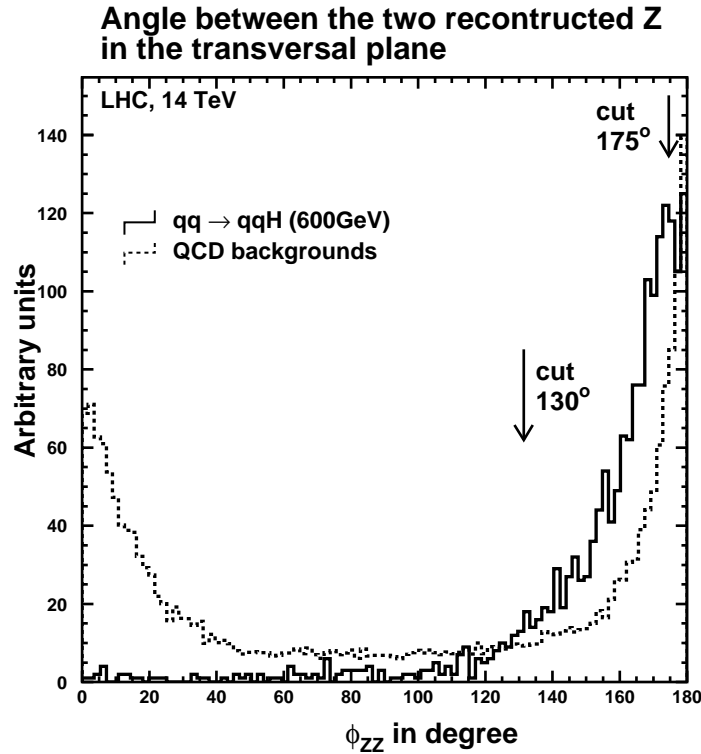


Figure 4.21: Angle between the two reconstructed Z, for the signal and the QCD background. The two histograms are not made for the same luminosity in order to compare the shapes. To have a number of events corresponding to the same luminosity for the signal and the background, the number of background events should be multiplied by $2 \cdot 10^6$.

Here are the cuts that were tried to isolate a signal with that signature:

- First we ask for four jets with $p_t > 20$ GeV and $|\eta| < 4.5$ and no isolated leptons in the event.

- We then took all jets combinations which gave a mass within an interval of 40 GeV centered in the shifted Z mass (85 GeV) and from these good combinations, the one with the highest p_t was chosen. The missing p_t vector is identified with the Z decaying into neutrinos.
- A cut on the angle in the transverse plane, ϕ , between the two reconstructed Z , was also made, asking it to be between 130° and 170° . This allows us to get rid of the half of the QCD background, as it is shown on Figure 4.21.
- A cut on the p_t 's of the two reconstructed Z 's is also done, asking $p_t(Z_{jj}) > 200 \text{ GeV}$, $p_t^{miss} > 200 \text{ GeV}$
- Finally, the mass of the tagging jets system has to be higher than 800 GeV or 1200 GeV.

The expected results for $\mathcal{L} = 100 \text{ fb}^{-1}$ and for a 600 GeV Higgs are given in Table 4.23. There is a big uncertainty on the QCD background results as its cross section is too high to generate the number of events corresponding to a luminosity of 100 fb^{-1} , even with hard cuts in the generation. We then had to multiply the number of QCD background events with 700 !

$H \rightarrow ZZ \rightarrow \nu\bar{\nu}jj$			
Channel	Generated	Number of events	
		With tagging	
		$m_{jj} > 800 \text{ GeV}$	$m_{jj} > 1200 \text{ GeV}$
$qq \rightarrow qqH \rightarrow \nu\bar{\nu}jj$	3'000	190	110
$gg \rightarrow H \rightarrow \nu\bar{\nu}jj$	16'400	30	20
Sum of all backgrounds	$7 \cdot 10^9$	4'700	1'600
Detailed backgrounds			
$qq \rightarrow ZZ \rightarrow \nu\bar{\nu}jj$	320'000	0	0
$qq, gg \rightarrow Z + jets \rightarrow \nu\nu + jets$	81'100'000	300	100
$qq \rightarrow t\bar{t} \rightarrow WbWb \rightarrow \text{anything}$	62'200'000	200	100
QCD background	$7 \cdot 10^9$	4'200	1'400

Table 4.23: Expected results for $\mathcal{L} = 100 \text{ fb}^{-1}$ for a 600 GeV Higgs (NLO cross sections) in the $H \rightarrow ZZ \rightarrow \nu\bar{\nu}jj$ channel. We give the expected number of events after all cuts. Once the mass of the tagging jets is asked to be higher than 800 GeV and once it is asked to be higher than 1200 GeV.

What is interesting to notice here is that if the QCD background is not taken into account, a signal can be isolated (130 signal events against 200 background events). Further studies need to be done to see if additional cuts against the QCD background could be found. Then, there would be a chance to observe a Higgs signal also in that channel. For example, the cut on the angle allowed already to get rid of the half of the QCD background.

Note that it would be relevant, not only for that channel, to know better the kinematic properties of the QCD background. This background could reduce the significance of other channels, if, for example, the jets are misidentified as missing energy or leptons.

Chapter 5

Discussion

In the following, we will combine the results obtained for the different channels studied, namely: $H \rightarrow ZZ \rightarrow llll$, $H \rightarrow ZZ \rightarrow ll\nu\nu$, $H \rightarrow WW \rightarrow l\nu l\nu$, $H \rightarrow WW \rightarrow l\nu jj$, $H \rightarrow ZZ \rightarrow lljj$ and $H \rightarrow ZZ \rightarrow \nu\nu jj$.

We concentrate on the following questions:

- How can a heavy Higgs, with a mass between 300 and 600 GeV be discovered at the LHC ? Which channels can give significant results for this purpose ? We will especially consider what the jet tagging technique can bring.
- Then we will discuss how precisely the ratio between the two decay branching fractions $H \rightarrow WW$ and $H \rightarrow ZZ$ can be measured.
- Finally, we will ask ourselves with which statistical precision the weak boson fusion and gluon fusion cross sections can be measured.

As already said, these two last measurements are crucial tests of the theoretical predictions about how the Higgs couples to top quarks and W and Z bosons.

5.1 Discovery luminosity for heavy Higgs

First of all, we want to find out with which luminosity a heavy Higgs boson can be discovered at the LHC. Two things are important to consider for a channel to give a signal: Firstly, the signal to background ratio has to be high enough to reduce the effect of the systematic errors. Secondly, enough statistics have to be left after the selection cuts, to minimize the statistical errors which are proportional to \sqrt{N} . In that study, only the statistical errors are taken into account. However, only the signatures where signal to background ratio was high enough (> 0.5) are kept. This gives a safety margin on the results, if the systematic errors are subsequently taken into account.

A summary of the expected discovery luminosities for every channel studied is made in Table 5.1. Always two values for the discovery luminosity were obtained:

A first one without using the jet tagging technique and a second one using the jet tagging technique. We chose to give only the most significant result of these two.

We see that we have mainly two types of channels. The first ones, which are more significant when no jet tagging is used, namely: $H \rightarrow ZZ \rightarrow \ell\ell\ell$ and $H \rightarrow ZZ \rightarrow \ell\ell\nu\nu$. The second ones, which only give a significant signal when the jet tagging technique is used: $H \rightarrow ZZ \rightarrow \ell\ell jj$, $H \rightarrow WW \rightarrow \ell\nu\ell\nu$ and $H \rightarrow WW \rightarrow \ell\nu jj$.

The forward jet tagging technique allows to get good signal to background ratios in several channels. However, the price to pay as soon as it is used, is a strong reduction of signal events. This would be a problem for channels with a small branching ratio, typically the ones where only leptonic decays are present.

Therefore, even if the jet tagging technique selects essentially a particular way of producing the Higgs, it can lead to a more significant Higgs signal than a signal obtained when no particular production mechanism of the Higgs is favored. This is especially the case when hadronic decays of W and Z are present in the signature.

As can be seen from Table 5.1, the four leptons channel is giving very good results for Higgs masses of 300 and 450 GeV, leading to an expected discovery luminosity of 4 and $8 fb^{-1}$ respectively. The ability of this signature to give significant results relies essentially on the possibility to reconstruct a narrow signal peak in the ZZ mass spectrum. However as for high Higgs masses, the natural width of the Higgs becomes wider, this signature is not as powerful as for lower Higgs masses. Furthermore, its branching fraction begins to be very small for high Higgs masses.

The $H \rightarrow ZZ \rightarrow \ell\ell\nu\nu$ has a good significance for higher Higgs masses. An expected discovery luminosity for that channel of 5 and $6 fb^{-1}$ for a 450 and 600 GeV Higgs respectively is expected. This channel works well for a Higgs with a high mass, because the decay products of a Higgs which has a high mass receive more p_t and therefore more missing p_t is present in the signal events. This will allow harder cuts on the missing p_t to be done, leading to a good signal significance, as the background has a missing p_t spectrum which steeply falls down.

Finally the third channel which can bring a good significance for a Higgs discovery is the $H \rightarrow WW \rightarrow \ell\nu qq$ channel, having expected discovery luminosities of 6, 3 and $6 fb^{-1}$ for a 300, 450 and 600 GeV Higgs respectively. Note that this last signature is obtain with the jet tagging technique. As it has a rather high branching fraction, this method works well here.

The two last channels $H \rightarrow WW \rightarrow \ell\nu\ell\nu$ and $H \rightarrow ZZ \rightarrow \ell\ell jj$ are giving smaller contributions to the total significance.

The last column of Table 5.1 shows the signal significance obtained for a luminosity of $5 fb^{-1}$, which corresponds to half a year of LHC running at low luminosity or, expressed in another way, one year at 50% efficiency. We see that as for the discovery luminosity, almost all the significance comes from the four leptons channel, the $H \rightarrow ZZ \rightarrow \ell\ell\nu\nu$ channel and the $H \rightarrow WW \rightarrow \ell\nu jj$ channel.

If these significances are combined, we get 8, 10 and 8 standard deviations for a Higgs with a mass of 300, 450 and 600 GeV, respectively.

In Table 5.1, the expected discovery luminosities for the combined channels are also given. We find that a Higgs with has a mass between 300 and 600 GeV and

Channel	S	B	S/B	Signal significance S/\sqrt{B}	Discovery luminosity (fb^{-1})
	Luminosity: $100 fb^{-1}$			$5 fb^{-1}$	\mathcal{L}_{disc}
$m_{Higgs} = 300 GeV$					
$pp \rightarrow H \rightarrow ZZ \rightarrow llll$	140	4	35.00	≈ 6.0	4
$qq \rightarrow qqH \rightarrow ZZ \rightarrow ll\nu\nu$	62	66	0.94	≈ 1.5	43
$qq \rightarrow qqH \rightarrow WW \rightarrow \ell\nu\ell\nu$	90	90	1.00	≈ 2.0	28
$qq \rightarrow qqH \rightarrow WW \rightarrow \ell\nu jj$	330	280	1.18	≈ 4.5	6
$qq \rightarrow qqH \rightarrow ZZ \rightarrow lljj$	53	46	1.15	≈ 2.0	41
Combined				≈ 8.0	2-3
$m_{Higgs} = 450 GeV$					
$pp \rightarrow H \rightarrow ZZ \rightarrow llll$	90	6	15.00	≈ 3.5	8
$pp \rightarrow H \rightarrow ZZ \rightarrow ll\nu\nu$	810	1'313	0.62	≈ 5.0	5
$qq \rightarrow qqH \rightarrow WW \rightarrow \ell\nu\ell\nu$	150	90	1.67	≈ 3.5	12
$qq \rightarrow qqH \rightarrow WW \rightarrow \ell\nu jj$	420	200	2.10	≈ 7.0	3
$qq \rightarrow qqH \rightarrow ZZ \rightarrow lljj$	75	50	1.50	≈ 2.0	22
Combined				≈ 10.0	2
$m_{Higgs} = 600 GeV$					
$pp \rightarrow H \rightarrow ZZ \rightarrow llll$	40	10	4.00	≈ 2.0	30
$pp \rightarrow H \rightarrow ZZ \rightarrow ll\nu\nu$	410	400	1.03	≈ 4.5	6
$qq \rightarrow qqH \rightarrow WW \rightarrow \ell\nu\ell\nu$	130	90	1.44	≈ 3.0	13
$qq \rightarrow qqH \rightarrow WW \rightarrow \ell\nu jj$	260	150	1.73	≈ 5.0	6
$qq \rightarrow qqH \rightarrow ZZ \rightarrow lljj$	75	25	3.00	≈ 2.5	20
Combined				≈ 8.0	2-3

Table 5.1: Expected discovery luminosities (\mathcal{L}_{disc}) for the studied channels, without systematic errors taken into account. The signal (S) and background (B) are given for a luminosity of $100 fb^{-1}$. The third column shows the signal to background ratio (S/B). We also give the significance the signals reach with a luminosity of $5 fb^{-1}$, ie. corresponding to half a year of LHC low luminosity running. The total significance reached for this luminosity is also calculated. For every Higgs masses, we give first the channels which were more significant without jet tagging ($pp \rightarrow H$) and then the channels which were more significant with the jet tagging ($qq \rightarrow qqH$).

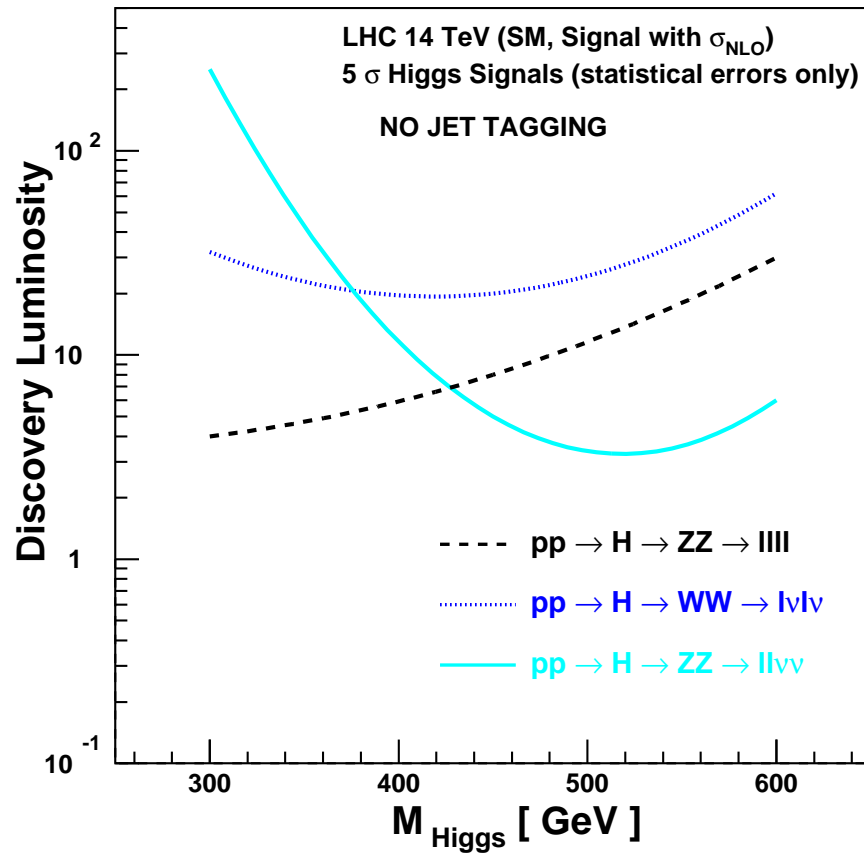


Figure 5.1: Expected luminosity for a 5σ standard deviation, for the 3 channels that give the most significant contribution when no jet tagging is made. Note that in the $H \rightarrow WW \rightarrow l\nu l\nu$ channel, the signal to background ratio is low (about 0.15). For the signal, NLO cross sections are used.

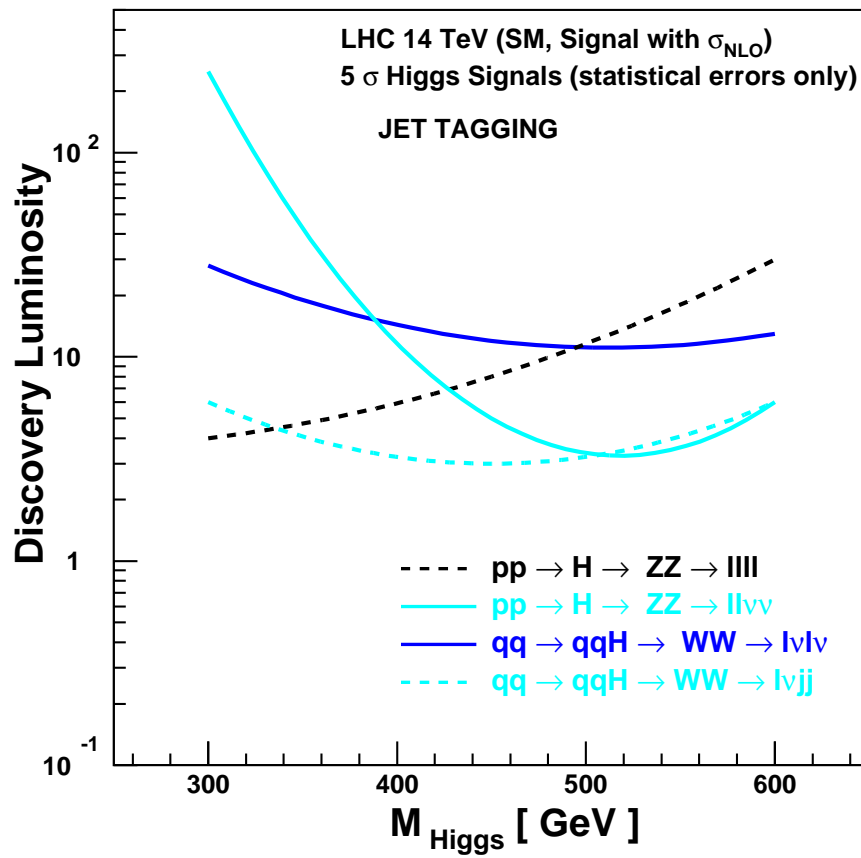


Figure 5.2: Expected luminosity for a 5σ standard deviation, for the channels that can give an interesting contribution. The channels where the jet tagging technique is used are taken here into account. For the signal, NLO cross sections are used.

SM-like couplings, should be discovered with a luminosity between 2 and 3 fb^{-1} and thus should be discovered already after one year of LHC low-luminosity running. Moreover, even if the gluon fusion process would not exist, such a Higgs could be observed within about a year, using then only the channels where that signal is isolated with the jet tagging technique.

Figures 5.1 and 5.2 give the expected required luminosity to discover a SM Higgs with a statistical significance of five standard deviations. The first plot is made with the expected discovery luminosities in the channels when no jet tagging technique is used. On the second plot, the corresponding results are shown with the channels where the jet tagging technique was used to get a signal. As said before, these alternative signatures, which are isolated with the jet tagging technique ($H \rightarrow WW \rightarrow \ell\nu\ell\nu$ and $H \rightarrow WW \rightarrow \ell\nu jj$), can contribute to lower the discovery luminosity brought by the standard Higgs discovery channels ($H \rightarrow ZZ \rightarrow \ell\ell\ell\ell$ and $H \rightarrow ZZ \rightarrow \ell\ell\nu\nu$).

Figure 5.3 gives the updated curve for the discovery luminosity over the all mass range taking into account the results brought by this study and as presented in the CMS meeting of 9th March 2001.

Finally, one last thing needs to be taken into account when one want to discuss the ability of a channel to discover the Higgs. Namely, how, in a potential discovery channel, the Higgs mass can be reconstructed. For the four leptons channels, it is not a problem, as it is directly obtained from the mass peak. That means that for masses up to 450 GeV, where this channel gives a good signal, the Higgs mass can be measured with the discovery luminosity. As already discussed, the Higgs mass peak can be also reconstructed with the $H \rightarrow WW \rightarrow \ell\nu jj$ signature, but slightly worse.

In contrast, in the $H \rightarrow ZZ \rightarrow \ell\ell\nu\nu$ channel, no mass peak can be reconstructed. One could still obtain the Higgs mass indirectly from a fit on the missing p_t spectrum or from the transverse mass spectrum.

Taking into account the results of the previous studies, we see that from 200 GeV up to 300 GeV, the four leptons channels contributes almost alone to the significance. It will then not be a problem to measure the Higgs mass if it lies in that interval. For higher masses, the $qq \rightarrow qqH \rightarrow WW \rightarrow \ell\nu jj$ channel can then be used to reconstruct a mass peak.

5.2 Measuring the ratio between the two decay branching fractions of a heavy SM Higgs, $H \rightarrow WW$ and $H \rightarrow ZZ$

From now on, the assumption that the Higgs was discovered and that its mass is known will be made. It will be assumed that the available luminosity is 100 fb^{-1} , ie. the luminosity corresponding to one year of LHC running at full capacity.

The next question we would like to study is how precisely one could measure the $\frac{BR(H \rightarrow WW)}{BR(H \rightarrow ZZ)}$ ratio. As said before, a Standard Model Higgs with a mass between

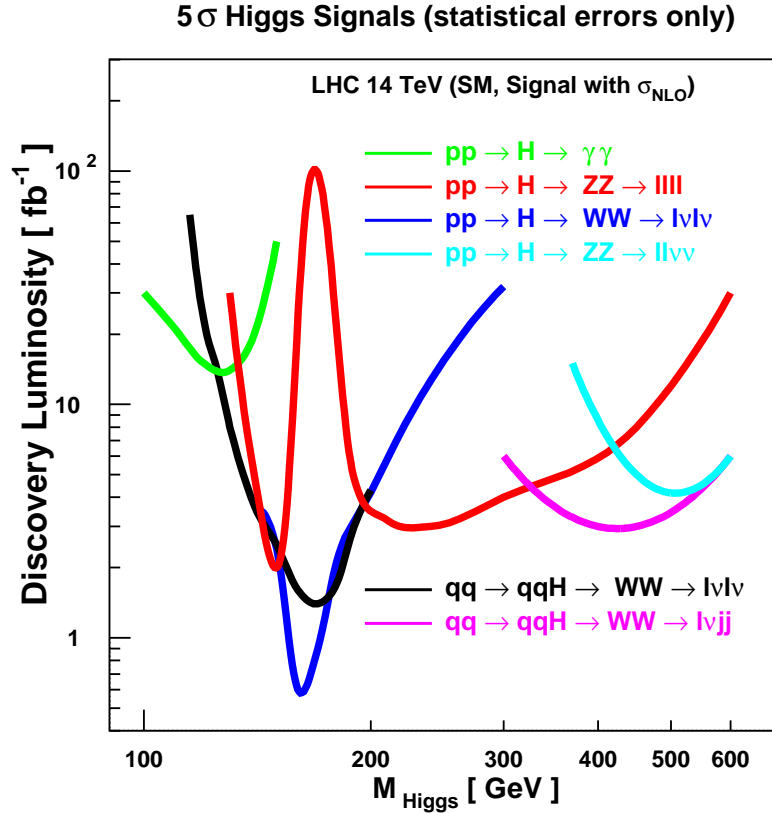


Figure 5.3: Expected luminosity for a 5 σ standard deviation, as presented in the CMS meeting of 9th March 2001. For the signal, NLO cross sections are used.

300 and 600 GeV will decay essentially in W 's and Z 's. The branching ratio (BR) for a Higgs decay in W is approximatively 2 times the branching ratio for a Higgs decay in Z 's.

It is favorable to take a ratio rather than a branching ratio alone as some hypothetical errors on cuts efficiencies caused by the simulation can be canceled. Let's take an example: We consider the cut on the tagging jet mass system and make the hypothesis that the rapidity of the tagging jets was not well simulated. If we assume that the same error in the $H \rightarrow WW$ channel than in the $H \rightarrow ZZ$ channel is introduced, then this error will be canceled when the ratio is taken. Actually, as soon as we divide the branching fractions obtained for these two channels, the efficiency of this cut does not really influence the final result.

By the way, we can compare the efficiencies of the tagging jets cuts in the different channels, which is done in Table 5.2. We see that the efficiency of the cut asking the invariant mass of the tagging jets being higher than 800 GeV is varying only by about 10% in the different channels. The efficiency of this cut will then not

influence the branching fractions rate.

Channel	$m_{Higgs} = 300 \text{ GeV}$	$m_{Higgs} = 600 \text{ GeV}$
$qq \rightarrow qqH \rightarrow ZZ \rightarrow \ell\ell\ell\ell$	0.52	0.60
$qq \rightarrow qqH \rightarrow ZZ \rightarrow \ell\nu\nu$	0.50	0.67
$qq \rightarrow qqH \rightarrow WW \rightarrow \ell\nu\ell\nu$	0.47	0.65
$qq \rightarrow qqH \rightarrow WW \rightarrow \ell\nu jj$	0.42	0.57
$qq \rightarrow qqH \rightarrow ZZ \rightarrow \ell\ell jj$	0.47	0.58

Table 5.2: Efficiency of the cut on the tagging jets mass, for the different channels studied, for weak boson fusion process.

Let's see how we can get a cross section:

Assuming that our simulation gives an efficiency of the cuts close to the reality, the cross section for a the process is given by the following formula:

$$\sigma = \frac{S}{\mathcal{L} \cdot \varepsilon_{cuts}} \quad (5.1)$$

Where \mathcal{L} is the luminosity, ε_{cuts} the efficiency of the cuts and $S (= N - B)$ the number of signal events, N the total number of events measured which survived the selection cuts minus and B the expected number of background events given by the simulation.

Given that formula, the error measured cross section depends these parameters:

- ΔN , which is given by $\pm\sqrt{S+B}$ when no systematical errors are taken into account,
- $\Delta\varepsilon_{cuts}$, which depends on the simulation used,
- ΔB , which in some cases depends strongly on the Monte Carlo used but which can be tuned through a estimation of the backgrounds in the regions where no signal is expected, using data events (this idea was discussed for the $H \rightarrow ZZ \rightarrow \ell\nu\nu$ channel, see page 47),
- and $\Delta\mathcal{L}$.

The only source of error being take into account in that study is the statistical error on N , $\pm\sqrt{S+B}$. It will give us a lower bound of the precision that could be reached.

To get the $\frac{BR(H \rightarrow WW)}{BR(H \rightarrow ZZ)}$ ratio, we have to measure separately the two ratios $\frac{\sigma(gg \rightarrow H \rightarrow WW)}{\sigma(gg \rightarrow H \rightarrow ZZ)}$ and $\frac{\sigma(qq \rightarrow qqH \rightarrow WW)}{\sigma(qq \rightarrow qqH \rightarrow ZZ)}$ and subsequently combine them, as the two Higgs production mechanisms are not the same.

We want to determine in a first step the $\frac{\sigma(qq \rightarrow qqH \rightarrow WW)}{\sigma(qq \rightarrow qqH \rightarrow ZZ)}$ ratio. The signal events are then only events where the Higgs was produced through weak boson fusion and

we will count the events with a Higgs produced through gluon fusion as background events.

We showed in the previous sections that the forward jet tagging technique allowed to isolate signal events containing Higgs produced through weak boson fusion as well from the background events, as the signal events produced through gluon fusion. Depending on the signatures considered, we find that after the jet tagging cuts, there was five to ten times more $qq \rightarrow qqH$ events than $gg \rightarrow H$ events.

Only the results from channels having a signal to background ratio higher than 0.1 are kept for the analysis¹. Table 5.3 gives the number of weak boson fusion signal events (S) and background events (B) expected for every signature studied, as well as their ratio (S/B). The statistical error on the measure of a particular branching fraction ($\sqrt{S+B}/S$) is given in the last column.

We can combine the different channels to get the final error. The formula used for the total error σ_{tot} , with the particular channels errors, σ_i is:

$$\sigma_{tot} = \frac{1}{\sqrt{w}}, \text{ where } w = \sum_i \frac{1}{\sigma_i^2} \quad (5.2)$$

We first combine the channels to get the error on the $qq \rightarrow qqH \rightarrow ZZ$ and $qq \rightarrow qqH \rightarrow WW$ branching fractions. Expected results are given in Table 5.4. Depending on the mass, we see that we have errors between 6.5% and 12.8%.

The second step is to determine the $\frac{\sigma(gg \rightarrow H \rightarrow WW)}{\sigma(gg \rightarrow H \rightarrow ZZ)}$ ratio. The results of the Higgs search when no jet tagging is applied can be used, as the contribution of this process is always larger than the contribution from weak boson fusion. The events coming from the weak boson fusion are considered as background events. Also in that case, only the channels where the signal to background ratio is higher than 10% are kept.

The results for the different channels are given in Table 5.5. Like for the weak boson fusion, we combine the results of the different channels to get the total error. Results are given in Table 5.6. We get errors between 4.3% and 17%.

We have now everything we need to make a prediction on the statistical error we can get on the measurement of the $\frac{BR(H \rightarrow WW)}{BR(H \rightarrow ZZ)}$ ratio. Let's see how we can get this information for a 450 GeV Higgs:

If we refer to Tables 5.4 and 5.6, we find that the branching ratio for $gg \rightarrow H \rightarrow ZZ$ for a 450 GeV Higgs is known up to a statistical error of 4.3% and the cross section for $gg \rightarrow H \rightarrow WW$ up to a statistical error of 10%². That means that in the best of the cases, we could measure the $\frac{\sigma(gg \rightarrow H \rightarrow WW)}{\sigma(gg \rightarrow H \rightarrow ZZ)}$ ratio for a 300 GeV Higgs up to an error of 11% in the first LHC year of full running. The formula used

¹ The minimal value required for the signal to background ratio is in that case smaller (0.1) than the value that was taken for the discovery (0.5). Actually, as we are working with higher luminosities, a better estimation of the background can be then assumed.

²It is sufficient to measure a given decay mode of the W 's, as the branching ratios of the different W 's decay modes are known from LEP.

Channel	S	B	S/B	$\sqrt{S+B}$	Stat. error
300 GeV Higgs, $qq \rightarrow qqH$					
$qq \rightarrow qqH \rightarrow ZZ \rightarrow llll$	15	2	7.50	4	27%
$qq \rightarrow qqH \rightarrow ZZ \rightarrow ll\nu\nu$	55	73	0.75	11	21%
$qq \rightarrow qqH \rightarrow WW \rightarrow l\nu l\nu$	80	100	0.80	13	17%
$qq \rightarrow qqH \rightarrow WW \rightarrow l\nu jj$	290	320	0.91	25	9%
$qq \rightarrow qqH \rightarrow ZZ \rightarrow lljj$	50	49	1.02	10	20%
450 GeV Higgs, $qq \rightarrow qqH$					
$qq \rightarrow qqH \rightarrow ZZ \rightarrow llll$	6	1	6.00	2	33%
$qq \rightarrow qqH \rightarrow ZZ \rightarrow ll\nu\nu$	55	43	1.28	10	18%
$qq \rightarrow qqH \rightarrow WW \rightarrow l\nu l\nu$	140	100	1.40	15	11%
$qq \rightarrow qqH \rightarrow WW \rightarrow l\nu jj$	330	290	1.14	25	8%
$qq \rightarrow qqH \rightarrow ZZ \rightarrow lljj$	60	65	0.92	11	18%
600 GeV Higgs, $qq \rightarrow qqH$					
$qq \rightarrow qqH \rightarrow ZZ \rightarrow llll$	5	0	-	2	40%
$qq \rightarrow qqH \rightarrow ZZ \rightarrow ll\nu\nu$	40	19	2.11	8	20%
$qq \rightarrow qqH \rightarrow WW \rightarrow l\nu l\nu$	110	110	1.00	15	14%
$qq \rightarrow qqH \rightarrow WW \rightarrow l\nu jj$	220	190	1.16	20	9%
$qq \rightarrow qqH \rightarrow ZZ \rightarrow lljj$	70	30	2.33	10	14%

Table 5.3: Expected statistical errors on the measurement of different branching fractions of the weak boson fusion process, for a luminosity of $100 fb^{-1}$. The Higgs events produced with gluon fusion are counted here as background events.

Combined results for weak boson fusion			
Channel	Statistical error		
	Higgs mass		
	300 GeV	450 GeV	600 GeV
$qq \rightarrow qqH \rightarrow ZZ$	12.8%	11.9%	11.0%
$qq \rightarrow qqH \rightarrow WW$	8.0%	6.5%	7.6%
$qq \rightarrow qqH$	6.8%	5.7%	6.2%

Table 5.4: Expected statistical errors when all channels contributions are combined and for luminosity of $100 fb^{-1}$ on the measurement of two Higgs branching fractions when it is produced through weak boson fusion. We also give the total cross section for weak boson fusion.

to get the error, ΔBR , on the ratio is

$$\Delta BR = \sqrt{\sum \Delta BR_i^2} \quad (5.3)$$

We can now repeat the same procedure for the weak boson fusion, where we have errors of 6.5% for $H \rightarrow WW$ and 11.9% for $H \rightarrow ZZ$, which gives a statistical error on the ratio of 14%. We combine the two results with the same method than the one used in the previous section, using the Formula 5.2 given on page 81, and we find a final statistical error of 9%.

A summary of all the results is given in Table 5.7.

From this, we can conclude that the $\frac{BR(H \rightarrow WW)}{BR(H \rightarrow ZZ)}$ ratio could be measured with a statistical precision of about 10%, when only statistical errors are taken into account and after one year of high luminosity LHC running.

5.3 Measuring the weak boson production and the gluon fusion cross sections

We now estimate how precisely the cross section for weak boson fusion can be measured, with a luminosity of $100 fb^{-1}$. We can actually directly refer to the Table 5.3. We only need to combine the results of the different branching ratios we have to get the total error, using Formula 5.2.

We find a statistical error on the measurement of the weak boson fusion cross section of 6.8%, 5.7% and 6.2% for a 300, 450 and 600 GeV Higgs respectively, see Table 5.4.

The channel which gives the smallest error for the weak boson fusion cross section is the $H \rightarrow WW \rightarrow \ell\nu jj$ channel, with statistical errors of 9%, 8% and 9% for a 300, 450 and 600 GeV Higgs respectively and largely contributes to improve the total resolution.

We can also estimate the statistical precision on a measurement of the gluon fusion cross section. This time, we refer to Tables 5.5 and 5.6. The main channel

Channel	S	B	S/B	$\sqrt{S+B}$	Stat. error
300 GeV Higgs, $gg \rightarrow H$					
$gg \rightarrow H \rightarrow ZZ \rightarrow llll$	90	54	1.67	12	13%
$gg \rightarrow H \rightarrow WW \rightarrow l\nu l\nu$	460	2'807	0.16	57	12%
450 GeV Higgs, $gg \rightarrow H$					
$gg \rightarrow H \rightarrow ZZ \rightarrow llll$	70	26	2.69	10	14%
$gg \rightarrow H \rightarrow ZZ \rightarrow ll\nu\nu$	700	1'423	0.49	46	7%
$gg \rightarrow H \rightarrow ZZ \rightarrow lljj$	2'290	18'760	0.12	145	6%
$gg \rightarrow H \rightarrow WW \rightarrow l\nu l\nu$	530	2'555	0.21	56	10%
600 GeV Higgs, $gg \rightarrow H$					
$gg \rightarrow H \rightarrow ZZ \rightarrow llll$	25	25	1.00	7	28%
$gg \rightarrow H \rightarrow ZZ \rightarrow ll\nu\nu$	330	480	0.69	28	9%
$gg \rightarrow H \rightarrow WW \rightarrow l\nu l\nu$	310	2'560	0.12	54	17%

Table 5.5: Expected statistical errors on the measurement of different branching fractions when the Higgs is produced through gluon fusion, for a luminosity of $100 fb^{-1}$. The Higgs events produced with weak boson fusion are counted here as background events.

Combined results for gluon fusion			
Channel	Statistical error		
	Higgs mass		
	300 GeV	450 GeV	600 GeV
$gg \rightarrow H \rightarrow ZZ$	13.0%	4.3%	8.6%
$gg \rightarrow H \rightarrow WW$	12.0%	10.0%	17.0%
$gg \rightarrow H$	8.9%	4.0%	7.7%

Table 5.6: Expected statistical errors on the measurement of the gluon fusion cross section, when all channels contributions are combined, for a luminosity of $100 fb^{-1}$. We first combine the channels to get the error on the $gg \rightarrow H \rightarrow ZZ$ and $gg \rightarrow H \rightarrow WW$ branching fractions. Then we combine all channels to get the $gg \rightarrow H$ cross section.

Higgs mass	Error determined in the process:		Combined $\frac{BR(H \rightarrow WW)}{BR(H \rightarrow ZZ)}$
	$\frac{\sigma(gg \rightarrow H \rightarrow WW)}{\sigma(gg \rightarrow H \rightarrow ZZ)}$	$\frac{\sigma(qq \rightarrow qqH \rightarrow WW)}{\sigma(qq \rightarrow qqH \rightarrow ZZ)}$	
300 GeV	18%	15%	12%
450 GeV	11%	14%	9%
600 GeV	19%	13%	11%

Table 5.7: Expected statistical precision that could be reached with a luminosity of 100 fb^{-1} on the measurement of the $\frac{BR(H \rightarrow WW)}{BR(H \rightarrow ZZ)}$ ratio.

which contribute to this measurement cross section is the $H \rightarrow ZZ \rightarrow \ell\nu\nu$ channel, which gives statistical errors of 7% and 9% for a 450 and 600 GeV Higgs respectively and largely contributes to lower the total error. The $H \rightarrow ZZ \rightarrow \ell\ell jj$ gives a contribution of 6% for a 450 GeV Higgs, but its signal to background ratio is small (0.12). Note that the four leptons channel does not bring a main contribution for that measurement, due to its too small branching ratio. We find a statistical error on the measurement of the gluon fusion cross section of 8.9%, 4.0% and 7.7% for a 300, 450 and 600 GeV Higgs respectively.

As a summary of the results obtained, we would like to present the errors we got for the different cross sections and branching ratios applied to the Standard Model predictions. If we assume that the values measured for the Higgs production through gluon fusion and weak boson fusion cross sections as well as the ratio between the two Higgs decay modes are the ones predicted by the Standard Model, which statistical error would they have ? Here is what was obtained for the different Higgs masses studied³:

$$\begin{array}{l}
 m_{Higgs} = 300 \text{ GeV} : \\
 \frac{BR(H \rightarrow WW)}{BR(H \rightarrow ZZ)} = 2.3 \pm 0.3 \\
 \sigma(qq \rightarrow qqH) = 1.5 \pm 0.1 \text{ pb} \\
 \sigma(gg \rightarrow H) = 7.8 \pm 0.7 \text{ pb}
 \end{array}$$

$$\begin{array}{l}
 m_{Higgs} = 450 \text{ GeV} : \\
 \frac{BR(H \rightarrow WW)}{BR(H \rightarrow ZZ)} = 2.1 \pm 0.2 \\
 \sigma(qq \rightarrow qqH) = 0.65 \pm 0.04 \text{ pb} \\
 \sigma(gg \rightarrow H) = 2.7 \pm 0.1 \text{ pb}
 \end{array}$$

$$\begin{array}{l}
 m_{Higgs} = 600 \text{ GeV} : \\
 \frac{BR(H \rightarrow WW)}{BR(H \rightarrow ZZ)} = 2.1 \pm 0.2 \\
 \sigma(qq \rightarrow qqH) = 0.40 \pm 0.02 \text{ pb} \\
 \sigma(gg \rightarrow H) = 1.8 \pm 0.1 \text{ pb}
 \end{array}$$

We see that the statistical precision reached with a luminosity of 100 fb^{-1} is already quite good !

A last point we would like to treat is how can this study, developed here within the Standard Model, be used in other theoretical Models. Actually the possibility to use the forward emitted jets produced in the weak boson fusion process depends only on the coupling of the Higgs to vector bosons, as the requirement for a Higgs to be produced through weak boson fusion is that it can couple to vectors bosons. Moreover the Higgs signatures studied were always characterized by a Higgs decaying into vector bosons. So if the Higgs can be produced through weak boson fusion, it can also decay in the studied modes.

The jet tagging method will then be usable in the frame of every theory assuming a Higgs coupling at vector bosons without a too small branching fraction.

Zeppenfeld and *al.* developed for example a theoretical method based on the

³The values for the different cross sections and branching ratios are taken from [18].

forward emitted jets coming from weak boson fusion processes to isolate light MSSM Higgs [22].

Note finally that the Higgs produced through gluon fusion relies on the Higgs coupling to the top quarks. If we assume a theory where a Higgs can couple in the same time to vector bosons and top quarks, a similar study can be repeated, taking into account that the ratio between the gluon fusion and weak boson cross section can be different from the one of the Standard Model (about 2 for high Higgs masses).

Summary

A possibility to detect a Higgs, with Standard Model - like couplings, having a mass lying between 300 and 600 GeV was discussed for the following signatures:

$$\begin{aligned} H &\rightarrow ZZ \rightarrow \ell\ell\ell \\ H &\rightarrow ZZ \rightarrow \ell\nu\nu \\ H &\rightarrow WW \rightarrow \ell\nu\ell\nu \\ H &\rightarrow WW \rightarrow \ell\nu jj \\ H &\rightarrow ZZ \rightarrow \ell\ell jj \\ H &\rightarrow ZZ \rightarrow \nu\nu jj \end{aligned}$$

We could isolate a Higgs signal in all of these channels except for the $H \rightarrow ZZ \rightarrow \nu\nu jj$ where too high QCD background was present. We found that a very powerful selection cut for the channels where hadronic decays were present was to use the two forward emitted jets present in the weak boson fusion Higgs production process.

It was shown that a 300 GeV Higgs signal, with the NLO cross section, could be detected already with a luminosity between 2 and $3 fb^{-1}$. The two best channels were $H \rightarrow ZZ \rightarrow \ell\ell\ell$ and $qq \rightarrow qqH \rightarrow WW \rightarrow \ell\nu jj$. A 450 GeV Higgs could be discovered with a luminosity of $2 fb^{-1}$, using mainly the following processes: $H \rightarrow ZZ \rightarrow \ell\nu\nu$ and $qq \rightarrow qqH \rightarrow WW \rightarrow \ell\nu jj$. Finally, a 600 GeV Higgs could be discovered with a luminosity between 2 and $3 fb^{-1}$, primarily from the $H \rightarrow ZZ \rightarrow \ell\nu\nu$ and $qq \rightarrow qqH \rightarrow WW \rightarrow \ell\nu jj$ channels.

With the use of the jet tagging technique, the weak boson fusion process was isolated. It was shown that the cross section for this process could be measured with a statistical precision of 6.8%, 5.7% and 6.2% for a 300, 450 and 600 GeV Higgs respectively, with a luminosity of $100 fb^{-1}$. The gluon fusion cross section could be measured with a statistical precision of 8.9%, 4.0% and 7.7% for a 300, 450 and 600 GeV Higgs respectively. The ratio between the two decay branching fractions for a heavy SM Higgs, $H \rightarrow WW$ and $H \rightarrow ZZ$ could be measured with a statistical precision of about 10%, with a luminosity of $100 fb^{-1}$.

These results need be refined in the future. The simulations did not include a full detector simulation. Hence no systematic errors were taken into account. For

example, it would be interesting to consider the error on the energy or momentum measurement in the simulation and to study how well the detector is actually able to reconstruct jets. Especially for the high luminosity phase, many proton proton interactions take place in one bunch crossing. Furthermore proton proton interactions in the previous bunch crossing influence the measurement (pile-up effects). They affect in particular the detection of the Higgs from the decay modes involving jets. Another point is that the Monte Carlo programs which simulate the backgrounds are based only on LO calculations. The next step would be to include NLO corrections.

Although the reconstruction of the Higgs from the hadronic decay mode is more difficult than that from the leptonic decay mode, it increases significantly the signal statistics. This not only enhances the chance of the discovery but also allows to study the Higgs production and decay modes.

What I am asking myself after these four months of work on that topic is if there is in Nature a Higgs with a mass between 300 and 600 GeV and Standard Model - like couplings... To get an answer to this question, see you in five years !

Bibliography

- [1] S. Glashow, Nucl. Phys. **22** (1961) 579;
S. Weinberg, Phys. Rev. Lett. **19** (1967) 1264;
A. Salam, Elementary Particle Theory, (Almqvist and Wiksells, 1968).
- [2] P. Higgs, Phys. Lett. **12** (1964) 132;
P. Higgs, Phys. Rev. **145** (1966) 1156.
- [3] T. Hambye and K. Riesselmann, *Matching conditions and Higgs mass upper bounds revisited*, Phys. Rev. D **55** (1997) 7255 [hep-ph/9610272].
- [4] CMS collaboration, *The Compact Muon Solenoid, Technical Proposal*, CERN/LHCC 94-38, December 15, 1994.
- [5] For the Higgs discovery studies made by CMS, see:
CMS collaboration, *The Compact Muon Solenoid, Technical Proposal*, CERN/LHCC 94-38, December 15, 1994.
or under the page:
http://cmsdoc.cern.ch/cgi-doc/Grep_Search_F/documents/all.html?STRING=Higgs.
- [6] For the Higgs discovery studies made by ATLAS, see:
ATLAS collaboration, *ATLAS detector and physics performance, Technical Design Report*, Volume II, ATLAS TDR 15, CERN/LHCC 99-15, May 25, 1999.
- [7] M. E. Peskin and J. D. Wells, *How can a heavy Higgs boson be consistent with the precision electroweak measurements?*, hep-ph/0101342.
- [8] M. Spira, *QCD effects in Higgs physics*, Fortsch. Phys. **46** (1998) 203 [hep-ph/9705337].
- [9] M. Dittmar, *Perspectives of SM Higgs measurements at the LHC*, Pramana-journal of physics, Indian Academy of Sciences, Vol. **55**, Nos 1 & 2, July & August 2000, pp.151-160.
- [10] R. Barate *et al.* [ALEPH Collaboration], *Observation of an excess in the search for the standard model Higgs boson at ALEPH*, Phys. Lett. **B495** (2000) 1 [hep-ex/0011045].

- [11] A. Djouadi, J. Kalinowski, M. Spira, *HDECAY: A program for Higgs boson decays in the Standard Model and its supersymmetric extension*, Comput. Phys. Commun. **108** (1998) 56-74 [hep-ph 9704448]
- [12] M. Dittmar, *Searching for the Higgs and other exotic objects (A "How to" Guide from LEP to LHC)*, Lectures given at the 30^{ème} école d'été de physique des particules Marseille 7-11 septembre 1998, ETHZ-IPP PR-98-10.
- [13] A. Holzner, *LHC Higgs Search with $\ell\nu\tau\nu$ final state*, Diploma Thesis of ETH Zürich, Spring 1998.
D. Hug, *Analyse der Signatur $H^0 \rightarrow ZZ \rightarrow \ell^+\ell^-\tau^+\tau^-$ am LHC*, Diplomarbeit am ETH Zürich, Spring 1998.
- [14] H. Ruiz Pérez, *Discovery potential of a heavy Standard Model Higgs bosons through the $H \rightarrow ZZ \rightarrow \ell\nu\nu$ channel at the LHC with the ATLAS detector*, Treball de recerca del Tercer cicle de Física, September 1998.
- [15] More informations about PYTHIA can be found under <http://shakespeare.thep.lu.se/~torbjorn/Pythia.html>.
- [16] H. L. Lai *et al.* [CTEQ Collaboration], *Global QCD analysis of parton structure of the nucleon: CTEQ5 parton distributions*, Eur. Phys. J. C **12** (2000) 375 [hep-ph/9903282].
- [17] R. K. Ellis, I. Hinchliffe, M. Soldate and J. J. van der Bij, *Higgs Decay To Tau+ Tau-: A Possible Signature Of Intermediate Mass Higgs Bosons At The Ssc*, Nucl. Phys. B **297** (1988) 221.
I. Hinchliffe and S. F. Novaes, *On The Mean Transverse Momentum Of Higgs Bosons At The Ssc*, Phys. Rev. D **38** (1988) 3475.
R. P. Kauffman, *Higher order corrections to Higgs boson $p(T)$* , Phys. Rev. D **45** (1992) 1512 and *Higgs boson $p(T)$ in gluon fusion*, Phys. Rev. D **44** (1991) 1415,
C. P. Yuan, *Kinematics of the Higgs boson at hadron colliders: NLO QCD gluon resummation*, Phys. Lett. B **283** (1992) 395.C.-P. Yuan, Phys. Lett. B **283** (1992) 395,
C. Kao, *Production of CP odd Higgs bosons with large transverse momentum at Hadron supercolliders*, Phys. Lett. B **328** (1994) 420 [hep-ph/9310206].
- [18] M. Dittmar, M. Spira, *Standard Model Higgs cross sections (NLO) and PYTHIA*, CMS Note 1997/080, October 6, 1997.
- [19] D. Zürcher, in *1999 CERN Workshop on Standard Model Physics (and more) at the LHC*, CERN, Geneva, Switzerland, May 25, 1999, Ed. by Altarelli, G and Mangano, M L - CERN, Geneva, 2000. [CERN-2000-004] - p.163.
- [20] M. H. Seymour, *The Higgs boson line shape and perturbative unitarity*, Phys. Lett. B **354** (1995) 409 [hep-ph/9505211].

-
- [21] M. Dittmar, H. Dreiner, *LHC Higgs Search with $l^+\nu l^-\bar{\nu}$ final states*, CMS Note 1997/083, October 10, 1997.
- [22] T. Plehn, D. Rainwater and D. Zeppenfeld, *Probing the MSSM Higgs sector via weak boson fusion at the LHC*, Phys. Lett. B **454** (1999) 297 [hep-ph/9902434].

Acknowledgments

For these acknowledgments, I prefer to switch to French.

Ces quatre mois de travail de diplôme ont été pour moi très intéressants et riches en découvertes. Je tiens à remercier de tout mon coeur toutes les personnes qui ont contribué à rendre cette expérience possible.

Tout d'abord, j'aimerais remercier Felicitas Pauss pour la possibilité qu'elle m'a donnée de faire mon travail de diplôme dans le groupe de l'ETHZ au CERN.

Ensuite, mes remerciements vont spécialement à Michael Dittmar, qui m'a "supervisée" tout au long de ce travail et qui a su me guider et me conseiller, en faisant preuve d'une patience sans bornes. Merci d'avoir contribué à m'ouvrir de nouveaux horizons aussi variés que la physique du Higgs, la grammaire allemande (jetzt weiß ich, daß man nicht sagt: "das fastfertige Kriminalroman"...) ou encore le théâtre de marionnettes !

J'aimerais aussi remercier tous les gens du groupe de l'ETHZ et spécialement Steve pour la salsa et les pauses café: "salade de fruits, jolie, jolie, jolie...", Dario pour les inoubliables soupers du mercredi soir, Radek et André pour l'aide inconditionnelle à faire fonctionner les ordinateurs (maintenant je crois que je sais rebooter le PC de Michael les yeux fermés...).

Merci enfin à ma famille qui a su me soutenir tout au long de mes études et m'encourager dans la voie, parfois pénible, que j'ai choisie.

Encore deux mentions spéciales à Stéphane qui m'a donné l'idée du titre lors d'une mémorable sortie à peaux de phoque et à Olivier pour sa relecture attentive de l'introduction.